



Charged-hadron production in $p p$, $p+\text{Pb}$, $\text{Pb}+\text{Pb}$, and $\text{Xe}+\text{Xe}$ collisions at $\sqrt{s_{\text{NN}}} = 5 \text{ TeV}$ with the ATLAS detector at the LHC

The ATLAS Collaboration

This paper presents measurements of charged-hadron spectra obtained in $p p$, $p+\text{Pb}$, and $\text{Pb}+\text{Pb}$ collisions at \sqrt{s} or $\sqrt{s_{\text{NN}}} = 5.02 \text{ TeV}$, and in $\text{Xe}+\text{Xe}$ collisions at $\sqrt{s_{\text{NN}}} = 5.44 \text{ TeV}$. The data recorded by the ATLAS detector at the LHC have total integrated luminosities of 25 pb^{-1} , 28 nb^{-1} , 0.50 nb^{-1} , and $3 \mu\text{b}^{-1}$, respectively. The nuclear modification factors $R_{p\text{Pb}}$ and R_{AA} are obtained by comparing the spectra in heavy-ion and $p p$ collisions in a wide range of charged-particle transverse momenta and pseudorapidity. The nuclear modification factor $R_{p\text{Pb}}$ shows a moderate enhancement above unity with a maximum at $p_{\text{T}} \approx 3 \text{ GeV}$; the enhancement is stronger in the Pb-going direction. The nuclear modification factors in both $\text{Pb}+\text{Pb}$ and $\text{Xe}+\text{Xe}$ collisions feature a significant, centrality-dependent suppression. They show a similar distinct p_{T} -dependence with a local maximum at $p_{\text{T}} \approx 2 \text{ GeV}$ and a local minimum at $p_{\text{T}} \approx 7 \text{ GeV}$. This dependence is more distinguishable in more central collisions. No significant $|\eta|$ -dependence is found. A comprehensive comparison with several theoretical predictions is also provided. They typically describe R_{AA} better in central collisions and in the p_{T} range from about 10 to 100 GeV.

Contents

1	Introduction	2
2	ATLAS detector	4
3	Data and Monte Carlo simulation samples	5
3.1	Data samples	5
3.2	Monte Carlo simulation samples	6
4	Centrality	7
5	Event and track selection	8
5.1	Event selection	8
5.2	Track selection	9
6	Analysis procedure	10
7	Systematic uncertainties	16
8	Results	18
9	Conclusions	34

1 Introduction

Collisions of heavy nuclei at high centre-of-mass energy produce a hot and dense state of matter in which quarks and gluons are no longer confined, the quark–gluon plasma (QGP) [1, 2]. In these collisions, soft (low-energy) particles are produced mainly by the thermalizing QGP [3], while hard (high-energy) particles are mostly found in jets.

Jets originating from high transverse momentum (p_T) partons are modified because of interactions with the QGP medium [4, 5]. Previous measurements of jets performed by the ATLAS, ALICE, and CMS Collaborations in Pb+Pb collisions at $\sqrt{s_{NN}} = 5.02$ TeV revealed that the energy loss of high- p_T partons results in a lower jet yield at a fixed p_T [6–8]. The jet yield is about one half to three quarters of what it would have been in the absence of the medium’s effects. The medium’s effects also modify the jet fragmentation functions [9]. The measurements show an enhancement of the charged-hadron yield inside jets at $p_T \lesssim 4$ GeV, suppression at $4 \lesssim p_T \lesssim 30$ GeV, and a small enhancement at $p_T \gtrsim 30$ GeV independent of jet p_T for jets up to $p_T^{jet} \approx 400$ GeV.

Jet p_T spectra, jet fragmentation functions, and (inclusive) charged-hadron p_T spectra are three complementary observables and it is thus expected that the production of charged hadrons will be modified by the presence of the QGP as well. The results from the LHC experiments show that hadron production in Pb+Pb and Xe+Xe (hereinafter collectively referred to as A+A) collisions is suppressed by a factor of about seven at $p_T \approx 7$ GeV [10–14] in the most central collisions. The suppression diminishes towards higher p_T . The results can test models of jet quenching in fine detail. The models often incorporate radial flow [15, 16] as well.

The observed modifications in A+A collisions are interpreted as arising mainly from the modifications of the parton showering processes in the final stages of the collisions because of the presence of QGP. However, initial-state effects arising from the presence of a large nucleus may also play a role. For example, nucleons bound in a nucleus are expected to have a somewhat different structure than free nucleons [17], or partons may lose energy in the nuclear environment before hard scattering [18]. Proton–ion collisions are used to distinguish between the initial- and final-state effects. The results from the LHC experiments show no more than a mild enhancement of hadron production at $p_T \gtrsim 2$ GeV in p +Pb collisions [11, 12, 19], indicating that initial-state effects do not influence hadron production to any large extent. The significant suppression of charged-hadron yields in A+A collisions is thus a result of the final-state effects.

The suppression of hadron production in heavy-ion (HI) collisions, encompassing both A+A and p +Pb collisions, can be quantified using the nuclear modification factor, R_{AB} . It is a ratio of the measured charged-particle production yield in HI collisions to the appropriately scaled yield in nucleon–nucleon collisions:

$$R_{AB} = \frac{1}{\langle T_{AB} \rangle} \frac{(1/N_{\text{evt}}) d^2N_{\text{ch}}/dp_T d\eta}{d^2\sigma_{pp}/dp_T d\eta}, \quad (1)$$

where N_{evt} is the number of HI events, $d^2N_{\text{ch}}/dp_T d\eta$ is the differential yield of charged hadrons in HI collisions, $d^2\sigma_{pp}/dp_T d\eta$ is the differential charged-hadron production cross-section measured in inelastic pp collisions, and $\langle T_{AB} \rangle$ is the mean nuclear thickness function. The nuclear modification factor also refers to quantities integrated over p_T or η variables,¹ or both. The mean nuclear thickness function $\langle T_{AB} \rangle$ is estimated as the number of nucleon–nucleon collisions divided by their cross-section [20]. The nucleon–nucleon hadron-production cross-section can be approximated by the corresponding pp cross-section if isospin effects are neglected [21]. To eliminate any centre-of-mass energy dependence of the charged-hadron cross-section, both the HI and pp collisions are measured at the same $\sqrt{s_{\text{NN}}}$.

The HI colliding systems considered in this study are p +Pb, Pb+Pb, and Xe+Xe. The nuclear modification factors measured for p +Pb collisions are denoted by $R_{p\text{Pb}}$ and they use $\langle T_{p\text{Pb}} \rangle$; the nuclear modification factors measured for Pb+Pb and Xe+Xe collisions are collectively denoted by R_{AA} and they use their respective $\langle T_{AA} \rangle$. It is expected that in the absence of initial- and final-state effects, the nuclear modification factor will be unity in the region of p_T where hadron production is dominated by hard scattering processes. All three nuclear modification factors are estimated as functions of p_T and η , and in intervals of collision centrality. In p +Pb collisions, the rapidity in the nucleon–nucleon centre-of-mass frame, y^* , is used instead of η [19]; the same applies for its pp baseline in $R_{p\text{Pb}}$. Collision centrality is further discussed in Section 4.

This analysis uses pp , p +Pb, Pb+Pb, and Xe+Xe data recorded by the ATLAS detector to measure charged-hadron spectra and nuclear modification factors. The pp , p +Pb, and Pb+Pb collisions have nucleon–nucleon centre-of-mass energy $\sqrt{s} = \sqrt{s_{\text{NN}}} = 5.02$ TeV while the Xe+Xe collisions have $\sqrt{s_{\text{NN}}} = 5.44$ TeV. The pp reference for Xe+Xe collisions is obtained by an extrapolation of the existing pp data at lower \sqrt{s} . The pp data were recorded in 2015 with an integrated luminosity of 25 pb^{-1} ; the p +Pb collisions were recorded in 2013 and they have an integrated luminosity of 28 nb^{-1} ; the Pb+Pb collisions recorded in 2015 have 0.50 nb^{-1} of data; and the Xe+Xe collisions were recorded in 2017 with an integrated luminosity of

¹ ATLAS uses a right-handed coordinate system with its origin at the nominal interaction point (IP) in the centre of the detector and the z -axis along the beam pipe. The x -axis points from the IP to the centre of the LHC ring, and the y -axis points upwards. Cylindrical coordinates (r, ϕ) are used in the transverse plane, ϕ being the azimuthal angle around the z -axis. The pseudorapidity is defined in terms of the polar angle θ as $\eta = -\ln \tan(\theta/2)$ and the rapidity of the components of the beam, y , are defined in terms of their energy, E , and longitudinal momentum, p_z , as $y = 0.5 \ln[(E + p_z)/(E - p_z)]$. Angular distance is measured in units of $\Delta R \equiv \sqrt{(\Delta\eta)^2 + (\Delta\phi)^2}$.

$3\,\mu\text{b}^{-1}$. The measurements use tracks with $p_{\text{T}} > 0.3\,\text{GeV}$ for all samples except for the Pb+Pb sample, where the p_{T} threshold is increased to $0.5\,\text{GeV}$. The measurements cover $|\eta| < 2.5$ for all samples, apart from $p+\text{Pb}$, which uses $-2.5 < y^* < 2.0$. Unlike the others, the $p+\text{Pb}$ collisions are asymmetric; protons with $E = 4\,\text{TeV}$ collide with lead nuclei of energy $E = 82 \times 4\,\text{TeV}$. The resulting $p+\text{Pb}$ centre-of-mass reference frame is boosted relative to the laboratory frame with a rapidity shift of $\Delta y = \pm 0.465$.

This paper is organized in nine sections: Section 2 reviews the ATLAS detector; Section 3 introduces the data and simulation samples; Section 4 provides a brief overview of the centrality definition; Section 5 outlines the event and track selection; Section 6 describes all the corrections applied to the data; Section 7 summarizes the systematic uncertainties of this measurement; Section 8 presents the results; and finally Section 9 contains the conclusions.

2 ATLAS detector

The ATLAS detector [22] at the LHC is a multipurpose particle detector with a forward/backward symmetric cylindrical geometry that covers nearly the entire solid angle around the collision point. It consists of an inner tracking detector surrounded by a thin superconducting solenoid, electromagnetic and hadronic calorimeters, and a muon spectrometer incorporating three large superconducting toroid magnets.

The inner-detector system (ID) is immersed in a $2\,\text{T}$ axial magnetic field and provides charged particle tracking in the range $|\eta| < 2.5$. The high-granularity silicon pixel detector (Pixel) covers the vertex region and typically provides three or four measurements per track; the original three layers have been augmented by the insertable B-layer [23, 24], a new innermost layer operating as a part of the pixel detector since 2015. It is surrounded by the silicon microstrip tracker (SCT) which usually provides four two-dimensional measurement points per track. These silicon detectors are complemented by the transition radiation tracker, which enables radially extended track reconstruction up to $|\eta| = 2.0$.

The calorimeter system covers the pseudorapidity range $|\eta| < 4.9$. In the region $|\eta| < 3.2$, electromagnetic calorimetry is provided by barrel and endcap high-granularity lead/liquid-argon (LAr) electromagnetic calorimeters, with an additional thin LAr presampler covering $|\eta| < 1.8$ to correct for energy loss in material upstream of the calorimeters. Hadronic calorimetry is provided by the steel/scintillator-tile calorimeter, segmented into three barrel structures within $|\eta| < 1.7$, and two copper/LAr hadronic endcap calorimeters. The system is completed with forward copper/LAr and tungsten/LAr calorimeter modules (FCal) covering $3.1 < |\eta| < 4.9$, optimized for electromagnetic and hadronic measurements respectively.

The muon spectrometer comprises separate trigger and high-precision tracking chambers. A set of precision chambers covers the pseudorapidity range $|\eta| < 2.7$ with three layers of monitored drift tubes, complemented by cathode-strip chambers in the forward region. The muon trigger system covers the range $|\eta| < 2.4$ with resistive-plate chambers in the barrel, and thin-gap chambers in the endcap regions.

The minimum-bias trigger scintillator (MBTS) counters are located at $z = \pm 3.56\,\text{m}$ along the beamline from the centre of the ATLAS detector and cover $2.1 < |\eta| < 3.9$ on each side. The number of scintillator pads forming each MBTS counter was reduced from the original 16 to 12 in 2015 [25].

The zero-degree calorimeter (ZDC) consists of two arms, positioned at $z = \pm 140\,\text{m}$ from the centre of the ATLAS detector, and detects neutrons and photons with $|\eta| > 8.3$. Signals from the ZDC are used by the trigger systems. The ZDC thresholds were set to select events with even a single neutron reaching the ZDC. The ZDC was installed only during the Pb+Pb data-taking.

An extensive software suite [26] is used in data simulation, in the reconstruction and analysis of real and simulated data, in detector operations, and in the trigger and data acquisition systems of the experiment. A two-level trigger system was used to select events [25], with a first-level (L1) trigger implemented in hardware followed by a software-based high-level trigger (HLT) that reconstructs the event in a manner similar to the final offline reconstruction, accessing information from all ATLAS subdetectors. Events used for the analysis were selected using several carefully designed triggers.

3 Data and Monte Carlo simulation samples

3.1 Data samples

A summary of all data samples used in the measurement, including triggers, luminosities, and years of data-taking is given in Table 1.

The $p\bar{p}$ events were required to either satisfy a minimum-bias (MB) trigger or one of several jet triggers with different E_T thresholds. The MB trigger required an event to be randomly selected at L1, requiring only filled bunch crossings, and a track to be reconstructed in the ID at the HLT. Jet triggers used an anti- k_t jet algorithm [27–29] with a radius parameter of $R = 0.4$ and one of seven different E_T thresholds at the HLT; the events were preselected in different ways at L1. The jet trigger with an HLT threshold of $E_T = 20$ GeV required an event to be randomly selected at L1. The jet triggers with thresholds of $E_T = 30$ GeV and 40 GeV required at L1 the total transverse energy (TE) measured in the calorimeter system to be greater than 5 GeV and 10 GeV, respectively. The jet triggers with thresholds of $E_T = 50$ GeV, 60 GeV, 75 GeV, and 85 GeV required the identification of a jet by the L1 jet trigger algorithm with thresholds of 12 GeV, 15 GeV, 20 GeV, and again 20 GeV, respectively.

The $p+\text{Pb}$ events were recorded in two data-taking periods with proton and lead beam directions swapped in the LHC rings: period A with ‘Pb+ p ’ geometry and period B with ‘ $p+\text{Pb}$ ’ geometry. Regardless of the period, the physics results of $p+\text{Pb}$ collisions are presented such that the p -going direction is towards positive rapidity; this is the convention used in previous ATLAS publications as well as in publications of other LHC experiments [30–32]. The events were required to either satisfy an MB trigger or one of several jet triggers with different thresholds. The MB trigger required an event to have signals on both sides of the MBTS. Jet triggers used an anti- k_t jet algorithm with a radius parameter of $R = 0.4$ and six different thresholds at the HLT, while the events were preselected in different ways at L1 [29]. The jet triggers with HLT thresholds of $E_T = 20$ GeV, 30 GeV, and 40 GeV required signals at L1 in both sides of the MBTS. The jet trigger with the $E_T = 50$ GeV threshold required the identification of a jet by the L1 jet trigger algorithm with a threshold of 10 GeV, and the triggers with 60 and 75 GeV thresholds required identification by the L1 jet trigger algorithm with a threshold of 15 GeV.

The Pb+Pb events were required to either satisfy one of the MB triggers or one of several jet triggers with different thresholds. The first MB trigger required an event to have TE below 50 GeV, signals in both sides of the ZDC, and a track in the ID. The second MB trigger was complementary and it required TE above 50 GeV. Jet triggers used an anti- k_t jet algorithm with a radius parameter of $R = 0.4$ and three different thresholds at the HLT, while the events were preselected in the same way at L1 [9]. The jet triggers had thresholds of $E_T = 60$ GeV, 75 GeV, and 100 GeV. They required the identification of a jet by the L1 jet trigger algorithm with a threshold of 50 GeV.

Table 1: Summary of the data samples used in the analysis. The entire luminosity is sampled only by the triggers indicated in bold font. For the MB triggers, ‘track’ means a track must be reconstructed in the ID; ‘MBTS’ means a signal is required in both sides of the MBTS; ‘ZDC’ means a signal is required in both sides of the ZDC; ‘TE50’ and ‘TE4’ means the total energy deposited in the calorimeter must be above 50 GeV and 4 GeV, respectively; ‘VTE50’ and ‘VTE4’ means a veto of the complementary trigger. More details are provided in the text.

Sample	Year	MB triggers	Jet trigger thresholds [GeV]	Luminosity	$\sqrt{s}, \sqrt{s_{\text{NN}}}$
pp	2015	track	20, 30, 40, 50, 60, 75, 85	25.0 pb^{-1}	5.02 TeV
$p+\text{Pb}$	2013	MBTS	20, 30, 40, 50, 60, 75	28.1 nb^{-1}	5.02 TeV
$\text{Pb}+\text{Pb}$	2015	TE50, VTE50+ZDC+track	60, 75, 100	0.50 nb^{-1}	5.02 TeV
$\text{Xe}+\text{Xe}$	2017	TE4 , VTE4+track	—	$3 \mu\text{b}^{-1}$	5.44 TeV

The Xe+Xe events were required to satisfy one of the MB triggers. The first MB trigger required an event to have TE smaller than 4 GeV and have a track in the ID. The second MB trigger was complementary and it required TE greater than 4 GeV. No jet triggers were used for Xe+Xe collisions.

3.2 Monte Carlo simulation samples

Several Monte Carlo (MC) simulation samples are used to evaluate the impact of the detector performance on the obtained data and to estimate necessary corrections to derive particle-level results.

For pp data, MC samples were generated at leading order using PYTHIA 8.2 [33] with NNPDF2.3LO [34] parton distribution functions (PDFs), the A14 set of tuned parameters [35], and the same \sqrt{s} as in the data. Since the production of the MC samples requires significant resources, a special effort was made to optimize it. The event production was split into 12 subsamples according to the p_T of the leading charged particle in the range of $|\eta| < 2.6$. The samples used p_T ranges of 0–3 GeV, 3–7 GeV, 7–10 GeV, 10–15 GeV, 15–20 GeV, 20–30 GeV, 30–45 GeV, 45–65 GeV, 65–90 GeV, 90–140 GeV, 140–200 GeV, and above 200 GeV. For each subsample, PYTHIA was set up with high momentum transfer² that still covered the production of all tracks within the given range; if PYTHIA produced an event with the leading charged-particle p_T too high for the given range, the event was discarded. This procedure ensures the statistical significance of the MC sample is approximately uniform in the p_T range studied. There are $4.8 \cdot 10^6$ simulated events in total.

Another three sets of PYTHIA samples are required for the pp data extrapolation as described in Section 6. Each set is also split into 12 subsamples with the same p_T ranges as those described above. There are $3 \times 19.2 \cdot 10^6$ events in total. The sets have $\sqrt{s} = 5.44 \text{ TeV}$, 5.02 TeV , and 2.76 TeV . The first two sets are used for extrapolation of data with $\sqrt{s} = 5.02 \text{ TeV}$ to $\sqrt{s} = 5.44 \text{ TeV}$ as required for the calculation of R_{AA} for Xe+Xe collisions. The last two sets are used to estimate the systematic uncertainty in this extrapolation. For these three sets of PYTHIA samples, only the generation was performed. The simulation of the detector response and consequent reconstruction, described later in this section, were not performed.

For $p+\text{Pb}$ data, separate HIJING (version 1.38b) [36] and ‘data overlay’ MC samples [37] were used. There are separate MC samples for each data-taking period. The samples using the HIJING event generator consist of $9.7 \cdot 10^6$ minimum-bias events in total. For the overlay samples, the PYTHIA hard-scattering events, using the same parameter tune and PDFs as for pp simulation, were embedded in real $p+\text{Pb}$ data events specifically recorded for this purpose with dedicated triggers. Thus, data overlay events contain

² Denoted by ‘PhaseSpace:pTHatMin’ in PYTHIA.

an underlying-event contribution identical to that in data. Only one hard-scattering event is embedded in each p +Pb event. The events are split into five subsamples according to the generated jet p_T : 0–20 GeV, 20–80 GeV, 80–200 GeV, 200–500 GeV, and 500–1000 GeV. The data overlay samples consist of $33.9 \cdot 10^6$ events in total.

The samples for Pb+Pb data also use HIJING and ‘data overlay’. The HIJING sample has $1.5 \cdot 10^6$ events. The PYTHIA events, split into 12 subsamples analogous to those of pp , were embedded in real Pb+Pb data events, recorded for this purpose with dedicated triggers. The data overlay sample has $16 \cdot 10^6$ events in total. For Xe+Xe data, ‘HIJING overlay’ and ‘data overlay’ MC samples are used. The PYTHIA events, split into 12 subsamples analogous to those of pp , were embedded either in HIJING events or in real Xe+Xe data events, recorded for this purpose with dedicated triggers. There are $2.9 \cdot 10^6$ HIJING overlay events and $16 \cdot 10^6$ data overlay events in total.

Once the MC events were generated, GEANT4 [38] simulated the detector response. It was configured with geometry and digitization parameters matching those of the data [37]. The MC events were reconstructed using the same configuration as the corresponding data [39].

To achieve precise correspondence between data and MC samples, a reweighting of the MC samples is necessary. This is done on an event-by-event basis as well as on a particle-by-particle basis. Events in the data overlay MC samples are reweighted on an event-by-event basis such that they have the same distributions of total transverse energy deposited in the FCal (FCal E_T) as in data. Events in the HIJING and HIJING overlay MC samples are reweighted on an event-by-event basis such that they have the same charged-particle multiplicity distributions as those in data; HIJING does not reproduce the correlation between FCal E_T and multiplicity reliably. No reweighting on an event-by-event basis is applied to PYTHIA MC samples. Particles in all MC samples are reweighted on a particle-by-particle basis such that the relative abundances of particle types match those measured in data by the ALICE Collaboration [40, 41]. The abundances in Xe+Xe collisions are approximated by those measured in Pb+Pb collisions in centrality intervals with the same $\langle dN/d\eta \rangle$ [14]. Since ALICE measured only pions, kaons, and protons in sufficiently wide p_T ranges in all systems (except Xe+Xe), abundances of strange baryons are estimated with another procedure. It is assumed that the number of particles follows the dependency described in Ref. [42]. The unknown parameters that are independent of the particle species are calculated using known ratios of kaons to pions and protons to pions [40, 41], while also accounting for differences between the model and the data [43]. The estimate yields about 15% strange baryons in the most central Pb+Pb collisions at around 3 GeV and less elsewhere. This is significantly higher than the 6% expected from PYTHIA. Their contribution is a result of the combination of several effects: the particle production cross-sections, kinematics and phase spaces of the decay modes, and momentum distributions of parent and child particles.

4 Centrality

In HI collisions, the event centrality reflects the overlap of the two colliding nuclei. The description of the centrality is based on the Monte Carlo Glauber model [20]. ATLAS analyses determine centrality by a measurement of the event activity in the FCal. In the case of p +Pb collisions, only the Pb-going side of the FCal is used [30], whereas in the case of Pb+Pb and Xe+Xe collisions, the sum of energies measured on both sides is used [44, 45]. The centrality intervals used in this analysis are defined according to successive percentiles of the FCal E_T distribution obtained from MB-triggered HI events ordered from the most central (highest FCal E_T , smallest impact parameter, centrality interval 0–5%) to the most peripheral collisions

Table 2: Average values and the uncertainties of centrality parameters evaluated by a Glauber model analysis of the FCal E_T distributions. Only values of the centrality intervals used in this analysis are mentioned. The calculations use the value of $\sigma_{\text{NN}} = 67.6 \pm 0.5 \text{ mb}$ at 5.02 TeV [46] and $71 \pm 3 \text{ mb}$ at 5.44 TeV. The uncertainties are discussed in Ref. [47].

Centrality	$p+\text{Pb}$		$\text{Pb}+\text{Pb}$		$\text{Xe}+\text{Xe}$	
	$\langle T_{p\text{Pb}} \rangle [\mu\text{b}^{-1}]$	$\langle N_{\text{part}} \rangle$	$\langle T_{\text{AA}} \rangle [\text{mb}^{-1}]$	$\langle N_{\text{part}} \rangle$	$\langle T_{\text{AA}} \rangle [\text{mb}^{-1}]$	$\langle N_{\text{part}} \rangle$
0–5%	222^{+25}_{-6}	$16.5^{+1.9}_{-0.9}$	26.0 ± 0.1	383.7 ± 0.4	13.9 ± 0.1	237.4 ± 0.6
5–10%	194^{+14}_{-4}	$14.6^{+1.2}_{-0.9}$	20.4 ± 0.1	331.4 ± 0.9	10.9 ± 0.1	208.6 ± 1.2
10–20%	172^{+7}_{-3}	$13.1^{+0.8}_{-0.7}$	14.4 ± 0.1	262.3 ± 1.5	7.54 ± 0.09	166.6 ± 1.5
20–30%	148^{+4}_{-2}	$11.4^{+0.6}_{-0.6}$	8.77 ± 0.13	188.2 ± 1.9	4.48 ± 0.10	119.9 ± 1.7
30–40%	126^{+3}_{-4}	$9.8^{+0.6}_{-0.6}$	5.09 ± 0.12	131.0 ± 2.0	2.55 ± 0.08	83.6 ± 1.7
40–50%			2.75 ± 0.09	87.2 ± 2.0	1.37 ± 0.06	55.6 ± 1.6
40–60%	92^{+4}_{-6}	$7.4^{+0.4}_{-0.5}$				
50–60%			1.35 ± 0.07	54.4 ± 1.8	0.69 ± 0.04	34.9 ± 1.4
60–80%			0.42 ± 0.03	23.4 ± 1.2	0.23 ± 0.02	15.5 ± 0.9
60–90%	43^{+3}_{-4}	$4.0^{+0.2}_{-0.3}$				

(lowest FCal E_T , larger impact parameter, centrality intervals 60–90% or 60–80%). The hard-scattering rate is higher in more central collisions. Such an enhancement is expected because the number of binary nucleon–nucleon collisions is greater in central than in peripheral collisions. The bias in FCal E_T from activity related to the triggering jet is negligible.

A Glauber model analysis of the FCal E_T distribution is used to evaluate geometric quantities together with their systematic uncertainties [30, 44, 45]; they are summarized in Table 2. The number of participants, N_{part} , corresponds to the number of nucleons that interacted inelastically at least once. The number of nucleon–nucleon collisions, N_{coll} , can be derived from their total inelastic cross-section and the nuclear thickness function:

$$N_{\text{coll}} = \langle T_{AB} \rangle \sigma_{\text{NN}}$$

5 Event and track selection

5.1 Event selection

Offline event selection always requires a vertex to be reconstructed less than 150 mm from the centre of the detector in the z direction [10]. In $\text{Pb}+\text{Pb}$ and $\text{Xe}+\text{Xe}$ data-taking the instantaneous luminosities resulted in less than 2×10^{-4} interactions per bunch crossing, and reconstruction of only one vertex is attempted because the probability of having pile-up vertices is very small. In pp and $p+\text{Pb}$ data, with instantaneous luminosity reaching 1.5 interactions and 2×10^{-3} interactions per bunch crossing, respectively, multiple collision vertices are possible.

In pp collisions, pile-up events are not rejected, as the measured observable is the total inelastic cross-section. On the other hand, the measured observable in HI collisions is the per-event yield, and thus the pile-up events are rejected. This is achieved by multiple means: by requiring correlations between FCal E_T and the number of reconstructed tracks (in the case of Pb+Pb and Xe+Xe collisions), by requiring signals in both sides of the ZDC (in Pb+Pb collisions), by requiring energy deposits in both the positive and negative intervals of $2.9 < |\eta| < 5.0$ (in p +Pb, Pb+Pb, and Xe+Xe collisions) and by requiring that there is only one reconstructed vertex (in p +Pb collisions). Beam–gas events are also rejected by this procedure.

5.2 Track selection

This analysis of the charged-particle spectra refers to primary charged particles with a mean lifetime greater than 0.3×10^{-10} s, directly produced in the nucleus–nucleus interactions or long-lived charged particles created by subsequent decays of particles with shorter lifetimes [48]. All other particles are considered secondary. Tracks produced by primary and secondary particles are referred to as primary and secondary tracks, respectively. Reconstructed tracks arising from spuriously associated detector-layer hits that originate from different particles are considered to be fake tracks. Tracks are reconstructed in the pseudorapidity region $|\eta| < 2.5$ and over the full azimuth [39, 49]. Tracks with $p_T > 0.3$ GeV from pp , p +Pb, and Xe+Xe collisions are reconstructed; tracks with $p_T > 0.5$ GeV from Pb+Pb collisions are reconstructed.

In the MC simulation, the categorization of tracks relies on their matching to generated particles. This is based on the hits produced in the detector layers by the generated particles. A reconstructed track is matched to a generated particle that contributed the most to the hits used to build this track. The matching procedure is explained in more detail in Ref. [50].

To enhance the fraction of primary tracks and suppress secondary and fake tracks, all reconstructed tracks are required to satisfy quality criteria. These criteria are the same for tracks in both the data and MC samples. In pp collisions, tracks are required not to miss any hits in the Pixel detector and no more than two hits in the SCT detector if such hits are expected from the track trajectory. Tracks are allowed to share either one hit in the Pixel detector or two hits in the SCT detector with other tracks. Tracks are also required to have at least one hit in one of the two innermost layers of the Pixel detector if the reconstructed track passed through an active sensor. Tracks with $|\eta| < 1.65$ ($|\eta| > 1.65$) are required to have at least 9 (11) hits in the Pixel and the SCT detectors combined. Since primary tracks are more likely than secondary or fake tracks to originate from the collision vertex, a p_T -dependent requirement on d_0 , the distance of the closest approach to the vertex in the transverse direction, is imposed on tracks. There is no requirement on z_0 , the longitudinal separation between the vertex and the point where d_0 is measured.

In p +Pb collisions, tracks must have at least two hits in the Pixel detector and at least six hits in the SCT detector. Tracks are not allowed to have a missing hit in the innermost layer of the Pixel detector if such a hit is expected from the track trajectory. Tracks must not share any hits with other tracks. To ensure a good match to the vertex, the significances $|d_0|/\sigma_{d_0}$ and $|z_0 \sin \theta|/\sigma_{z_0 \sin \theta}$ may not exceed 3 where σ_{d_0} and $\sigma_{z_0 \sin \theta}$ are the uncertainties in d_0 and $z_0 \sin \theta$, respectively, and θ is the polar angle of the track.

In Pb+Pb and Xe+Xe collisions, requirements on tracks are similar to those in pp collisions but a match to the vertex is required as for p +Pb collisions. Tracks are required not to miss any hits in the Pixel or SCT detectors if such hits are expected from the track trajectory; no restrictions on shared hits are imposed.

These track selection requirements produce a sufficiently clean track sample up to $p_T \lesssim 50$ GeV. Above that, a significant number of tracks originate from lower-momentum primary particles whose track p_T is mismeasured. The probability for this to occur increases with p_T , rapidity, and the detector occupancy and was studied in the simulated samples in detail. To eliminate the problem, high- p_T tracks are counted only in the vicinity of jets, within an angular distance $\Delta R = 0.4$. The jets are reconstructed in the calorimeter with the anti- k_t algorithm using a radius parameter of $R = 0.4$; the jet reconstruction and underlying-event subtraction is further described in Refs. [6, 30]. The relative difference of track p_T and p_T^{jet} may not exceed three times their measurement uncertainties combined. The limitation arising from a low jet reconstruction efficiency at low p_T^{jet} is also taken into account. The described requirement is not imposed if the track may originate from a jet whose reconstruction efficiency is less than 99%.

Leptons are excluded from the measured charged-hadron spectra. Tracks forming part of reconstructed muons are identified, and their contribution is subtracted with a weight that also accounts for tracks of electrons. The probability of missing a track from a muon is very small ($\lesssim 1\%$).

6 Analysis procedure

Events in pp , $p+\text{Pb}$, and $\text{Pb}+\text{Pb}$ collisions are recorded by MB and jet triggers. The spectra obtained with different triggers are combined to construct the spectra equivalent to the MB spectra, which extend to the highest p_T reachable with their luminosities [10].

With N denoting the number of jet triggers used in the data-taking for each analysed system as listed in Table 1, the jet triggers are numbered $n = 0, \dots, N - 1$ and to each one an *interval of full efficiency* $[p_{T,n}^{\text{jet}}, p_{T,n+1}^{\text{jet}}]$ is assigned. The values of $p_{T,n}^{\text{jet}}$ are defined as the momentum at which the n -th jet trigger is fully efficient. Due to differences between the online and offline estimates of p_T^{jet} , they are somewhat higher than the nominal momenta of the jet triggers listed in Table 1. These values form an incremental sequence: $p_{T,0}^{\text{jet}}, p_{T,1}^{\text{jet}}, \dots, p_{T,N-1}^{\text{jet}}$. The interval $[0, p_{T,0}^{\text{jet}}]$ is assigned to the MB trigger. The highest-threshold triggers have no upper limit, i.e. $p_{T,N}^{\text{jet}} = \infty$.

In events acquired with the MB trigger, tracks that do not match to any jet are also selected. In events acquired with the jet triggers, tracks are required to be matched only to the jets whose p_T^{jet} fall in the interval of full efficiency corresponding to the given jet trigger.

After scaling the spectrum of each trigger by its appropriate effective integrated luminosity, spectra from all triggers are summed. The procedure is illustrated in Figure 1. The low- p_T part of the combined spectrum is covered by the MB trigger with negligible contributions from other triggers. With increasing p_T , the importance of the MB trigger diminishes and that of jet triggers increases. At the highest p_T measured, all tracks are taken from the jet trigger with the highest p_T^{jet} .

After the summation, several subsequent corrections are applied in this order: for fake and secondary tracks, for p_T resolution, for η (or y^*) resolution, and for track reconstruction efficiency. Moreover, an extrapolation to $\sqrt{s} = 5.44$ TeV is applied as a final correction to the pp distributions used as a baseline for the R_{AA} values measured in Xe + Xe collisions. Corrections accounting for the generated distribution of particle masses are applied to $p+\text{Pb}$ distributions and their pp baseline. All corrections together modify the measured distributions by several tens of percent.

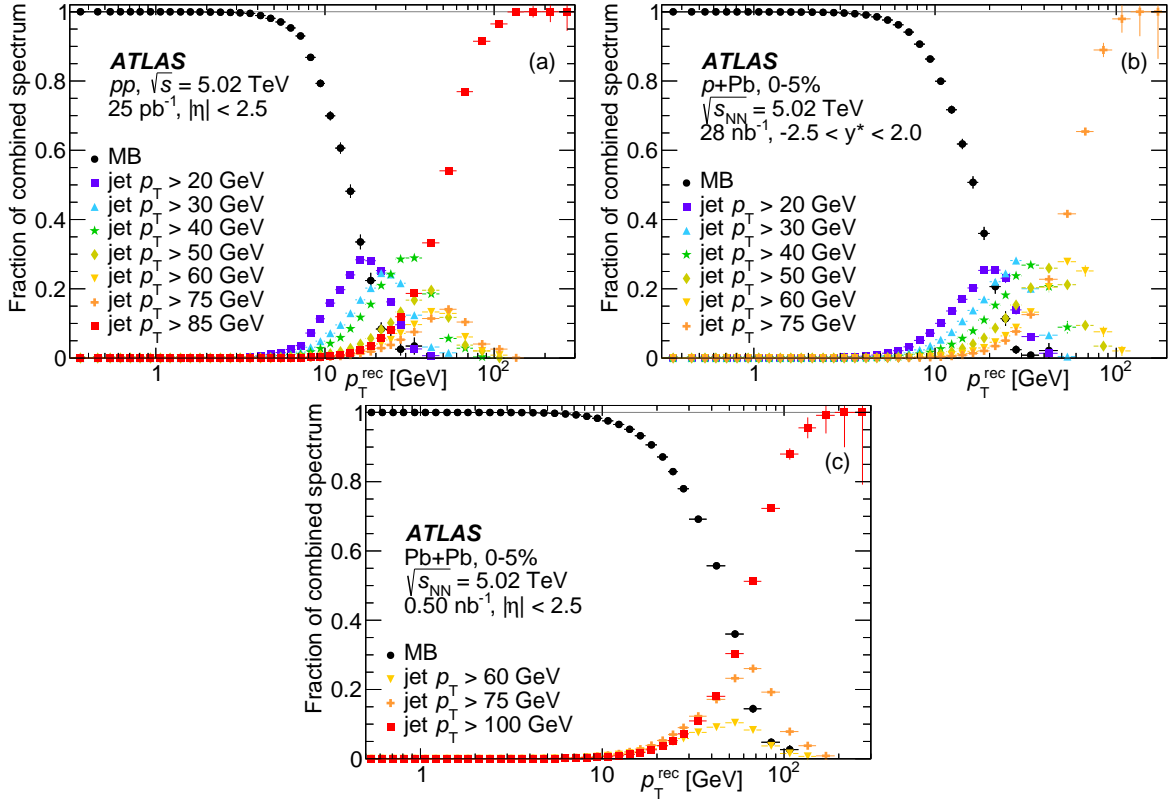


Figure 1: The relative contributions of different triggers to the combined reconstructed track p_T spectra in (a) pp , (b) $p+Pb$, and (c) $Pb+Pb$ collisions. The $p+Pb$ and $Pb+Pb$ results are shown for the 0–5% centrality interval. The statistical uncertainties are shown with vertical lines.

The corrections are estimated by using MC samples. In the case of pp collisions, all corrections use PYTHIA samples. In the case of HI collisions, the corrections for fake and secondary tracks are derived using HIJING samples, while the other corrections are derived using data overlay samples.

The first applied correction is for fake and secondary tracks. The merged spectra are multiplied by the fraction of primary tracks, which is defined as the number of primary tracks divided by the total number of tracks, i.e. including fake and secondary tracks. The fractions are estimated in the MC simulation as a function of p_T , η (or y^*), collision system, and centrality.

Figure 2 shows examples of the fraction of primary tracks in several η (or y^*) ranges. For HI collisions, only the most central collisions are shown. The decrease at low p_T is a feature common to all centrality intervals, although it is milder for more peripheral collisions.

To correct for the p_T resolution, iterative Bayesian unfolding [51] is used with migration matrices describing the relationship of the reconstructed p_T of the tracks (p_T^{rec}) to the generated p_T of the matched particles.

The unfolding accuracy is limited by the number of MC events through statistical fluctuations within the migration matrices. Therefore, a procedure to ‘smooth’ the migration matrices via fitting is implemented.

First, the response r defined as:

$$r = p_T / p_T^{\text{rec}} - 1,$$

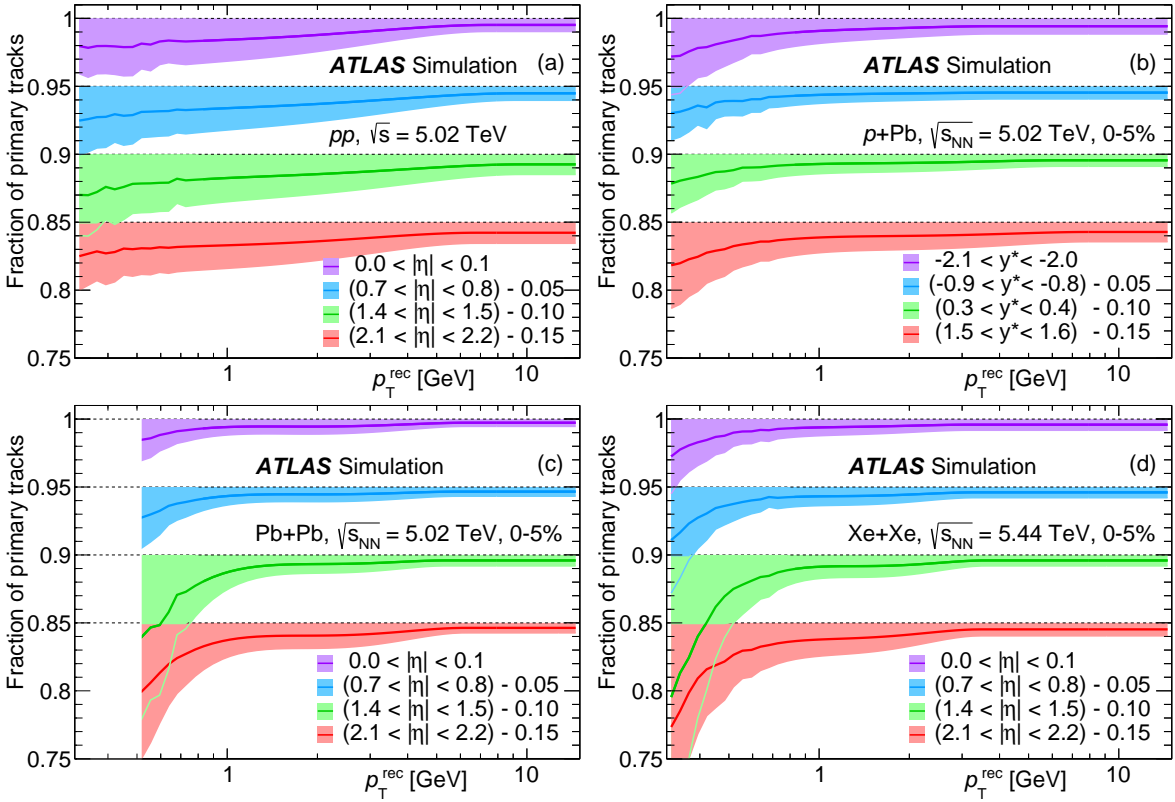


Figure 2: The fraction of reconstructed tracks matched to primary particles as a function of reconstructed p_T for (a) pp , (b) $p+Pb$, (c) $Pb+Pb$, and (d) $Xe+Xe$ collisions and for four ranges of (pseudo)rapidity. The widths of the bands represent the systematic uncertainties; see Section 7 for further details. The values are vertically offset for clarity.

is estimated for each collision system and centrality interval, and in small ranges of generated p_T and $|\eta|$ (or y^*) that coincide with the binning of the final distributions. Every response distribution is fitted; the central part ($|r| \lesssim 0.2$) is described by two Gaussian distributions, while the positive ($r \gtrsim 0.2$) and negative ($r \lesssim -0.2$) tails are described by two independent exponential functions.

Figure 3 shows examples of the response distributions and their fits in a few p_T ranges. Migration matrices are built separately for each collision system, centrality interval, and small range of $|\eta|$ (or y^*). The matrices have fixed generated p_T in rows and fixed reconstructed p_T^{rec} in columns. To fill one bin of the matrix, an integral of the response fit with appropriate ranges has to be calculated. The same fit is used for all bins in the same row, i.e. for the same generated p_T . Examples of the migration matrices after smoothing are shown in Figure 4 with the same centrality intervals and $|\eta|$ (or y^*) ranges as the response fits in Figure 3. The migration matrices are used in the iterative Bayesian unfolding. The procedure converges within two iterations.

Iterative Bayesian unfolding is also used to correct for the η (or y^*) resolution. In contrast to the p_T resolution, the η (and y^*) resolution is better, the migration matrices are more diagonal, and therefore no smoothing procedure is required for the migration matrices used in unfolding. Migration matrices are estimated separately for each collision system and centrality interval, and in small p_T ranges. The procedure converges within two iterations.

The unfolded spectra are corrected for the reconstruction efficiency, defined as the number of primary

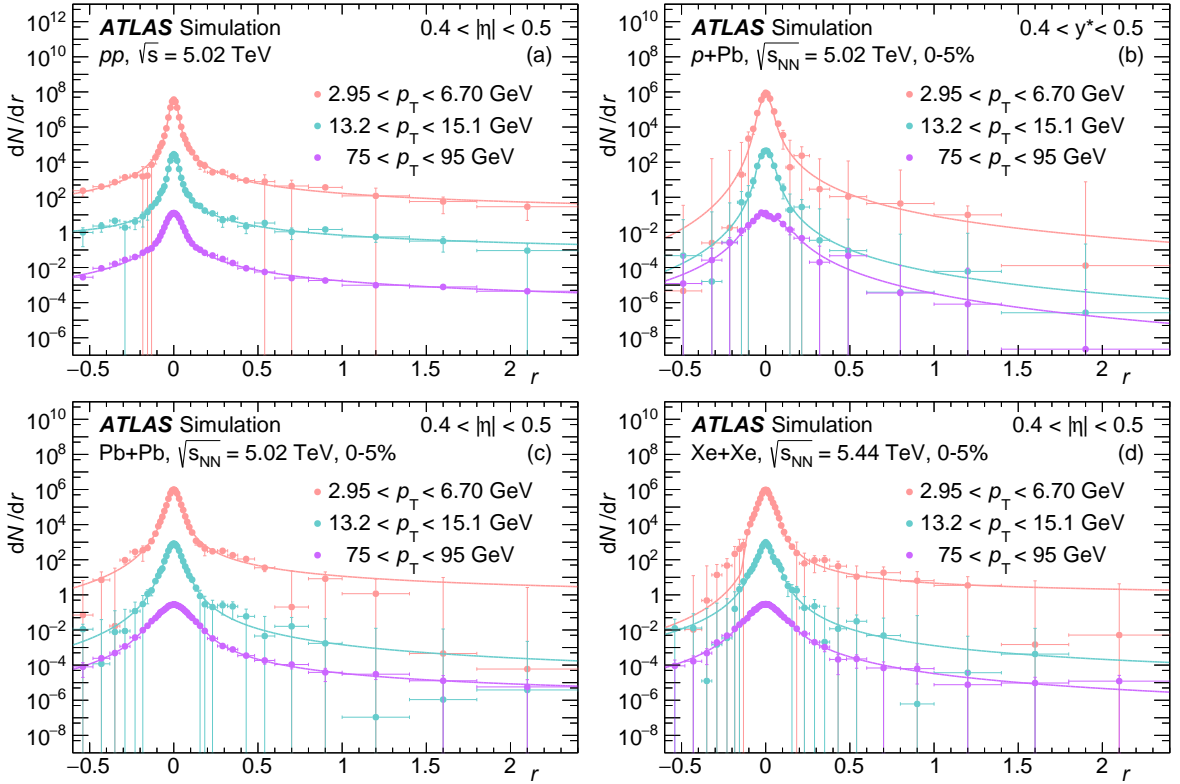


Figure 3: The track p_T response as a function of r for (a) pp , (b) $p+Pb$, (c) $Pb+Pb$, and (d) $Xe+Xe$ collisions and for three ranges of generated p_T . The vertical bars represent the statistical uncertainties. The curves represent the corresponding fits.

particles matched to reconstructed tracks divided by the total number of generated primary particles. The reconstruction efficiency is calculated as a function of p_T , η (or y^*), collision system, and centrality. To remove statistical fluctuations, the efficiency is fitted by a polynomial of the sixth order in $\log(p_T)$.

Figure 5 shows examples of the track reconstruction efficiency in several η (or y^*) ranges. For HI collisions, only the most central collisions are shown. The efficiency is typically higher for more peripheral collisions. The efficiencies for different collision systems also reflect changing detector conditions and reconstruction software, which are implemented in the simulation. The decrease at low p_T is a feature common to all centrality intervals. The decrease in reconstruction efficiency around p_T of 3 GeV is due to a large number of strange baryons, which according to the definition in Section 5.2 are considered primary particles. At this p_T , they are still unlikely to fully traverse the ID – with the probability growing at higher momentum. The reconstruction efficiency is expected to deteriorate at high p_T due to the higher likelihood of mismeasuring tracks in the dense core of high- p_T jets [9].

To construct the charged-hadron R_{AA} in the $Xe+Xe$ system at $\sqrt{s} = 5.44$ TeV the reference pp spectrum is extrapolated from the measured pp spectrum at $\sqrt{s} = 5.02$ TeV. A multiplicative extrapolation factor is estimated as a ratio of the generated spectrum at $\sqrt{s} = 5.44$ TeV to that at $\sqrt{s} = 5.02$ TeV. To remove statistical fluctuations, the extrapolation factor is fitted by a polynomial of the third order in $\log(p_T)$. The extrapolation factor is estimated as a function of p_T and η .

Figure 6 shows the extrapolation factor in several η ranges. At low p_T , the factor is almost independent of

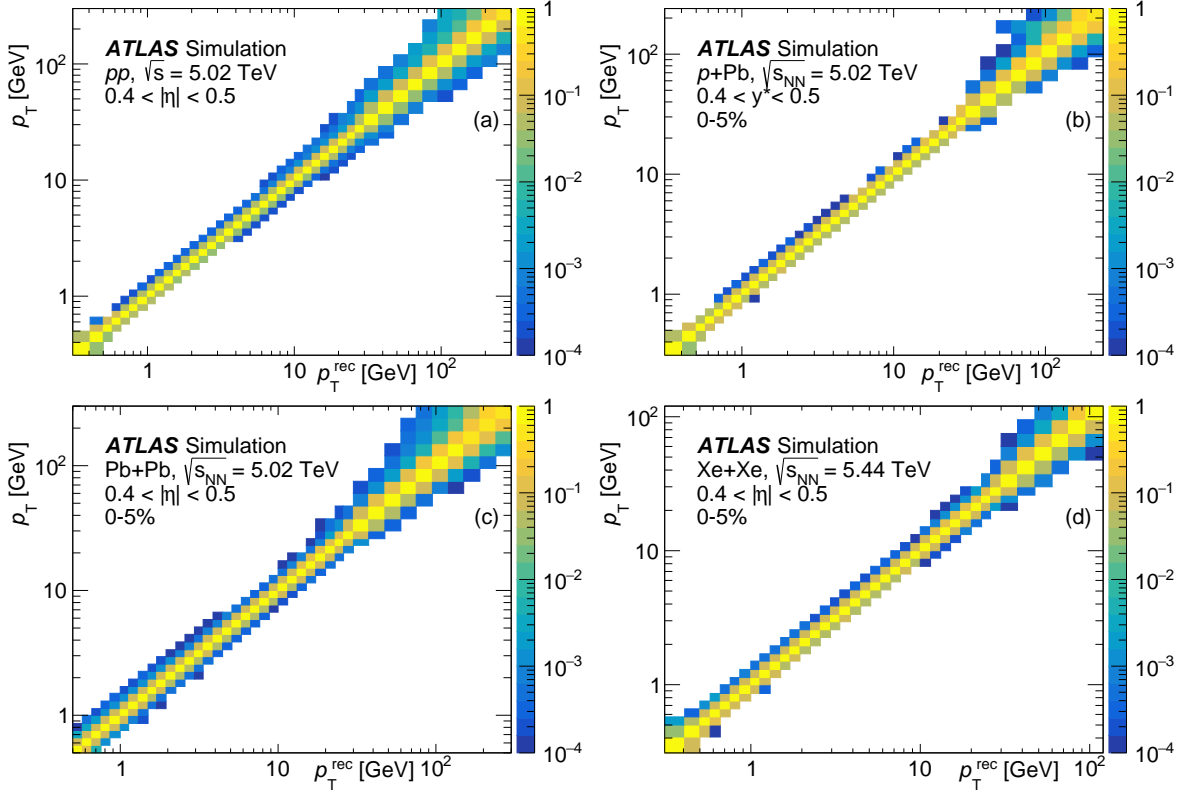


Figure 4: The p_T migration matrices for (a) pp , (b) $p+Pb$, (c) $Pb+Pb$, and (d) $Xe+Xe$ collisions. The integral of the distribution in each row is normalized to unity.

$|\eta|$. At high p_T , the factor is higher for high $|\eta|$ ranges.

For the measurements of $p+Pb$ collisions as well as of the corresponding pp baseline, all the corrections are estimated as a function of y^* , assuming the pion mass for all particles. The same assumption is made for the tracks from the data samples. To account for the generated mass of the particles, a correction similar to the one in Ref. [19] is applied. It is defined as a ratio of the generated particle spectrum using the correct mass to the spectrum using the mass of the pion. It is estimated as a function of p_T , y^* , and centrality. It has an effect only at low p_T and high $|y^*|$, where it corrects for migration in y^* ; there the correction factor can fall to about 0.85, from values closer to unity elsewhere.

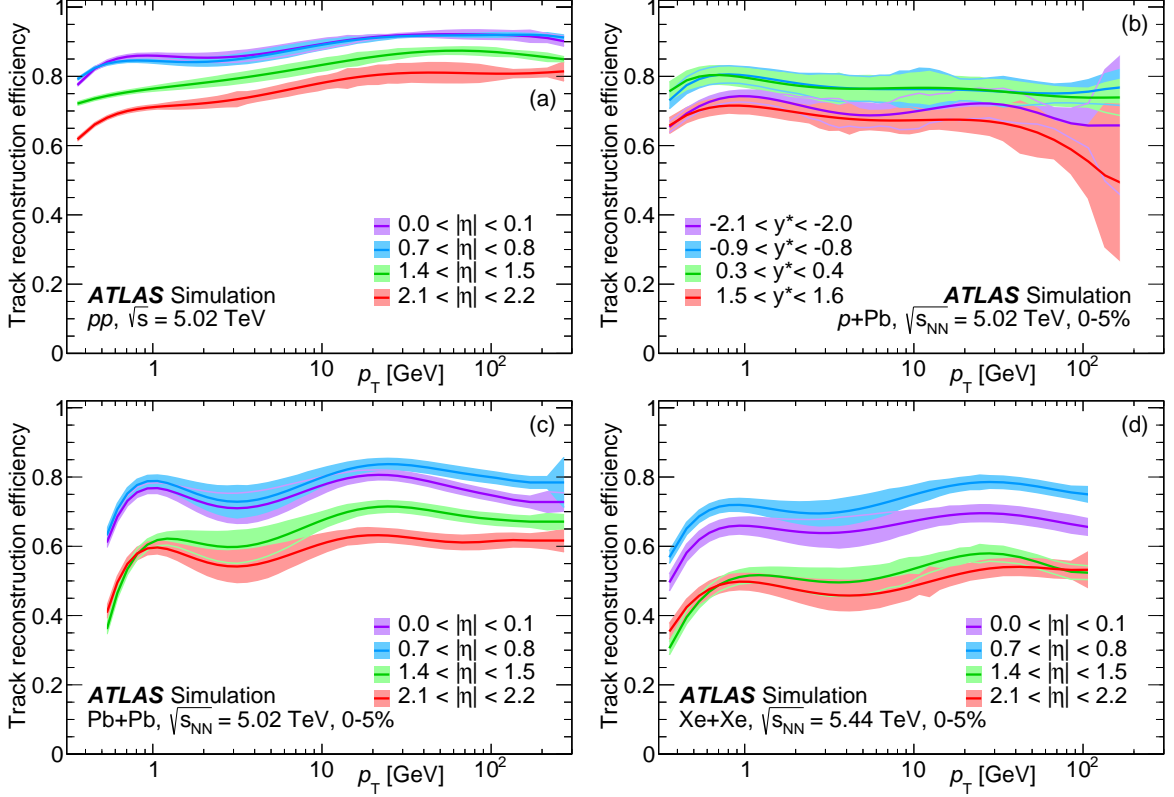


Figure 5: Track reconstruction efficiency as a function of p_T for (a) pp , (b) $p+\text{Pb}$, (c) $\text{Pb}+\text{Pb}$, and (d) $\text{Xe}+\text{Xe}$ collisions and for four ranges of (pseudo)rapidity. The widths of the bands represent the systematic uncertainties; see Section 7 for further details.

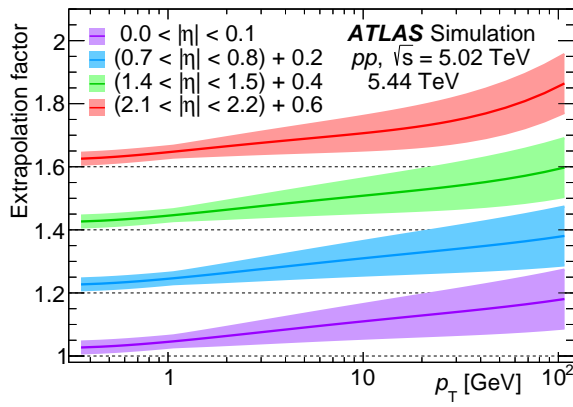


Figure 6: Extrapolation factors as a function of p_T for four ranges of pseudorapidity. The widths of the bands represent the systematic uncertainties; see Section 7 for further details. The values are vertically offset for clarity.

7 Systematic uncertainties

The systematic uncertainties of the measurements arise from several independent sources. The contribution of each source is estimated by varying the corresponding parameters of the analysis and propagating the impact of the source to the final result by performing the full analysis chain.

The total systematic uncertainties are determined by adding the contributions from all relevant sources in quadrature. All systematic uncertainties are summarized in Table 3.

Track selection. In addition to the track selection requirements explained in Section 5.2, two other sets of requirements are considered. The more restrictive criteria, with more required hits per track and stricter pointing-to-vertex requirements, provide a higher fraction of primary tracks but with lower efficiency. On the other hand, the relaxed criteria, with fewer required hits per track and looser pointing-to-vertex requirements, offer higher track reconstruction efficiency at the expense of more fake and secondary tracks. The average of the absolute values of the deviations from the default selection defines the systematic uncertainty. The uncertainty is higher in more central collisions and at higher p_T .

Momentum bias. A residual detector misalignment present in Pb+Pb data causes a momentum bias that is absent in the MC simulations. An additional correction is introduced to compensate for this effect. Its uncertainty is propagated to the measured distributions. No such misalignment is present in other data samples. The uncertainty is higher at high p_T and in more peripheral collisions.

Track-to-particle matching quality. The efficiency corrections used in the analysis rely on matching the reconstructed tracks to generated particles. To account for ambiguities in the matching procedure, the matching probability, defined in Ref. [50], is varied to assess the systematic uncertainty. This uncertainty is most pronounced at low p_T in the most central collisions.

Particle composition. The systematic uncertainty of the measurements of particle compositions [40, 41], as well as the full difference between the model and the data [43, 52], are taken into account when estimating particle weights for the analysis as described in Section 3. The resulting systematic uncertainty reaches its maximum at $3 \lesssim p_T \lesssim 5$ GeV.

Correction for fake and secondary tracks. The systematic uncertainty due to the fake and secondary tracks is estimated to be 100% of the secondary and fake rate. This is independent of the track selection criteria.

Resolution correction procedures in p_T and η . To test the stability of p_T and η resolution corrections, the content of each bin in the p_T resolution distributions or in the η migration matrices is individually changed following a Poisson distribution, reflecting the statistical uncertainties of a bin. The statistical uncertainties for p_T resolutions are shown in Figure 3.

Unfolding procedure. In the analysis, the measured spectra are first unfolded to correct for p_T resolution and then to correct for η (or y^*) resolution. To check the impact of this arbitrary choice, the order of these two steps is swapped.

Track reconstruction efficiency. The track reconstruction efficiency is fitted to produce a smooth correction. The difference between the fit and the data points is used to estimate an uncertainty in the track reconstruction efficiency; the difference is driven by the limited number of events in the MC samples.

Table 3: The summary of systematic uncertainties. The first listed numbers are typical values and the second numbers are maximum values of the uncertainties. All values are in percent. More details are given in the text.

Source	Spectra [%]				Ratios [%]		
	pp	$p+Pb$	$Pb+Pb$	$Xe+Xe$	$p+Pb/pp$	$Pb+Pb/p\bar{p}$	$Xe+Xe/p\bar{p}$
Track selection	2 / 12	5 / 33	2 / 13	2 / 9	5 / 32	4 / 18	3 / 12
Momentum bias	—	—	2 / 28	—	—	2 / 28	—
Track-to-part. match.	<1 / <1	1 / 3	1 / 6	1 / 5	1 / 3	1 / 6	1 / 5
Particle composition	1 / 2	2 / 8	2 / 8	2 / 4	1 / 8	1 / 7	1 / 2
Fake & second. tracks	1 / 2	1 / 2	1 / 4	1 / 6	<1 / 1	<1 / 2	1 / 3
p_T resolution correct.	<1 / <1	<1 / 2	<1 / 2	<1 / 1	<1 / 3	<1 / 2	<1 / 1
η resolution correct.	<1 / <1	<1 / 6	<1 / 1	<1 / 1	<1 / 6	<1 / 1	<1 / 1
Unfolding procedure	<1 / <1	<1 / 1	<1 / 1	<1 / 2	<1 / 2	<1 / 1	<1 / 2
Track reconstr. effic.	<1 / <1	1 / 2	2 / 2	2 / 2	1 / 2	2 / 2	2 / 2
Detector material	2 / 4	3 / 6	2 / 4	2 / 4	3 / 7	—	—
Luminosity	2 / 2	—	—	—	2 / 2	2 / 2	2 / 2
$\langle T_{pPb} \rangle$ or $\langle T_{AA} \rangle$	—	6 / 11	4 / 7	4 / 8	6 / 11	4 / 7	4 / 8
Extrapolation of pp	—	—	—	—	—	—	5 / 9
Total	4 / 12	8 / 38	6 / 33	6 / 11	9 / 37	7 / 35	8 / 18

Detector material. This systematic uncertainty is associated with possible mis-modelling of the detector material [50], effectively lowering the track reconstruction efficiency.

Luminosity, $\langle T_{pPb} \rangle$, and $\langle T_{AA} \rangle$. The integrated luminosity determined for the pp data is calibrated using data from dedicated beam separation scans, using procedures described in Ref. [53]. The systematic uncertainties in the mean nuclear thickness functions arise from the geometric modelling uncertainties and from the uncertainties in the fraction of selected inelastic HI collisions. The uncertainties are adapted from Refs. [30, 44, 45] and are listed in Table 2.

Extrapolation of the pp baseline to $\sqrt{s} = 5.44$ TeV. The measured pp spectrum at $\sqrt{s} = 2.76$ TeV [10] is extrapolated to $\sqrt{s} = 5.02$ TeV in a way analogous to that described in Section 6, using generated spectra at $\sqrt{s} = 2.76$ TeV and 5.02 TeV. The extrapolated spectrum at $\sqrt{s} = 5.02$ TeV is compared with the pp spectrum at $\sqrt{s} = 5.02$ TeV measured by this analysis. At $p_T \approx 100$ GeV, the cross-section increase in the extrapolation is about 40% less than it should be; it is more accurate at lower p_T . It is assumed that the cross-section increase is underestimated by the same percentage, with its associated uncertainty, when extrapolating the pp spectrum measured at $\sqrt{s} = 5.02$ TeV to $\sqrt{s} = 5.44$ TeV.

Some sources of systematic uncertainty are considered correlated between the HI and pp systems and their variations can lead to their impacts partially cancelling out when the ratios R_{pPb} and R_{AA} are calculated. This is the case for the uncertainties in track selection, track-to-particle matching quality, particle composition, the correction for fake and secondary tracks, and the unfolding procedure. In these cases, the parameters are varied simultaneously for the HI and pp collisions, so that the contributions properly reflect the correlated changes in the numerator and denominator of the ratio.

On the other hand, some sources are considered uncorrelated; this is the case for the uncertainties in resolution correction procedures in p_T and η , and the track reconstruction efficiency.

The uncertainties in detector material are considered correlated when comparing two samples from Run 2, which is the case for $\text{Pb+Pb}/pp$ and $\text{Xe+Xe}/pp$. The uncertainties from Run 1 and Run 2 are not correlated by more than half of their combined values. Since it is not feasible to work out the exact fractions, uncertainties are taken as uncorrelated when comparing a sample from Run 1 with a sample from Run 2, which is the case for $p+\text{Pb}/pp$.

The rest of the sources contribute only to either the numerator or the denominator.

The systematic uncertainties in the track quality selection, the momentum bias in Pb+Pb collisions, the extrapolation of the pp baseline, and $\langle T_{p\text{Pb}} \rangle$ or $\langle T_{\text{AA}} \rangle$ are the largest contributions to the total systematic uncertainty. The uncertainties associated with other individual sources typically do not exceed 3%.

8 Results

This section presents the results for all observables measured in this analysis. It also compares them between centralities and different collision systems as well as with theoretical models and other experiments.

The corrected charged-hadron spectra from $p+\text{Pb}$ collisions at $\sqrt{s_{\text{NN}}} = 5.02 \text{ TeV}$ measured as a function of p_T for the rapidity range $-2.5 < y^* < 2.0$ and for four centrality intervals are shown in Figure 7. The $p+\text{Pb}$ spectra are divided by the $\langle T_{p\text{Pb}} \rangle$ of the corresponding centrality intervals and are compared with the charged-hadron production cross-section measured in the pp collisions at the same nucleon–nucleon centre-of-mass energy and in the same rapidity range.

The corrected charged-hadron spectra from Pb+Pb and Xe+Xe collisions at $\sqrt{s_{\text{NN}}} = 5.02 \text{ TeV}$ and 5.44 TeV , respectively, measured as a function of p_T for the pseudorapidity range $|\eta| < 2.5$ and for five centrality intervals are shown in Figures 8 and 9, respectively. Both sets of A+A spectra are divided by the $\langle T_{\text{AA}} \rangle$ of the corresponding centrality intervals and are compared with the charged-hadron production pp cross-section in the same pseudorapidity range and at the same centre-of-mass energy as the corresponding A+A collisions.

The nuclear modification factor, defined by Eq. (1), quantifies the difference between HI and pp collisions. The difference is visible in all centrality intervals. Figure 10 shows the nuclear modification factor $R_{p\text{Pb}}$ in the centrality interval 0–90%. The $R_{p\text{Pb}}$ values exhibit only weak p_T dependence at $p_T > 4 \text{ GeV}$ and level off at a value $R_{p\text{Pb}} = 1.14^{+0.06}_{-0.08}$ (syst.); this is obtained by fitting a constant to the data points in this p_T range. Figure 11 shows the nuclear modification factors $R_{p\text{Pb}}$ for the same centrality intervals and y^* ranges as in the case of the charged-hadron spectra. In the central collisions, $R_{p\text{Pb}}$ rises up to $p_T \approx 3 \text{ GeV}$ where it has a local maximum. In the more peripheral collisions, the maximum vanishes. Above 3 GeV , the values of $R_{p\text{Pb}}$ in different centrality intervals converge and have very similar values at $p_T \approx 40 \text{ GeV}$. At higher momenta, $R_{p\text{Pb}}$ values from different centrality intervals follow different trends, but their values are consistent within the uncertainties.

Figures 12 and 13 show the nuclear modification factors R_{AA} in Pb+Pb and Xe+Xe collisions, respectively, for the same centrality intervals and $|\eta|$ ranges as in the case of the charged-hadron spectra. In both cases, the R_{AA} distributions have a characteristic shape seen previously [11–14, 19, 54, 55]; the modification is stronger in central collisions. First, R_{AA} increases to a local maximum at around 2 GeV , then it decreases to a local minimum at around 7 GeV , and then rises again. In Pb+Pb collisions at $p_T \approx 100 \text{ GeV}$, the slope of the distributions becomes smaller. At higher p_T , R_{AA} is consistent with a plateau with a magnitude between 0.6 for central collisions and 0.8 for peripheral collisions. No similar conclusion can be drawn

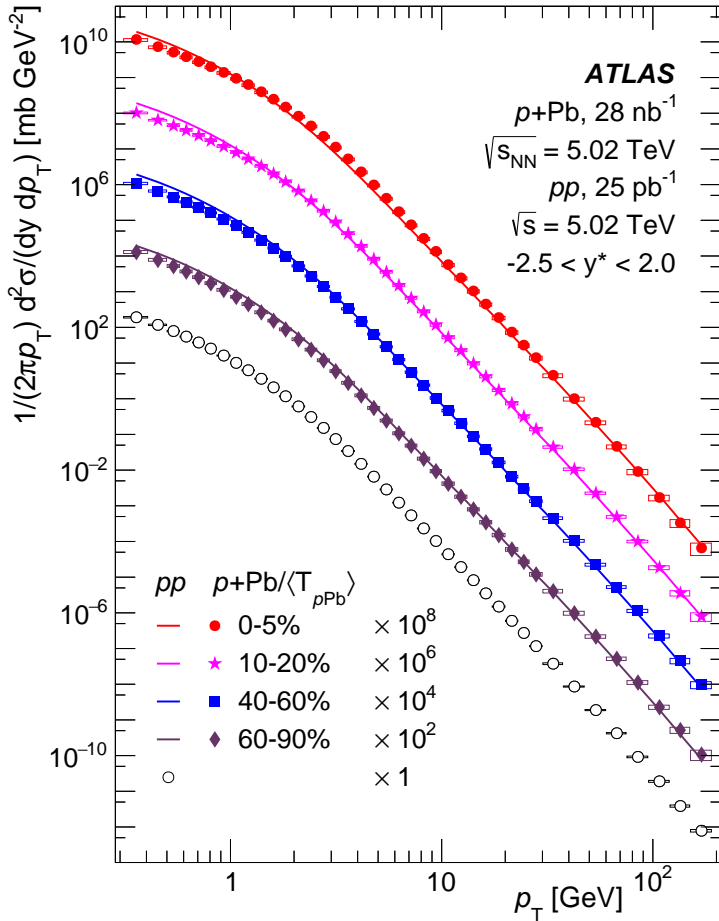


Figure 7: Charged-hadron spectra divided by the nuclear thickness function in $p+Pb$ collisions and the cross-section in pp collisions measured in the rapidity range $-2.5 < y^* < 2.0$ at $\sqrt{s_{NN}} = \sqrt{s} = 5.02$ TeV. Measurements in centrality intervals are scaled by powers of ten for clarity in the plot. Systematic uncertainties are shown with boxes; statistical uncertainties are smaller than the marker size. All the lines represent the same pp data, scaled by the same factor as the corresponding centrality interval.

for the Xe+Xe data above $p_T \approx 100$ GeV due to their lower integrated luminosity and, therefore, higher statistical uncertainty.

Figure 14 shows $R_{p\text{Pb}}$ as a function of rapidity in four p_T ranges. They correspond to low p_T where $R_{p\text{Pb}}$ is below unity ($0.66 < p_T < 0.76$ GeV), the local maximum for central collisions ($3.0 < p_T < 3.4$ GeV), and two ranges where $R_{p\text{Pb}}$ decreases towards unity ($7.7 < p_T < 8.8$ GeV and $15 < p_T < 17$ GeV). The asymmetry is present in the central collisions even for lower p_T ranges, but it only reveals its full magnitude at about 3 GeV. On the proton-going side, it is consistent with, or close to, unity; it shows an excess of up to a factor of ~ 2 on the Pb-going side, with fragmentation of Pb nuclei. With increasing centrality percentile and increasing p_T , the asymmetry diminishes. This is in agreement with previous observations [19].

Figures 15 and 16 show R_{AA} in Pb+Pb and Xe+Xe collisions, respectively, as a function of pseudorapidity in several p_T ranges corresponding to the local maximum ($1.7 < p_T < 2.0$ GeV), the minimum ($6.7 < p_T < 7.7$ GeV), the region of increasing R_{AA} ($20 < p_T < 23$ GeV), and the plateau ($60 < p_T < 95$ GeV; only for Pb+Pb). The values of R_{AA} show no strong dependence on η .

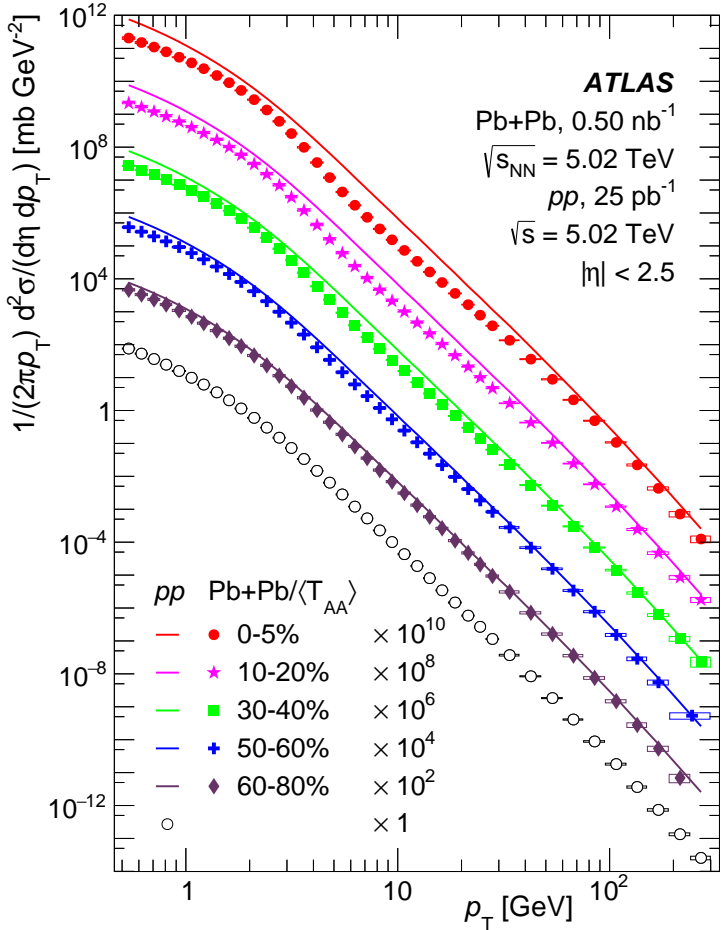


Figure 8: Charged-hadron spectra divided by the nuclear thickness function in Pb+Pb collisions and the cross-section in pp collisions measured in the pseudorapidity range $|\eta| < 2.5$ at $\sqrt{s_{NN}} = \sqrt{s} = 5.02$ TeV. Measurements in centrality intervals are scaled by powers of ten for clarity in the plot. Systematic uncertainties are shown with boxes; statistical uncertainties are smaller than the marker size. Any data point with more than 30% statistical uncertainty is not shown. All the lines represent the same pp data, scaled by the same factor as the corresponding centrality interval.

The nuclear modification factor R_{AA} measured in Pb+Pb and Xe+Xe collisions as a function of the mean number of participants $\langle N_{\text{part}} \rangle$ and the mean number of collisions $\langle N_{\text{coll}} \rangle$ in two momentum intervals is shown in Figures 17 and 18, respectively. These p_T intervals correspond to the local minimum in the region $6.7 < p_T < 7.7$ GeV, and to the interval where R_{AA} has an intermediate value, in the region $26 < p_T < 30$ GeV. In both momentum intervals, R_{AA} decreases in more central collisions; this decrease is stronger for the p_T range corresponding to the local minimum. Neither of the comparisons remove the dependency of R_{AA} on the collision system.

Comparisons of measurements from this analysis with the measurements of CMS [11, 13] and ALICE [12, 14] for p +Pb, Pb+Pb, and Xe+Xe collisions are shown in Figures 19, 20, and 21, respectively. For $R_{p\text{Pb}}$, the results of all three experiments generally agree with each other at lower p_T , within their uncertainties. The ALICE result is lower than ATLAS and CMS results at $p_T \gtrsim 10$ GeV. Nevertheless, the experiments do not report results in the same ranges of y^* . Considering the asymmetry of $R_{p\text{Pb}}$ in y^* , as seen in Figure 14,

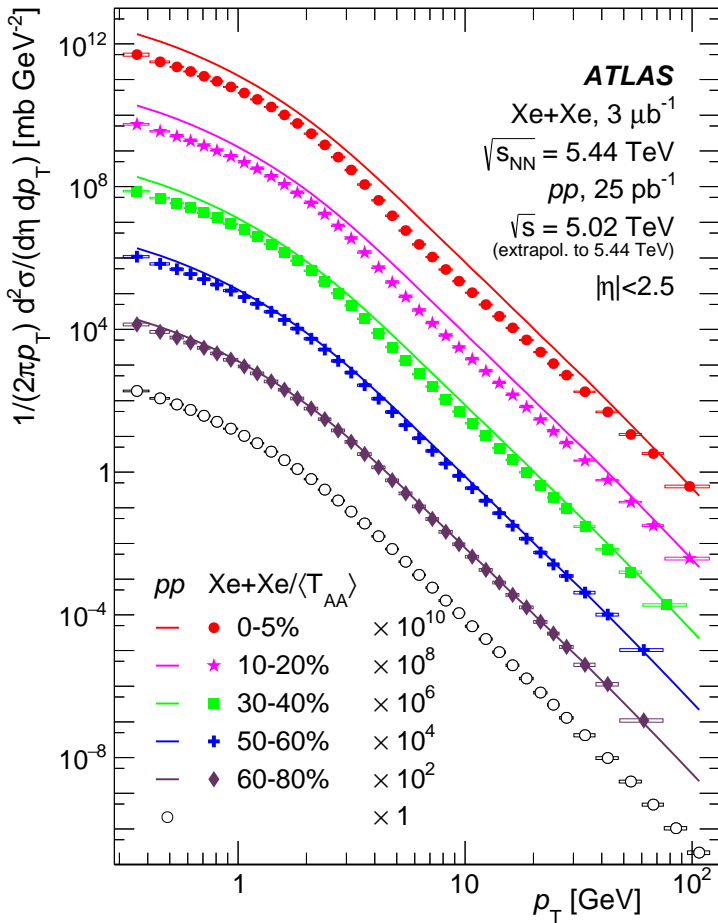


Figure 9: Charged-hadron spectra divided by the nuclear thickness function in Xe+Xe collisions measured in the pseudorapidity range $|\eta| < 2.5$ at $\sqrt{s_{NN}} = 5.44$ TeV. Measurements in centrality intervals are scaled by powers of ten for clarity in the plot. Also shown is the cross-section measured in pp collisions in the same pseudorapidity range and extrapolated to the same nucleon–nucleon centre-of-mass energy. Systematic uncertainties are shown with boxes; statistical uncertainties are smaller than the marker size. Any data point with more than 30% statistical uncertainty is not shown. All the lines represent the same pp data, scaled by the same factor as the corresponding centrality interval.

ALICE results would be expected to be somewhat lower than CMS results, and CMS results somewhat lower than ATLAS results. The differences should diminish at $p_T \approx 10$ GeV. The R_{AA} measured in Pb+Pb collisions by CMS at $p_T \gtrsim 60$ GeV is above the one measured by ATLAS. The discrepancy becomes larger at higher p_T . The ALICE results are consistent with ATLAS results within the range of the ALICE measurement. For Xe+Xe collisions, all three experiments are consistent. The systematic uncertainty in $\langle T_{AA} \rangle$ is often the largest among all systematic uncertainties. Although estimated independently by each collaboration, it is always fully correlated across the whole p_T region.

The measured distributions are also compared with several theoretical calculations. The models cover different dynamical ranges; the comparison is performed in the ranges provided by the authors of the models.

The Linear Boltzmann Transport (LBT) model [56, 57] uses linear Boltzmann equations to describe parton

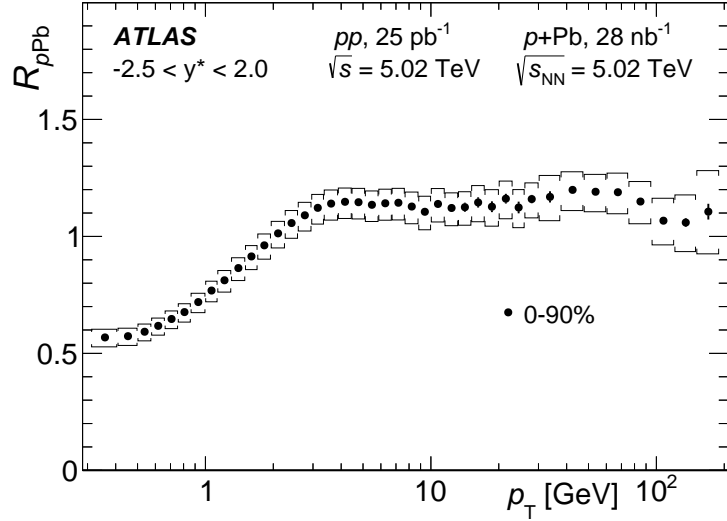


Figure 10: Charged-hadron nuclear modification factor $R_{p\text{Pb}}$ in the rapidity region $-2.5 < y^* < 2.0$. The markers show $R_{p\text{Pb}}$ for centrality interval 0–90%. Systematic uncertainties are shown with brackets; statistical uncertainties are shown with vertical lines.

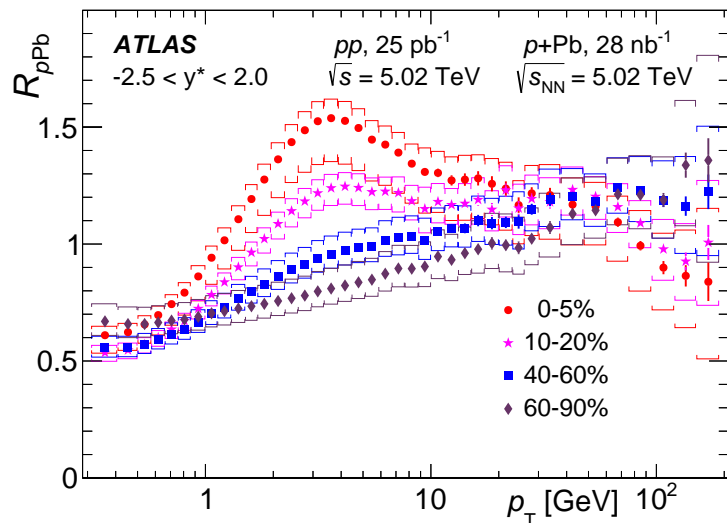


Figure 11: Charged-hadron nuclear modification factor $R_{p\text{Pb}}$ in the rapidity region $-2.5 < y^* < 2.0$. The full markers with different shapes show $R_{p\text{Pb}}$ for four different centralities. Systematic uncertainties are shown with brackets; statistical uncertainties are shown with vertical lines.

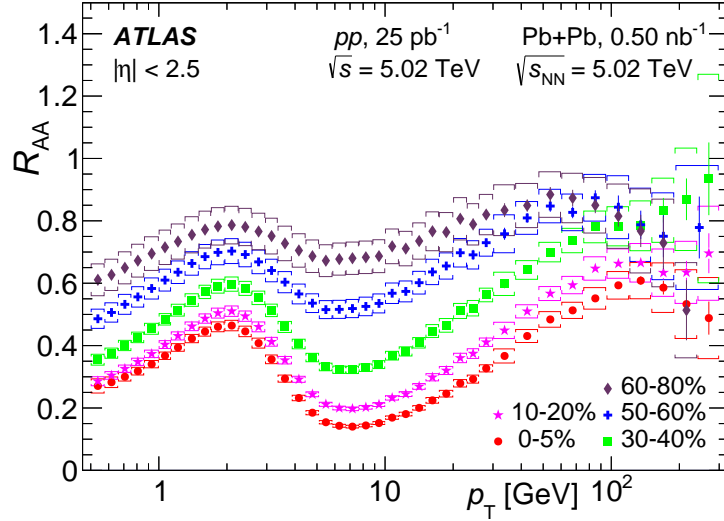


Figure 12: Charged-hadron nuclear modification factor R_{AA} for Pb+Pb collisions in the pseudorapidity region $|\eta| < 2.5$. Full markers with different shapes show R_{AA} for five different centralities. Systematic uncertainties are shown with brackets; statistical uncertainties are shown with vertical lines. Any data point with more than 30% statistical uncertainty is not shown.

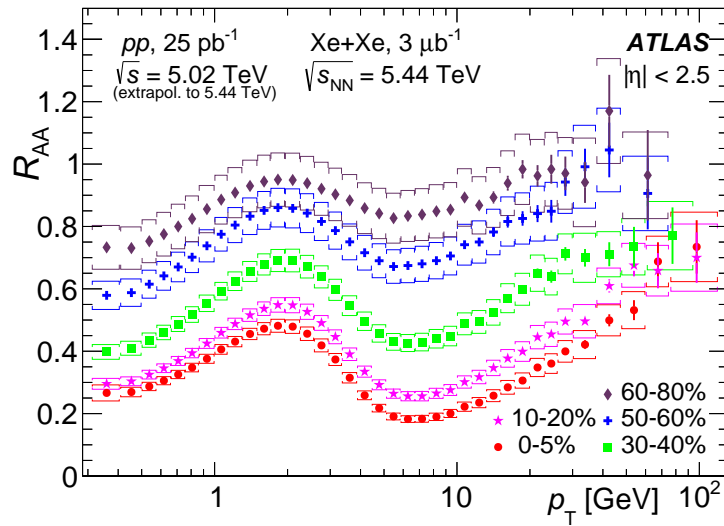


Figure 13: Charged-hadron nuclear modification factor R_{AA} for Xe+Xe collisions in the pseudorapidity region $|\eta| < 2.5$. Full markers with different shapes show R_{AA} for five different centralities. Systematic uncertainties are shown with brackets; statistical uncertainties are shown with vertical lines. Any data point with more than 30% statistical uncertainty is not shown.

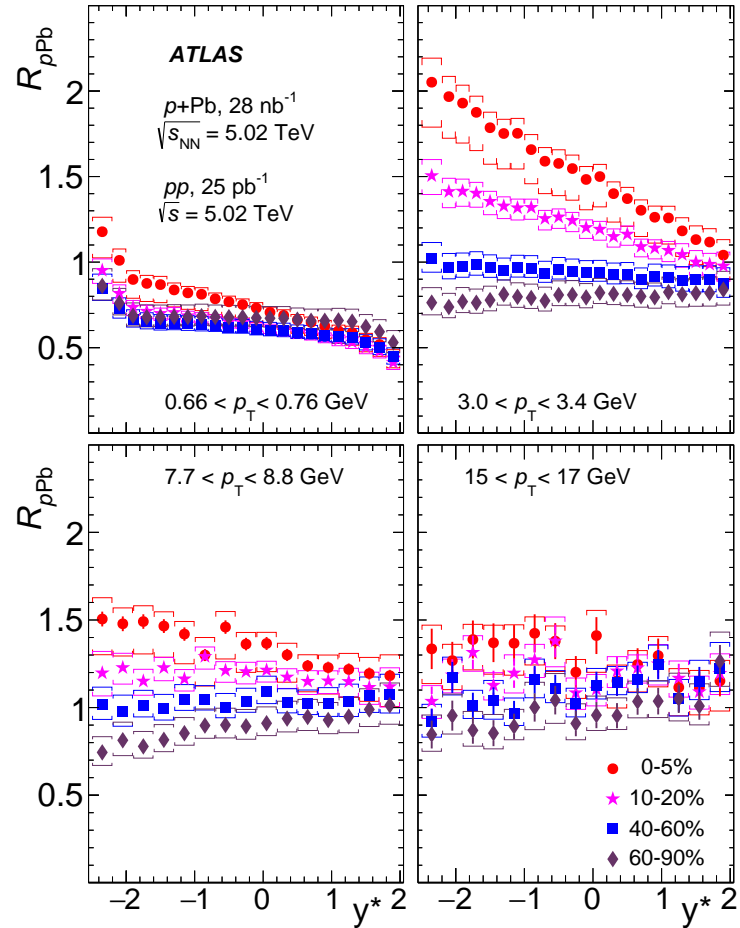


Figure 14: Charged-hadron nuclear modification factor $R_{p\text{Pb}}$ for $p+\text{Pb}$ collisions in four p_T regions. Full markers with different shapes show $R_{p\text{Pb}}$ for four different centralities. Systematic uncertainties are shown with brackets; statistical uncertainties are shown with vertical lines.

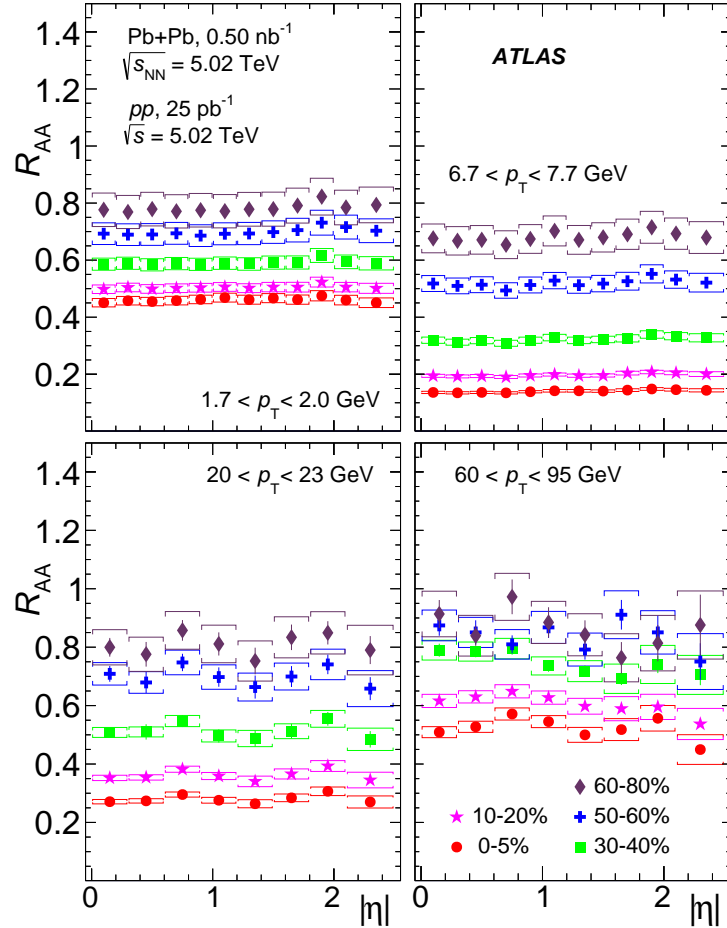


Figure 15: Charged-hadron nuclear modification factor R_{AA} for Pb+Pb collisions in four p_T regions. Full markers with different shapes show R_{AA} for five different centralities. Systematic uncertainties are shown with brackets; statistical uncertainties are shown with vertical lines.

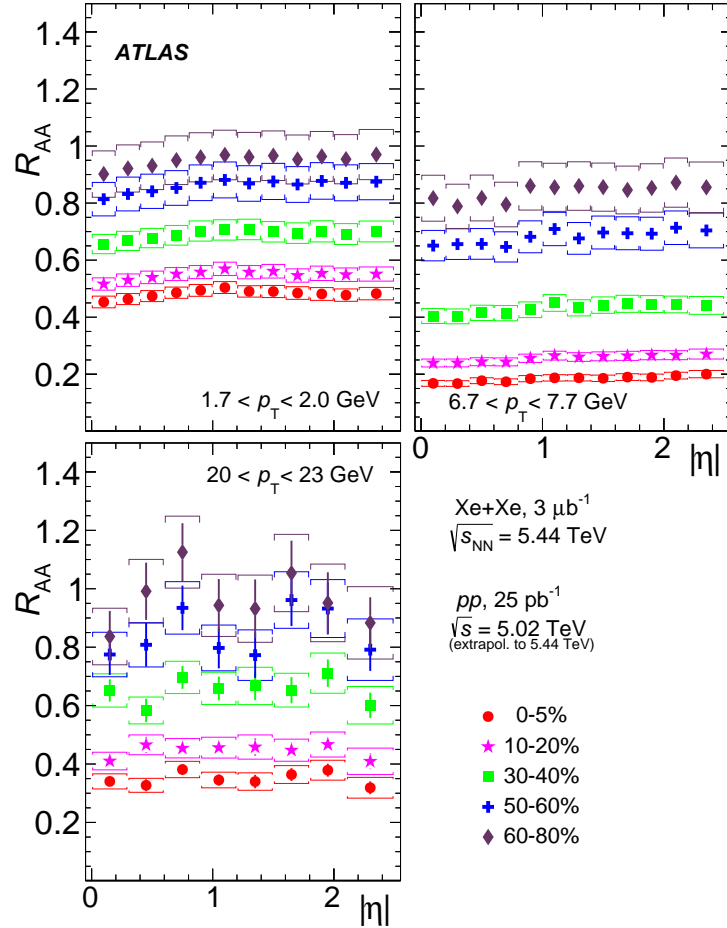


Figure 16: Charged-hadron nuclear modification factor R_{AA} for Xe+Xe collisions in three p_T regions. Full markers with different shapes show R_{AA} for five different centralities. Systematic uncertainties are shown with brackets; statistical uncertainties are shown with vertical lines.

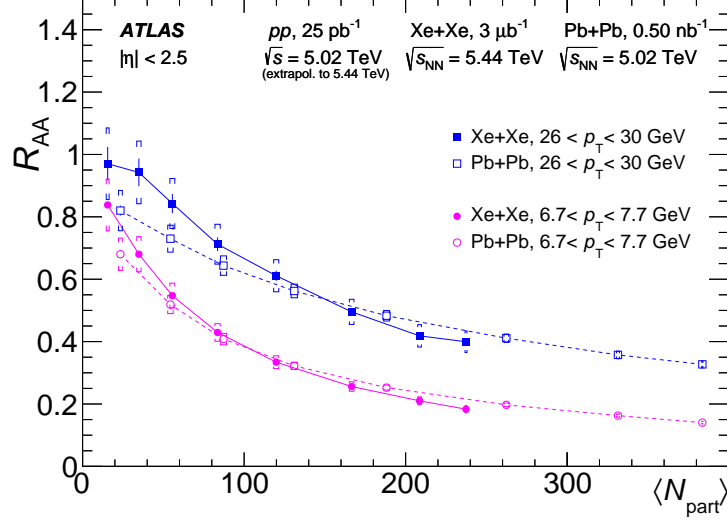


Figure 17: Nuclear modification factor R_{AA} as a function of $\langle N_{\text{part}} \rangle$ for selected ranges of p_T measured in Xe+Xe collisions (full markers) and in Pb+Pb collisions (open markers). Systematic uncertainties are shown with brackets; statistical uncertainties are shown with vertical lines. The horizontal widths of the brackets represent the systematic uncertainties in $\langle N_{\text{part}} \rangle$. The lines are to help guide the eye.

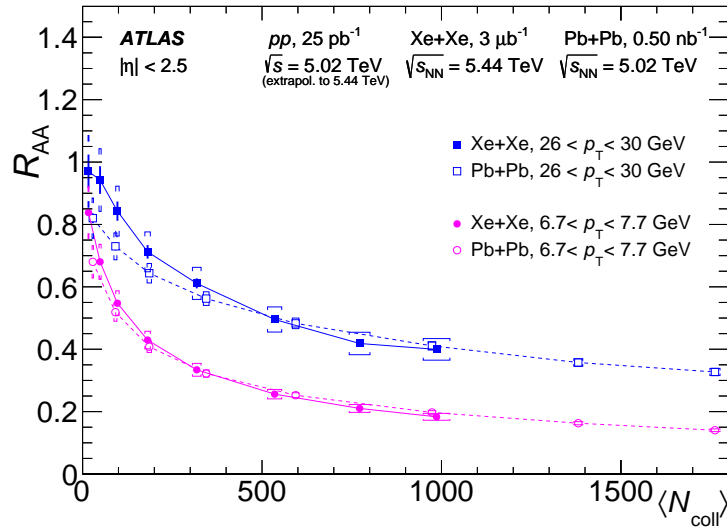


Figure 18: Nuclear modification factor R_{AA} as a function of $\langle N_{\text{coll}} \rangle$ for selected ranges of p_T measured in Xe+Xe collisions (full markers) and in Pb+Pb collisions (open markers). Systematic uncertainties are shown with brackets; statistical uncertainties are shown with vertical lines. The horizontal widths of the brackets represent the systematic uncertainties in $\langle N_{\text{coll}} \rangle$. The lines are to help guide the eye.

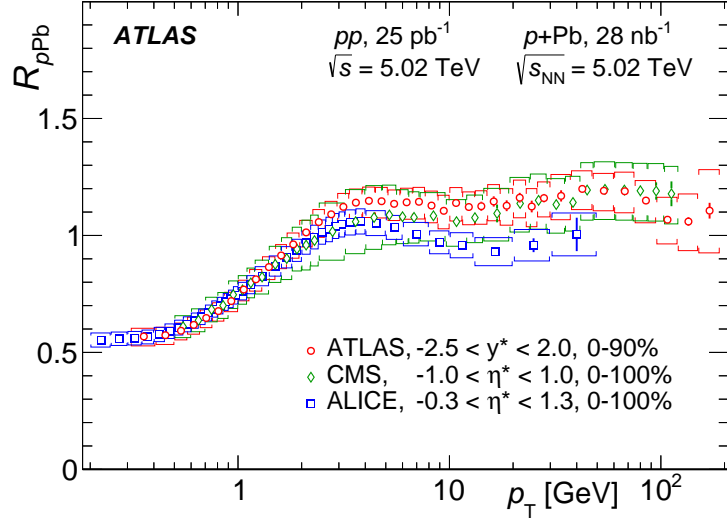


Figure 19: Charged-hadron nuclear modification factor $R_{p\text{Pb}}$ for $p+\text{Pb}$ collisions in the rapidity region $-2.5 < y^* < 2.0$ measured by ATLAS compared with results from CMS [11] and ALICE [12]. The centrality and (pseudo)rapidity intervals for CMS and ALICE data are different. Systematic uncertainties are shown with brackets; statistical uncertainties are shown with vertical lines.

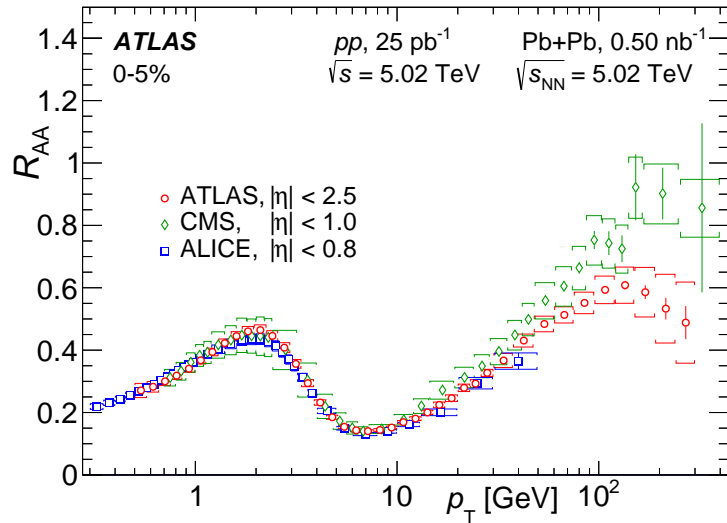


Figure 20: Charged-hadron nuclear modification factor R_{AA} for Pb+Pb collisions in the pseudorapidity region $|\eta| < 2.5$ measured by ATLAS compared with results from CMS [11] and ALICE [12]. Systematic uncertainties are shown with brackets; statistical uncertainties are shown with vertical lines.

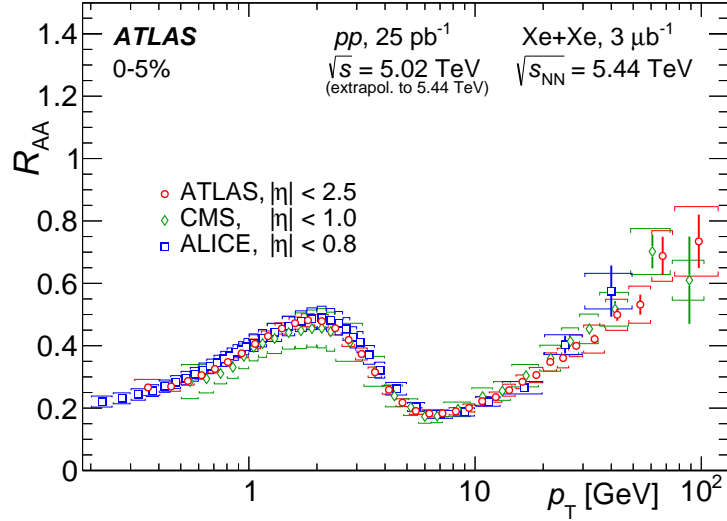


Figure 21: Charged-hadron nuclear modification factor R_{AA} for Xe+Xe collisions in the pseudorapidity region $|\eta| < 2.5$ measured by ATLAS compared with results from CMS [13] and ALICE [14]. Systematic uncertainties are shown with brackets; statistical uncertainties are shown with vertical lines.

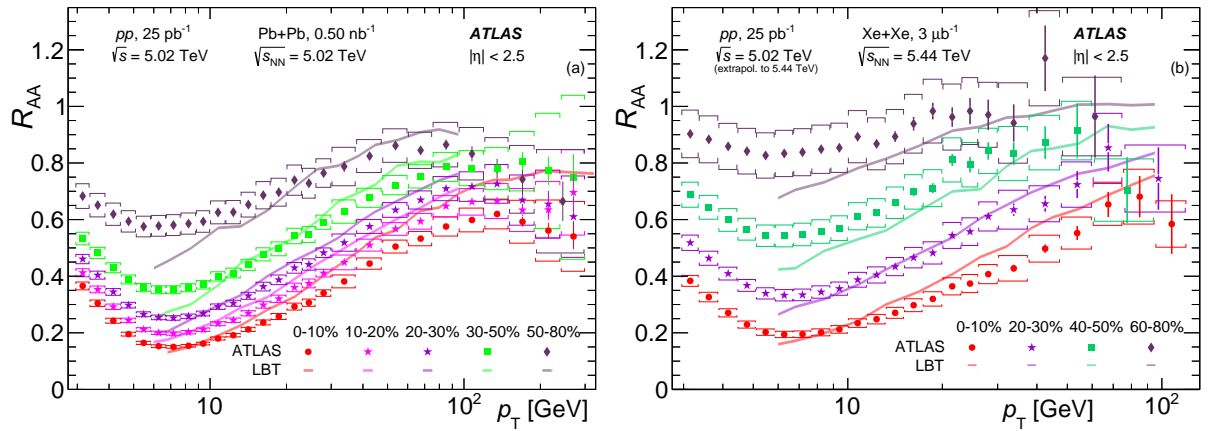


Figure 22: Charged-hadron nuclear modification factor R_{AA} for (a) Pb+Pb and (b) Xe+Xe collisions in the pseudorapidity region $|\eta| < 2.5$ measured by ATLAS compared with predictions of the LBT model [56, 57]. The width of the lines representing the model is chosen only for visibility; the model was not provided with any uncertainty.

transport in the QGP while considering 2→2 parton scattering. The rates of scattering in a medium follow relativistic hydrodynamic equations. A comparison of charged-hadron nuclear modification factors R_{AA} measured by ATLAS in Pb+Pb and Xe+Xe collisions with the LBT model predictions is shown in Figure 22. The model correctly describes the trends measured in the data, but has a somewhat shorter variational range, it overestimates the R_{AA} in the most central collisions in both the Pb+Pb and Xe+Xe systems, and underestimates it in the most peripheral Xe+Xe collisions.

The DREENA-B framework [58, 59] is based on Bjorken 1+1D medium evolution [60] that introduces different evolution scenarios before thermalization of the QGP and the same evolution after thermalization. It is also capable of describing charged-hadron R_{AA} and elliptic flow v_2 [61] at the same time. The model is compared with data in Figure 23. The model correctly describes Pb+Pb data for $p_T \gtrsim 8$ GeV, but predicts stronger suppression in peripheral Xe+Xe collisions than is measured in the data.

The CIBJET framework [62, 63] combines the bulk evolution calculated by the viscous hydrodynamic simulation VISHNU [64] with the high- p_T jet energy loss calculated in the CUJET model, which is a non-perturbative model integrating the suppression of chromo-electric degrees of freedom and emergence of the chromo-magnetic degrees of freedom. A comparison with the measured ATLAS data is shown in Figure 24. The CUJET model successfully describes R_{AA} in the entire Pb+Pb range of centrality intervals as well as in central Xe+Xe collisions, but it underestimates R_{AA} in peripheral Xe+Xe collisions. The VISHNU model correctly reproduces the R_{AA} distribution shape, but calculates values lower than the data at $p_T \gtrsim 2$ GeV.

The SCET_G model [65–67] uses soft-collinear effective theory, extends it to also include jet propagation in the QGP, and effectively describes in-medium parton shower formation. A comparison of the model predictions with data is shown in Figure 25. The model describes the R_{AA} values well in both collision systems and in almost the entire range of p_T . At very high p_T , the trend calculated by the model in the Pb+Pb system is different from the data.

The Higher Twist (HT) results [68, 69] obtained using the next-to-leading-order (NLO) parton model with higher-twist energy loss are shown in Figure 26. The HT model captures the shape of the R_{AA} distribution well in both systems across almost the entire p_T range of the prediction. In peripheral Pb+Pb collisions it predicts less suppression than is measured in data.

The model developed by Feal et al. [70] extracts the medium's parameter values with full resummation of scattering centres including the expected perturbative tails. The density of scattering centres qualitatively agrees with the QGP equation of state computed in lattice QCD. The predictions of the model are shown in Figure 27. It is not expected to describe R_{AA} distributions at lower p_T . At $8 \lesssim p_T \lesssim 80$ GeV, the model describes the data fairly accurately, although no predictions are available for peripheral collisions.

The HKMPSW model [71] has the BDMPS-Z formalism [72–74] as a starting point from which the probability distribution of parton energy loss in QGP is derived. A comparison with Pb+Pb, Xe+Xe, and p +Pb data is shown in Figure 28. For Pb+Pb and Xe+Xe collisions, the model describes the R_{AA} values in central and mid-central collisions in both systems well. In peripheral Pb+Pb collisions, the model predictions are above the R_{AA} values for the data. This model's prediction for $R_{p\text{Pb}}$ is also available. The shape appears nearly flat above 10 GeV, which is similar to the data, although lower than it.

In summary, the models generally describe the data between about 10 and 100 GeV well. Some difficulties arise in the most peripheral collisions, where agreement is worse for several models, although the data also has larger systematic uncertainties, driven by uncertainty associated with $\langle T_{AA} \rangle$. Above 100 GeV the ATLAS data show saturation in Pb+Pb collisions at values of about 0.6–0.8, depending on the centrality

interval. Some models show the same trend, but others keep rising, approaching unity. At high p_T , the accuracy of the measurements suffers from high systematic uncertainty and thus it is difficult to draw a definite conclusion.

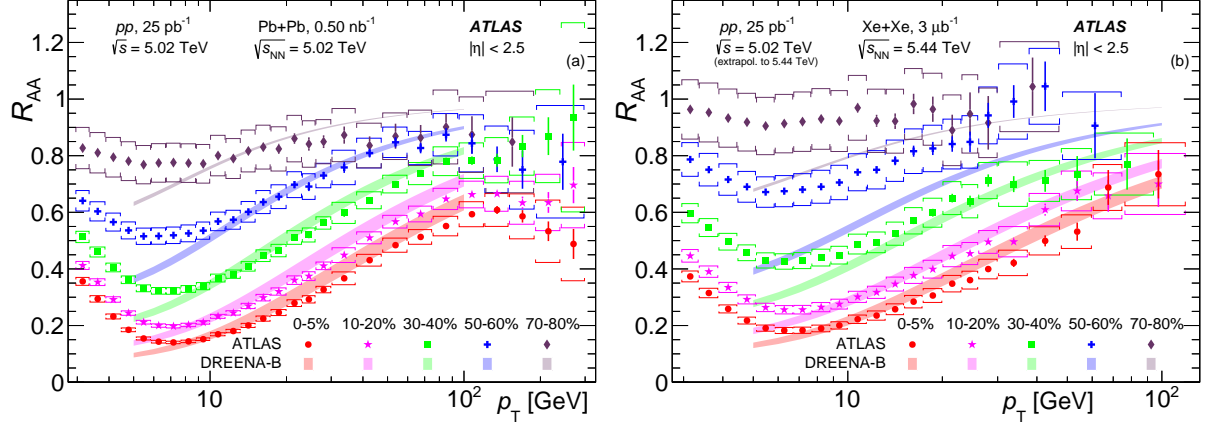


Figure 23: Charged-hadron nuclear modification factor R_{AA} for (a) $Pb+Pb$ and (b) $Xe+Xe$ collisions in the pseudorapidity region $|\eta| < 2.5$ measured by ATLAS compared with predictions of the DREENA-B model [58, 59]. The width of the model band represents the theoretical systematic uncertainty.

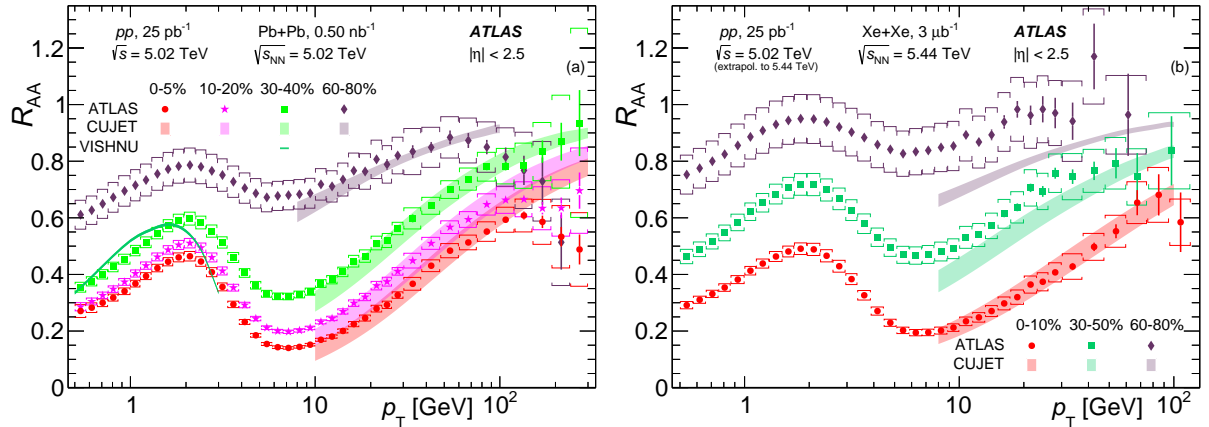


Figure 24: Charged-hadron nuclear modification factor R_{AA} for (a) $Pb+Pb$ and (b) $Xe+Xe$ collisions in the pseudorapidity region $|\eta| < 2.5$ measured by ATLAS compared with predictions of the CUJET [62, 63] and VISHNU [64] models. The width of the CUJET band represents the theoretical systematic uncertainty while the width of the VISHNU line is chosen only for visibility; the VISHNU model was not provided with any uncertainty.

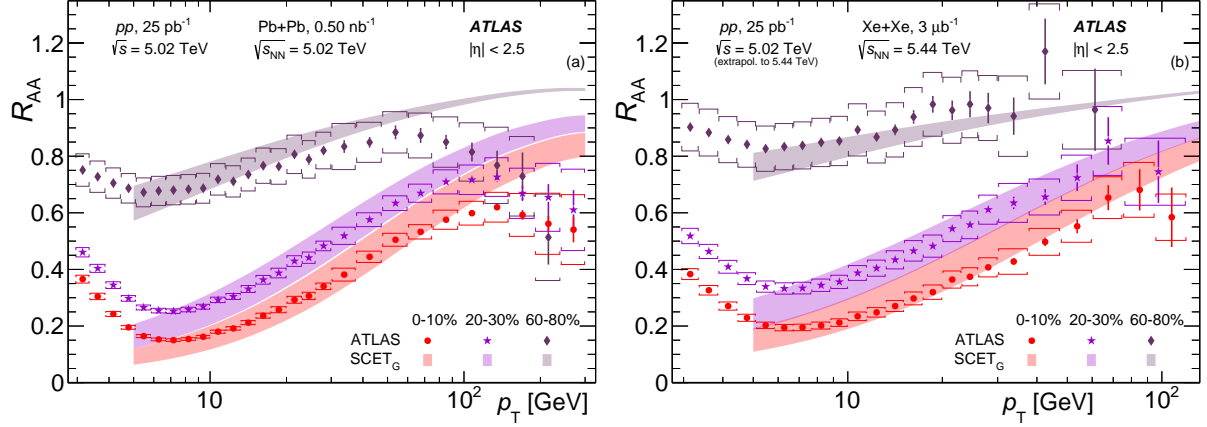


Figure 25: Charged-hadron nuclear modification factor R_{AA} for (a) Pb+Pb and (b) Xe+Xe collisions in the pseudorapidity region $|\eta| < 2.5$ measured by ATLAS compared with predictions of the SCET_G model [65–67]. The width of the model band represents the theoretical systematic uncertainty.

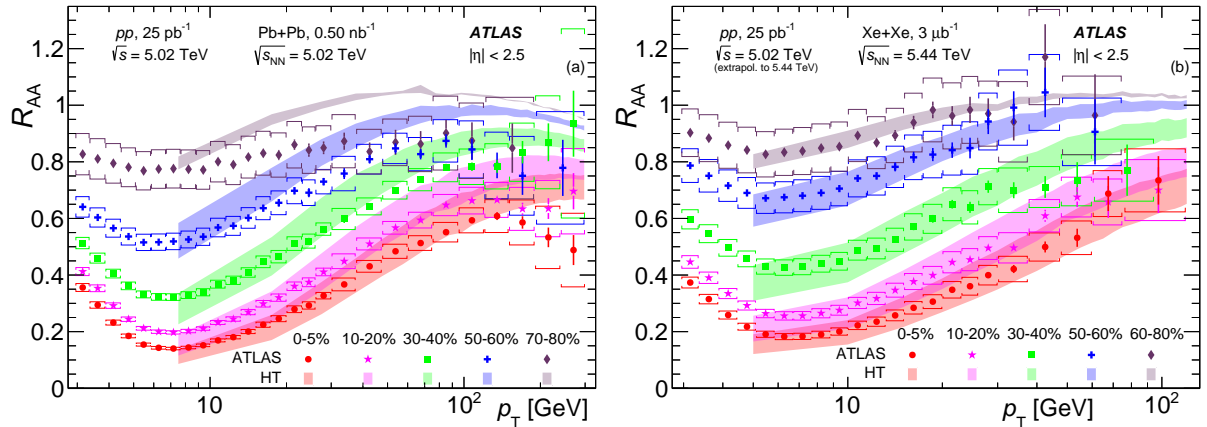


Figure 26: Charged-hadron nuclear modification factor R_{AA} for (a) Pb+Pb and (b) Xe+Xe collisions in the pseudorapidity region $|\eta| < 2.5$ measured by ATLAS compared with predictions of the HT model [68, 69]. The width of the model band represents the theoretical systematic uncertainty.

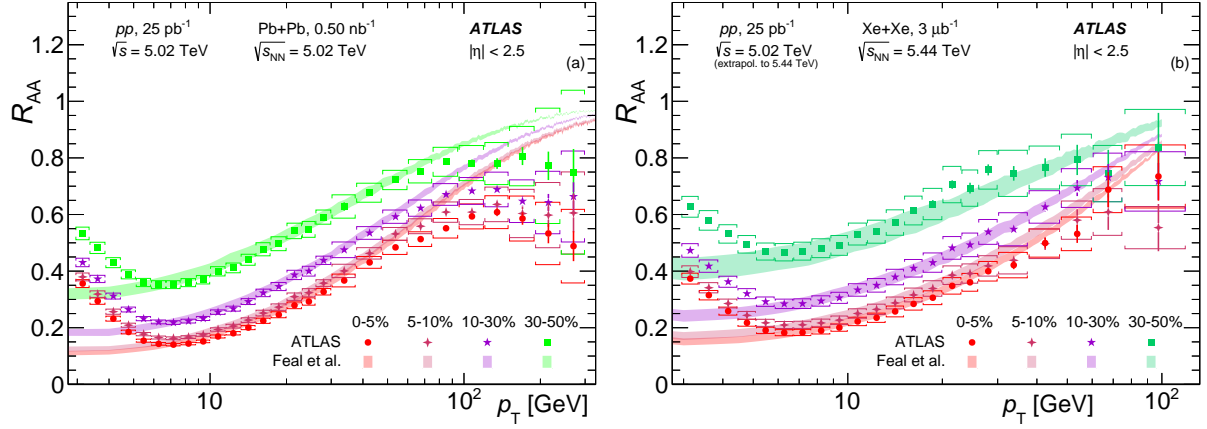


Figure 27: Charged-hadron nuclear modification factor R_{AA} for (a) Pb+Pb and (b) Xe+Xe collisions in the pseudorapidity region $|\eta| < 2.5$ measured by ATLAS compared with predictions of the model developed by Feal et al. [70]. The width of the model band represents the theoretical systematic uncertainty.

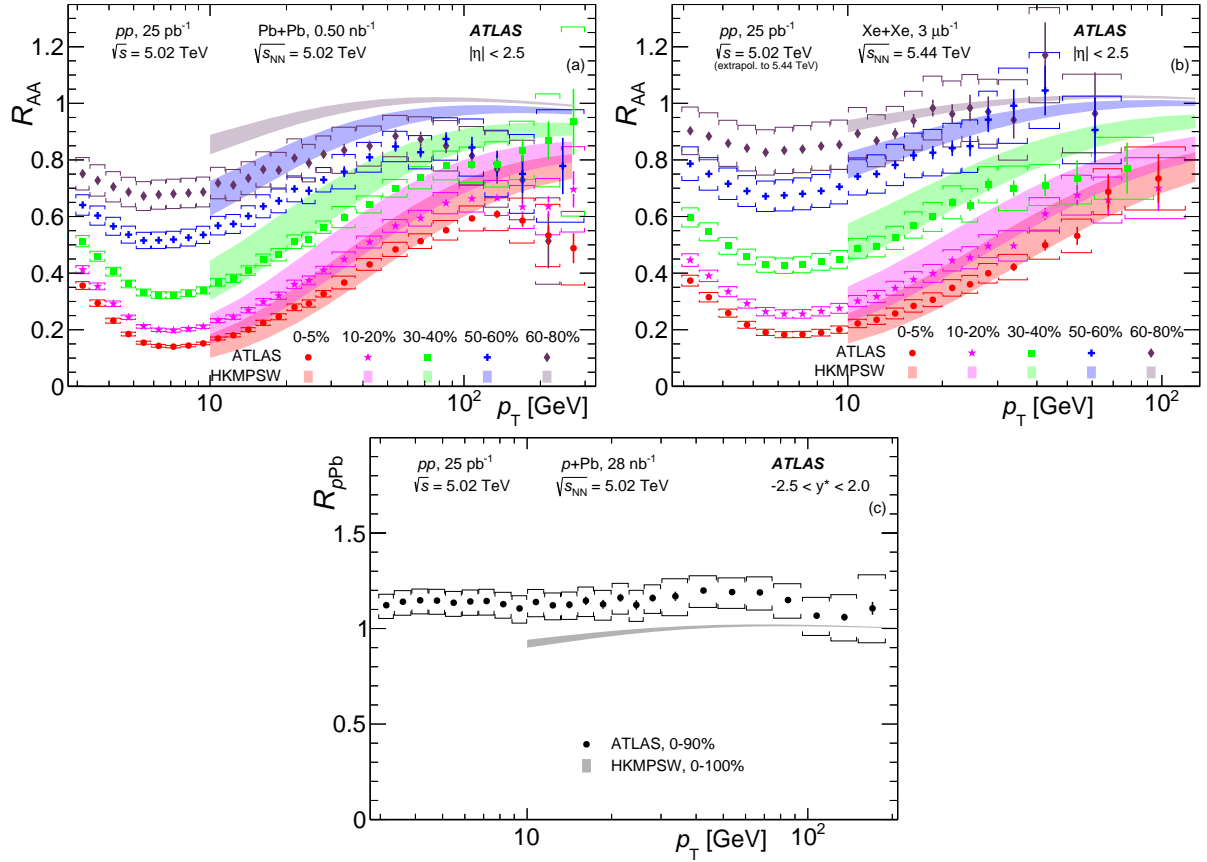


Figure 28: Charged-hadron nuclear modification factor R_{AA} for (a) Pb+Pb, (b) Xe+Xe, and (c) $p+Pb$ collisions in the pseudorapidity region $|\eta| < 2.5$ measured by ATLAS compared with predictions of the HKMPSW model [71]. The width of the model band represents the theoretical systematic uncertainty.

9 Conclusions

A precise measurement of inclusive charged-hadron production in all collision systems produced by the LHC at $\sqrt{s_{\text{NN}}} = 5.02$ or 5.44 TeV is presented by the ATLAS experiment in wide ranges of centrality, p_T and η (or y^*). The $p p$ data at $\sqrt{s} = 5.02$ TeV correspond to 28 pb^{-1} , the $p + \text{Pb}$ data at $\sqrt{s_{\text{NN}}} = 5.02$ TeV correspond to 25 nb^{-1} , the $\text{Pb} + \text{Pb}$ data at $\sqrt{s_{\text{NN}}} = 5.02$ TeV correspond to 0.50 nb^{-1} , and the $\text{Xe} + \text{Xe}$ data at $\sqrt{s_{\text{NN}}} = 5.44$ TeV correspond to $3 \mu\text{b}^{-1}$. These results extend similar ATLAS analyses of $\text{Pb} + \text{Pb}$ data at $\sqrt{s_{\text{NN}}} = 2.76$ TeV [10], and of $p + \text{Pb}$ data at $\sqrt{s_{\text{NN}}} = 5.02$ TeV [19].

In $p + \text{Pb}$ collisions, the nuclear modification factor $R_{p\text{Pb}}$ is not symmetric in rapidity, with more particles emitted in the Pb-going direction. This effect is most pronounced at low p_T and flattens out above 15 GeV. In the central collisions, a sharp local maximum at $p_T \approx 3$ GeV is followed by a decrease. As the collisions become more peripheral, the local maximum becomes less pronounced and wider. Above $p_T \approx 40$ GeV, the $R_{p\text{Pb}}$ values in different centrality intervals are consistent within their systematic uncertainties.

In $\text{Pb} + \text{Pb}$ and $\text{Xe} + \text{Xe}$ collisions, the nuclear modification factors, R_{AA} , show a characteristic shape observed previously: a local maximum at $p_T \approx 2$ GeV is followed by a decrease to a local minimum at $p_T \approx 7$ GeV and then a rise towards higher p_T . In $\text{Pb} + \text{Pb}$ collisions at around 100 GeV, the slope becomes smaller; no such conclusion is drawn for $\text{Xe} + \text{Xe}$ collisions because of the limited number of events. This shape is observed in all centrality intervals, but has its highest maximum-to-minimum ratio in the most central collisions. The suppression of charged-hadron production is also strongest in the most central collisions. At fixed p_T , the R_{AA} values have a very weak dependence on $|\eta|$.

The data presented here can provide comprehensive constraints on theoretical descriptions of soft and hard processes in the QGP in a variety of collision systems. Theoretical models typically describe R_{AA} better in central collisions and in the p_T range from 7–10 GeV to about 100 GeV. They tend to deviate from the data at higher p_T or in more peripheral collisions. Most of them do not attempt to describe low- p_T data.

Acknowledgements

We thank CERN for the very successful operation of the LHC, as well as the support staff from our institutions without whom ATLAS could not be operated efficiently.

We acknowledge the support of ANPCyT, Argentina; YerPhI, Armenia; ARC, Australia; BMWFW and FWF, Austria; ANAS, Azerbaijan; CNPq and FAPESP, Brazil; NSERC, NRC and CFI, Canada; CERN; ANID, Chile; CAS, MOST and NSFC, China; Minciencias, Colombia; MEYS CR, Czech Republic; DNRF and DNSRC, Denmark; IN2P3-CNRS and CEA-DRF/IRFU, France; SRNSFG, Georgia; BMBF, HGF and MPG, Germany; GSRI, Greece; RGC and Hong Kong SAR, China; ISF and Benoziyo Center, Israel; INFN, Italy; MEXT and JSPS, Japan; CNRST, Morocco; NWO, Netherlands; RCN, Norway; MEiN, Poland; FCT, Portugal; MNE/IFA, Romania; MESTD, Serbia; MSSR, Slovakia; ARRS and MIZŠ, Slovenia; DSI/NRF, South Africa; MICINN, Spain; SRC and Wallenberg Foundation, Sweden; SERI, SNSF and Cantons of Bern and Geneva, Switzerland; MOST, Taiwan; TENMAK, Türkiye; STFC, United Kingdom; DOE and NSF, United States of America. In addition, individual groups and members have received support from BCKDF, CANARIE, Compute Canada and CRC, Canada; PRIMUS 21/SCI/017 and UNCE SCI/013, Czech Republic; COST, ERC, ERDF, Horizon 2020 and Marie Skłodowska-Curie Actions, European Union; Investissements d’Avenir Labex, Investissements d’Avenir Idex and ANR, France; DFG and AvH Foundation, Germany; Herakleitos, Thales and Aristeia programmes co-financed by EU-ESF and the

Greek NSRF, Greece; BSF-NSF and MINERVA, Israel; Norwegian Financial Mechanism 2014–2021, Norway; NCN and NAWA, Poland; La Caixa Banking Foundation, CERCA Programme Generalitat de Catalunya and PROMETEO and GenT Programmes Generalitat Valenciana, Spain; Göran Gustafssons Stiftelse, Sweden; The Royal Society and Leverhulme Trust, United Kingdom.

The crucial computing support from all WLCG partners is acknowledged gratefully, in particular from CERN, the ATLAS Tier-1 facilities at TRIUMF (Canada), NDGF (Denmark, Norway, Sweden), CC-IN2P3 (France), KIT/GridKA (Germany), INFN-CNAF (Italy), NL-T1 (Netherlands), PIC (Spain), ASGC (Taiwan), RAL (UK) and BNL (USA), the Tier-2 facilities worldwide and large non-WLCG resource providers. Major contributors of computing resources are listed in Ref. [75].

References

- [1] G. Roland, K. Šafařík and P. Steinberg, *Heavy-ion collisions at the LHC*, *Prog. Part. Nucl. Phys.* **77** (2014) 70.
- [2] W. Busza, K. Rajagopal and W. van der Schee, *Heavy Ion Collisions: The Big Picture, and the Big Questions*, *Ann. Rev. Nucl. Part. Sci.* **68** (2018) 339, arXiv: [1802.04801](#) [hep-ph].
- [3] J. Berges, M. P. Heller, A. Mazeliauskas and R. Venugopalan, *QCD thermalization: Ab initio approaches and interdisciplinary connections*, *Rev. Mod. Phys.* **93** (2021) 035003, arXiv: [2005.12299](#) [hep-th].
- [4] ATLAS Collaboration, *Measurement of jet p_T correlations in Pb+Pb and pp collisions at $\sqrt{s_{NN}} = 2.76 \text{ TeV}$ with the ATLAS detector*, *Phys. Lett. B* **774** (2017) 379, arXiv: [1706.09363](#) [hep-ex].
- [5] CMS Collaboration, *Jet momentum dependence of jet quenching in PbPb collisions at $\sqrt{s_{NN}} = 2.76 \text{ TeV}$* , *Phys. Lett. B* **712** (2012) 176, arXiv: [1202.5022](#) [hep-ex].
- [6] ATLAS Collaboration, *Measurement of the nuclear modification factor for inclusive jets in Pb+Pb collisions at $\sqrt{s_{NN}} = 5.02 \text{ TeV}$ with the ATLAS detector*, *Phys. Lett. B* **790** (2019) 108, arXiv: [1805.05635](#) [hep-ex].
- [7] ALICE Collaboration, *Measurements of inclusive jet spectra in pp and central Pb-Pb collisions at $\sqrt{s_{NN}} = 5.02 \text{ TeV}$* , *Phys. Rev. C* **101** (2020) 034911, arXiv: [1909.09718](#) [nucl-ex].
- [8] CMS Collaboration, *First measurement of large area jet transverse momentum spectra in heavy-ion collisions*, *JHEP* **05** (2021) 284, arXiv: [2102.13080](#) [hep-ex].
- [9] ATLAS Collaboration, *Measurement of jet fragmentation in Pb+Pb and pp collisions at $\sqrt{s_{NN}} = 5.02 \text{ TeV}$ with the ATLAS detector*, *Phys. Rev. C* **98** (2018) 024908, arXiv: [1805.05424](#) [hep-ex].
- [10] ATLAS Collaboration, *Measurement of charged-particle spectra in Pb+Pb collisions at $\sqrt{s_{NN}} = 2.76 \text{ TeV}$ with the ATLAS detector at the LHC*, *JHEP* **09** (2015) 050, arXiv: [1504.04337](#) [hep-ex].

- [11] CMS Collaboration, *Charged-particle nuclear modification factors in PbPb and pPb collisions at $\sqrt{s_{NN}} = 5.02 \text{ TeV}$* , *JHEP* **04** (2017) 039, arXiv: [1611.01664 \[hep-ex\]](https://arxiv.org/abs/1611.01664).
- [12] ALICE Collaboration, *Transverse momentum spectra and nuclear modification factors of charged particles in pp, p-Pb and Pb-Pb collisions at the LHC*, *JHEP* **11** (2018) 013, arXiv: [1802.09145 \[nucl-ex\]](https://arxiv.org/abs/1802.09145).
- [13] CMS Collaboration, *Charged-particle nuclear modification factors in XeXe collisions at $\sqrt{s_{NN}} = 5.44 \text{ TeV}$* , *JHEP* **10** (2018) 138, arXiv: [1809.00201 \[hep-ex\]](https://arxiv.org/abs/1809.00201).
- [14] ALICE Collaboration, *Transverse momentum spectra and nuclear modification factors of charged particles in Xe-Xe collisions at $\sqrt{s_{NN}} = 5.44 \text{ TeV}$* , *Phys. Lett. B* **788** (2019) 166, arXiv: [1805.04399 \[nucl-ex\]](https://arxiv.org/abs/1805.04399).
- [15] G.-Y. Qin, H. Petersen, S. A. Bass and B. Müller, *Translation of collision geometry fluctuations into momentum anisotropies in relativistic heavy-ion collisions*, *Phys. Rev. C* **82** (2010) 064903, arXiv: [1009.1847 \[nucl-th\]](https://arxiv.org/abs/1009.1847).
- [16] S. Ryu et al., *Importance of the Bulk Viscosity of QCD in Ultrarelativistic Heavy-Ion Collisions*, *Phys. Rev. Lett.* **115** (2015) 132301, arXiv: [1502.01675 \[nucl-th\]](https://arxiv.org/abs/1502.01675).
- [17] C. A. Salgado et al., *Proton–nucleus collisions at the LHC: scientific opportunities and requirements*, *J. Phys. G* **39** (2012) 015010, arXiv: [1105.3919 \[hep-ph\]](https://arxiv.org/abs/1105.3919).
- [18] Z.-B. Kang, I. Vitev and H. Xing, *Effects of cold nuclear matter energy loss on inclusive jet production in p+A collisions at energies available at the BNL Relativistic Heavy Ion Collider and the CERN Large Hadron Collider*, *Phys. Rev. C* **92** (2015) 054911, arXiv: [1507.05987 \[hep-ph\]](https://arxiv.org/abs/1507.05987).
- [19] ATLAS Collaboration, *Transverse momentum, rapidity, and centrality dependence of inclusive charged-particle production in $\sqrt{s_{NN}} = 5.02 \text{ TeV}$ p+Pb collisions measured by the ATLAS experiment*, *Phys. Lett. B* **763** (2016) 313, arXiv: [1605.06436 \[hep-ex\]](https://arxiv.org/abs/1605.06436).
- [20] M. L. Miller, K. Reygers, S. J. Sanders and P. Steinberg, *Glauber Modeling in High-Energy Nuclear Collisions*, *Ann. Rev. Nucl. Part. Sci.* **57** (2007) 205, arXiv: [nucl-ex/0701025](https://arxiv.org/abs/nucl-ex/0701025).
- [21] PHENIX Collaboration, *Centrality dependence of charged hadron production in deuteron+gold and nucleon+gold collisions at $\sqrt{s_{NN}} = 200 \text{ GeV}$* , *Phys. Rev. C* **77** (2008) 014905, arXiv: [0708.2416 \[nucl-ex\]](https://arxiv.org/abs/0708.2416).
- [22] ATLAS Collaboration, *The ATLAS Experiment at the CERN Large Hadron Collider*, *JINST* **3** (2008) S08003.
- [23] ATLAS Collaboration, *ATLAS Insertable B-Layer Technical Design Report*, ATLAS-TDR-19; CERN-LHCC-2010-013, 2010, URL: <https://cds.cern.ch/record/1291633>, Addendum: ATLAS-TDR-19-ADD-1; CERN-LHCC-2012-009, 2012, URL: <https://cds.cern.ch/record/1451888>.
- [24] B. Abbott et al., *Production and integration of the ATLAS Insertable B-Layer*, *JINST* **13** (2018) T05008, arXiv: [1803.00844 \[physics.ins-det\]](https://arxiv.org/abs/1803.00844).

- [25] ATLAS Collaboration, *Performance of the ATLAS trigger system in 2015*, Eur. Phys. J. C **77** (2017) 317, arXiv: [1611.09661 \[hep-ex\]](#).
- [26] ATLAS Collaboration, *The ATLAS Collaboration Software and Firmware*, ATL-SOFT-PUB-2021-001, 2021, URL: <https://cds.cern.ch/record/2767187>.
- [27] M. Cacciari, G. P. Salam and G. Soyez, *The anti- k_t jet clustering algorithm*, JHEP **04** (2008) 063, arXiv: [0802.1189 \[hep-ph\]](#).
- [28] M. Cacciari, G. P. Salam and G. Soyez, *FastJet user manual*, Eur. Phys. J. C **72** (2012) 1896, arXiv: [1111.6097 \[hep-ph\]](#).
- [29] ATLAS Collaboration, *Measurement of jet fragmentation in 5.02 TeV proton–lead and proton–proton collisions with the ATLAS detector*, Nucl. Phys. A **978** (2018) 65, arXiv: [1706.02859 \[hep-ex\]](#).
- [30] ATLAS Collaboration, *Centrality and rapidity dependence of inclusive jet production in $\sqrt{s_{NN}} = 5.02$ TeV proton–lead collisions with the ATLAS detector*, Phys. Lett. B **748** (2015) 392, arXiv: [1412.4092 \[hep-ex\]](#).
- [31] CMS Collaboration, *Studies of dijet transverse momentum balance and pseudorapidity distributions in pPb collisions at $\sqrt{s_{NN}} = 5.02$ TeV*, Eur. Phys. J. C **74** (2014) 2951, arXiv: [1401.4433 \[hep-ex\]](#).
- [32] ALICE Collaboration, *Transverse momentum dependence of inclusive primary charged-particle production in p–Pb collisions at $\sqrt{s_{NN}} = 5.02$ TeV*, Eur. Phys. J. C **74** (2014) 3054, arXiv: [1405.2737 \[nucl-ex\]](#).
- [33] T. Sjöstrand et al., *An introduction to PYTHIA 8.2*, Comput. Phys. Commun. **191** (2015) 159, arXiv: [1410.3012](#).
- [34] R. D. Ball et al., *Parton distributions with LHC data*, Nucl. Phys. B **867** (2013) 244, arXiv: [1207.1303 \[hep-ph\]](#).
- [35] ATLAS Collaboration, *ATLAS Pythia 8 tunes to 7 TeV data*, ATL-PHYS-PUB-2014-021, 2014, URL: <https://cds.cern.ch/record/1966419>.
- [36] X.-N. Wang and M. Gyulassy, *hijing: A Monte Carlo model for multiple jet production in pp, pA, and AA collisions*, Phys. Rev. D **44** (11 1991) 3501.
- [37] ATLAS Collaboration, *The ATLAS Simulation Infrastructure*, Eur. Phys. J. C **70** (2010) 823, arXiv: [1005.4568 \[physics.ins-det\]](#).
- [38] S. Agostinelli et al., *GEANT4 — a simulation toolkit*, Nucl. Instrum. Meth. A **506** (2003) 250.
- [39] ATLAS Collaboration, *Performance of the ATLAS track reconstruction algorithms in dense environments in LHC Run 2*, Eur. Phys. J. C **77** (2017) 673, arXiv: [1704.07983 \[hep-ex\]](#).
- [40] ALICE Collaboration, *Production of charged pions, kaons, and (anti-)protons in Pb-Pb and inelastic pp collisions at $\sqrt{s_{NN}} = 5.02$ TeV*, Phys. Rev. C **101** (2020) 044907, arXiv: [1910.07678 \[nucl-ex\]](#).
- [41] ALICE Collaboration, *Multiplicity dependence of charged pion, kaon, and (anti)proton production at large transverse momentum in p-Pb collisions at $\sqrt{s_{NN}} = 5.02$ TeV*, Phys. Lett. B **760** (2016) 720, arXiv: [1601.03658 \[nucl-ex\]](#).

- [42] F. Grassi, Y. Hama, T. Kodama and O. Socolowski Jr., *Particle abundances and spectra in the hydrodynamical description of relativistic nuclear collisions with light projectiles*, *J. Phys. G* **30** (2004) 853, arXiv: [hep-ph/0307306](#).
- [43] A. Andronic, P. Braun-Munzinger, K. Redlich and J. Stachel, *Decoding the phase structure of QCD via particle production at high energy*, *Nature* **561** (2018) 321, arXiv: [1710.09425 \[nucl-th\]](#).
- [44] ATLAS Collaboration, *Measurement of longitudinal flow decorrelations in Pb+Pb collisions at $\sqrt{s_{NN}} = 2.76$ and 5.02 TeV with the ATLAS detector*, *Eur. Phys. J. C* **78** (2018) 142, arXiv: [1709.02301 \[hep-ex\]](#).
- [45] ATLAS Collaboration, *Measurement of the azimuthal anisotropy of charged-particle production in Xe+Xe collisions at $\sqrt{s_{NN}} = 5.44$ TeV with the ATLAS detector*, *Phys. Rev. C* **101** (2020) 024906, arXiv: [1911.04812 \[hep-ex\]](#).
- [46] C. Loizides, J. Kamin and D. d'Enterria, *Improved Monte Carlo Glauber predictions at present and future nuclear colliders*, *Phys. Rev. C* **97** (2018) 054910, arXiv: [1710.07098 \[nucl-ex\]](#), Erratum: *Phys. Rev. C* **99** (2018) 019901.
- [47] ATLAS Collaboration, *Measurement of W^\pm boson production in Pb+Pb collisions at $\sqrt{s_{NN}} = 5.02$ TeV with the ATLAS detector*, *Eur. Phys. J. C* **79** (2019) 935, arXiv: [1907.10414 \[hep-ex\]](#).
- [48] ATLAS Collaboration, *Charged-particle multiplicities in pp interactions measured with the ATLAS detector at the LHC*, *New J. Phys.* **13** (2011) 053033, arXiv: [1012.5104 \[hep-ex\]](#).
- [49] ATLAS Collaboration, *Charged-particle distributions in $\sqrt{s} = 13$ TeV pp interactions measured with the ATLAS detector at the LHC*, *Phys. Lett. B* **758** (2016) 67, arXiv: [1602.01633 \[hep-ex\]](#).
- [50] ATLAS Collaboration, *Early Inner Detector Tracking Performance in the 2015 Data at $\sqrt{s} = 13$ TeV*, ATL-PHYS-PUB-2015-051, 2015, URL: <https://cds.cern.ch/record/2110140>.
- [51] G. D'Agostini, *A multidimensional unfolding method based on Bayes' theorem*, *Nucl. Instrum. Methods Phys. Res. A* **362** (1995) 487, ISSN: 0168-9002.
- [52] ALICE Collaboration, *Multi-strange baryon production at mid-rapidity in Pb-Pb collisions at $\sqrt{s_{NN}} = 2.76$ TeV*, *Phys. Lett. B* **728** (2014) 216, arXiv: [1307.5543 \[nucl-ex\]](#), Erratum: *Phys. Lett. B* **734** (2014) 409.
- [53] ATLAS Collaboration, *Luminosity determination in pp collisions at $\sqrt{s} = 8$ TeV using the ATLAS detector at the LHC*, *Eur. Phys. J. C* **76** (2016) 653, arXiv: [1608.03953 \[hep-ex\]](#).
- [54] CMS Collaboration, *Study of high- p_T charged particle suppression in PbPb compared to pp collisions at $\sqrt{s_{NN}} = 2.76$ TeV*, *Eur. Phys. J. C* **72** (2012) 1945, arXiv: [1202.2554 \[hep-ex\]](#).
- [55] ALICE Collaboration, *Centrality dependence of charged particle production at large transverse momentum in Pb-Pb collisions at $\sqrt{s_{NN}} = 2.76$ TeV*, *Phys. Lett. B* **720** (2013) 52, arXiv: [1208.2711 \[hep-ex\]](#).

- [56] Y. He, T. Luo, X.-N. Wang and Y. Zhu, *Linear Boltzmann transport for jet propagation in the quark-gluon plasma: Elastic processes and medium recoil*, [Phys. Rev. C **91** \(2015\) 054908](#), arXiv: [1503.03313 \[nucl-th\]](#), Erratum: [Phys. Rev. C **97** \(2018\) 019902](#).
- [57] S. Cao, T. Luo, G.-Y. Qin and X.-N. Wang, *Heavy and light flavor jet quenching at RHIC and LHC energies*, [Phys. Lett. B **777** \(2018\) 255](#), arXiv: [1703.00822 \[nucl-th\]](#).
- [58] D. Zicic, B. Ilic, M. Djordjevic and M. Djordjevic, *Exploring the initial stages in heavy-ion collisions with high- p_\perp theory and data*, [Phys. Rev. C **101** \(2020\) 064909](#), arXiv: [1908.11866 \[hep-ph\]](#).
- [59] D. Zicic, I. Salom, J. Auvinen, M. Djordjevic and M. Djordjevic, *DREENA-B framework: First predictions of R_{AA} and v_2 within dynamical energy loss formalism in evolving QCD medium*, [Phys. Lett. B **791** \(2019\) 236](#), arXiv: [1805.04786 \[nucl-th\]](#).
- [60] J. D. Bjorken, *Highly relativistic nucleus-nucleus collisions: The central rapidity region*, [Phys. Rev. D **27** \(1983\) 140](#).
- [61] U. Heinz and R. Snellings, *Collective Flow and Viscosity in Relativistic Heavy-Ion Collisions*, [Ann. Rev. Nucl. Part. Sci. **63** \(2013\) 123](#), arXiv: [1301.2826 \[nucl-th\]](#).
- [62] S. Shi, J. Liao and M. Gyulassy, *Probing the color structure of the perfect QCD fluids via soft-hard-event-by-event azimuthal correlations*, [Chin. Phys. C **42** \(2018\) 104104](#), arXiv: [1804.01915 \[hep-ph\]](#).
- [63] S. Shi, J. Liao and M. Gyulassy, *Global constraints from RHIC and LHC on transport properties of QCD fluids in CUJET/CIBJET framework*, [Chin. Phys. C **43** \(2019\) 044101](#), arXiv: [1808.05461 \[hep-ph\]](#).
- [64] C. Shen et al., *The iEBE-VISHNU code package for relativistic heavy-ion collisions*, [Comput. Phys. Commun. **199** \(2016\) 61](#), arXiv: [1409.8164 \[nucl-th\]](#).
- [65] Y.-T. Chien, A. Emerman, Z.-B. Kang, G. Ovanesyan and I. Vitev, *Jet quenching from QCD evolution*, [Phys. Rev. D **93** \(2016\) 074030](#), arXiv: [1509.02936 \[hep-ph\]](#).
- [66] H. T. Li and I. Vitev, *Inverting the mass hierarchy of jet quenching effects with prompt b-jet substructure*, [Phys. Lett. B **793** \(2019\) 259](#), arXiv: [1801.00008 \[hep-ph\]](#).
- [67] H. T. Li and I. Vitev, *Inclusive heavy flavor jet production with semi-inclusive jet functions: from proton to heavy-ion collisions*, [JHEP **07** \(2019\) 148](#), arXiv: [1811.07905 \[hep-ph\]](#).
- [68] H. Zhang, J. F. Owens, E. Wang and X.-N. Wang, *Dihadron Tomography of High-Energy Nuclear Collisions in Next-to-Leading Order Perturbative QCD*, [Phys. Rev. Lett. **98** \(2007\) 212301](#), arXiv: [nucl-th/0701045](#).
- [69] H. Zhang, J. F. Owens, E. Wang and X.-N. Wang, *Tomography of High-Energy Nuclear Collisions with Photon-Hadron Correlations*, [Phys. Rev. Lett. **103** \(2009\) 032302](#), arXiv: [0902.4000 \[nucl-th\]](#).
- [70] X. Feal, C. A. Salgado and R. A. Vazquez, *Jet quenching test of the QCD matter created at RHIC and the LHC needs opacity-resummed medium induced radiation*, [Phys. Lett. B **816** \(2021\) 136251](#), arXiv: [1911.01309 \[hep-ph\]](#).

- [71] A. Huss et al., *Predicting parton energy loss in small collision systems*, Phys. Rev. C **103** (2021) 054903, arXiv: [2007.13758 \[hep-ph\]](#).
- [72] P. B. Arnold, *Simple formula for high-energy gluon bremsstrahlung in a finite, expanding medium*, Phys. Rev. D **79** (2009) 065025, arXiv: [0808.2767 \[hep-ph\]](#).
- [73] R. Baier, Y. L. Dokshitzer, A. H. Mueller, S. Peigne and D. Schiff, *Radiative energy loss of high energy quarks and gluons in a finite-volume quark-gluon plasma*, Nucl. Phys. B **483** (1997) 291, arXiv: [hep-ph/9607355](#).
- [74] B. G. Zakharov, *Fully quantum treatment of the Landau-Pomeranchuk-Migdal effect in QED and QCD*, JETP Lett. **63** (1996) 952, arXiv: [hep-ph/9607440](#).
- [75] ATLAS Collaboration, *ATLAS Computing Acknowledgements*, ATL-SOFT-PUB-2021-003, 2021, URL: <https://cds.cern.ch/record/2776662>.

The ATLAS Collaboration

G. Aad [ID¹⁰²](#), B. Abbott [ID¹²⁰](#), K. Abeling [ID⁵⁵](#), S.H. Abidi [ID²⁹](#), A. Aboulhorma [ID^{35e}](#), H. Abramowicz [ID¹⁵¹](#), H. Abreu [ID¹⁵⁰](#), Y. Abulaiti [ID¹¹⁷](#), A.C. Abusleme Hoffman [ID^{137a}](#), B.S. Acharya [ID^{69a,69b,p}](#), C. Adam Bourdarios [ID⁴](#), L. Adamczyk [ID^{85a}](#), L. Adamek [ID¹⁵⁵](#), S.V. Addepalli [ID²⁶](#), J. Adelman [ID¹¹⁵](#), A. Adiguzel [ID^{21c}](#), S. Adorni [ID⁵⁶](#), T. Adye [ID¹³⁴](#), A.A. Affolder [ID¹³⁶](#), Y. Afik [ID³⁶](#), M.N. Agaras [ID¹³](#), J. Agarwala [ID^{73a,73b}](#), A. Aggarwal [ID¹⁰⁰](#), C. Agheorghiesei [ID^{27c}](#), J.A. Aguilar-Saavedra [ID^{130f}](#), A. Ahmad [ID³⁶](#), F. Ahmadov [ID^{38,ab}](#), W.S. Ahmed [ID¹⁰⁴](#), S. Ahuja [ID⁹⁵](#), X. Ai [ID⁴⁸](#), G. Aielli [ID^{76a,76b}](#), M. Ait Tamlihat [ID^{35e}](#), B. Aitbenchikh [ID^{35a}](#), I. Aizenberg [ID¹⁶⁹](#), M. Akbiyik [ID¹⁰⁰](#), T.P.A. A+Akesson [ID⁹⁸](#), A.V. Akimov [ID³⁷](#), K. Al Khoury [ID⁴¹](#), G.L. Alberghi [ID^{23b}](#), J. Albert [ID¹⁶⁵](#), P. Albicocco [ID⁵³](#), S. Alderweireldt [ID⁵²](#), M. Aleksa [ID³⁶](#), I.N. Aleksandrov [ID³⁸](#), C. Alexa [ID^{27b}](#), T. Alexopoulos [ID¹⁰](#), A. Alfonsi [ID¹¹⁴](#), F. Alfonsi [ID^{23b}](#), M. Alhroob [ID¹²⁰](#), B. Ali [ID¹³²](#), S. Ali [ID¹⁴⁸](#), M. Aliev [ID³⁷](#), G. Alimonti [ID^{71a}](#), W. Alkakhi [ID⁵⁵](#), C. Allaire [ID⁶⁶](#), B.M.M. Allbrooke [ID¹⁴⁶](#), C.A. Allendes Flores [ID^{137f}](#), P.P. Allport [ID²⁰](#), A. Aloisio [ID^{72a,72b}](#), F. Alonso [ID⁹⁰](#), C. Alpigiani [ID¹³⁸](#), M. Alvarez Estevez [ID⁹⁹](#), A. Alvarez Fernandez [ID¹⁰⁰](#), M.G. Alviggi [ID^{72a,72b}](#), M. Aly [ID¹⁰¹](#), Y. Amaral Coutinho [ID^{82b}](#), A. Ambler [ID¹⁰⁴](#), C. Amelung [ID³⁶](#), M. Amerl [ID¹](#), C.G. Ames [ID¹⁰⁹](#), D. Amidei [ID¹⁰⁶](#), S.P. Amor Dos Santos [ID^{130a}](#), K.R. Amos [ID¹⁶³](#), V. Ananiev [ID¹²⁵](#), C. Anastopoulos [ID¹³⁹](#), T. Andeen [ID¹¹](#), J.K. Anders [ID³⁶](#), S.Y. Andrean [ID^{47a,47b}](#), A. Andreazza [ID^{71a,71b}](#), S. Angelidakis [ID⁹](#), A. Angerami [ID^{41,ae}](#), A.V. Anisenkov [ID³⁷](#), A. Annovi [ID^{74a}](#), C. Antel [ID⁵⁶](#), M.T. Anthony [ID¹³⁹](#), E. Antipov [ID¹⁴⁵](#), M. Antonelli [ID⁵³](#), D.J.A. Antrim [ID^{17a}](#), F. Anulli [ID^{75a}](#), M. Aoki [ID⁸³](#), T. Aoki [ID¹⁵³](#), J.A. Aparisi Pozo [ID¹⁶³](#), M.A. Aparo [ID¹⁴⁶](#), L. Aperio Bella [ID⁴⁸](#), C. Appelt [ID¹⁸](#), N. Aranzabal [ID³⁶](#), V. Araujo Ferraz [ID^{82a}](#), C. Arcangeletti [ID⁵³](#), A.T.H. Arce [ID⁵¹](#), E. Arena [ID⁹²](#), J-F. Arguin [ID¹⁰⁸](#), S. Argyropoulos [ID⁵⁴](#), J.-H. Arling [ID⁴⁸](#), A.J. Armbruster [ID³⁶](#), O. Arnaez [ID⁴](#), H. Arnold [ID¹¹⁴](#), Z.P. Arrubarrena Tame [ID¹⁰⁹](#), G. Artoni [ID^{75a,75b}](#), H. Asada [ID¹¹¹](#), K. Asai [ID¹¹⁸](#), S. Asai [ID¹⁵³](#), N.A. Asbah [ID⁶¹](#), J. Assahsah [ID^{35d}](#), K. Assamagan [ID²⁹](#), R. Astalos [ID^{28a}](#), R.J. Atkin [ID^{33a}](#), M. Atkinson [ID¹⁶²](#), N.B. Atlay [ID¹⁸](#), H. Atmani [ID^{62b}](#), P.A. Atmasiddha [ID¹⁰⁶](#), K. Augsten [ID¹³²](#), S. Auricchio [ID^{72a,72b}](#), A.D. Auriol [ID²⁰](#), V.A. Aastrup [ID¹⁷¹](#), G. Avner [ID¹⁵⁰](#), G. Avolio [ID³⁶](#), K. Axiotis [ID⁵⁶](#), G. Azuelos [ID^{108,ai}](#), D. Babal [ID^{28a}](#), H. Bachacou [ID¹³⁵](#), K. Bachas [ID^{152,s}](#), A. Bachiu [ID³⁴](#), F. Backman [ID^{47a,47b}](#), A. Badea [ID⁶¹](#), P. Bagnaia [ID^{75a,75b}](#), M. Bahmani [ID¹⁸](#), A.J. Bailey [ID¹⁶³](#), V.R. Bailey [ID¹⁶²](#), J.T. Baines [ID¹³⁴](#), C. Bakalis [ID¹⁰](#), O.K. Baker [ID¹⁷²](#), E. Bakos [ID¹⁵](#), D. Bakshi Gupta [ID⁸](#), R. Balasubramanian [ID¹¹⁴](#), E.M. Baldin [ID³⁷](#), P. Balek [ID¹³³](#), E. Ballabene [ID^{71a,71b}](#), F. Balli [ID¹³⁵](#), L.M. Baltes [ID^{63a}](#), W.K. Balunas [ID³²](#), J. Balz [ID¹⁰⁰](#), E. Banas [ID⁸⁶](#), M. Bandieramonte [ID¹²⁹](#), A. Bandyopadhyay [ID²⁴](#), S. Bansal [ID²⁴](#), L. Barak [ID¹⁵¹](#), E.L. Barberio [ID¹⁰⁵](#), D. Barberis [ID^{57b,57a}](#), M. Barbero [ID¹⁰²](#), G. Barbour [ID⁹⁶](#), K.N. Barends [ID^{33a}](#), T. Barillari [ID¹¹⁰](#), M.-S. Barisits [ID³⁶](#), T. Barklow [ID¹⁴³](#), P. Baron [ID¹²²](#), D.A. Baron Moreno [ID¹⁰¹](#), A. Baroncelli [ID^{62a}](#), G. Barone [ID²⁹](#), A.J. Barr [ID¹²⁶](#), L. Barranco Navarro [ID^{47a,47b}](#), F. Barreiro [ID⁹⁹](#), J. Barreiro Guimarães da Costa [ID^{14a}](#), U. Barron [ID¹⁵¹](#), M.G. Barros Teixeira [ID^{130a}](#), S. Barsov [ID³⁷](#), F. Bartels [ID^{63a}](#), R. Bartoldus [ID¹⁴³](#), A.E. Barton [ID⁹¹](#), P. Bartos [ID^{28a}](#), A. Basan [ID¹⁰⁰](#), M. Baselga [ID⁴⁹](#), I. Bashta [ID^{77a,77b}](#), A. Bassalat [ID^{66,b}](#), M.J. Basso [ID¹⁵⁵](#), C.R. Basson [ID¹⁰¹](#), R.L. Bates [ID⁵⁹](#), S. Batlamous [ID^{35e}](#), J.R. Batley [ID³²](#), B. Batool [ID¹⁴¹](#), M. Battaglia [ID¹³⁶](#), D. Battulga [ID¹⁸](#), M. Bauce [ID^{75a,75b}](#), P. Bauer [ID²⁴](#), J.B. Beacham [ID⁵¹](#), T. Beau [ID¹²⁷](#), P.H. Beauchemin [ID¹⁵⁸](#), F. Becherer [ID⁵⁴](#), P. Bechtle [ID²⁴](#), H.P. Beck [ID^{19,r}](#), K. Becker [ID¹⁶⁷](#), A.J. Beddall [ID^{21d}](#), V.A. Bednyakov [ID³⁸](#), C.P. Bee [ID¹⁴⁵](#), L.J. Beemster [ID¹⁵](#), T.A. Beermann [ID³⁶](#), M. Begalli [ID^{82d}](#), M. Begel [ID²⁹](#), A. Behera [ID¹⁴⁵](#), J.K. Behr [ID⁴⁸](#), C. Beirao Da Cruz E Silva [ID³⁶](#), J.F. Beirer [ID^{55,36}](#), F. Beisiegel [ID²⁴](#), M. Belfkir [ID¹⁵⁹](#), G. Bella [ID¹⁵¹](#), L. Bellagamba [ID^{23b}](#), A. Bellerive [ID³⁴](#), P. Bellos [ID²⁰](#), K. Beloborodov [ID³⁷](#), N.L. Belyaev [ID³⁷](#), D. Benchekroun [ID^{35a}](#), F. Bendebba [ID^{35a}](#), Y. Benhammou [ID¹⁵¹](#), M. Benoit [ID²⁹](#), J.R. Bensinger [ID²⁶](#), S. Bentvelsen [ID¹¹⁴](#), L. Beresford [ID³⁶](#),

M. Beretta [ID⁵³](#), E. Bergeaas Kuutmann [ID¹⁶¹](#), N. Berger [ID⁴](#), B. Bergmann [ID¹³²](#), J. Beringer [ID^{17a}](#), S. Berlendis [ID⁷](#), G. Bernardi [ID⁵](#), C. Bernius [ID¹⁴³](#), F.U. Bernlochner [ID²⁴](#), T. Berry [ID⁹⁵](#), P. Berta [ID¹³³](#), A. Berthold [ID⁵⁰](#), I.A. Bertram [ID⁹¹](#), S. Bethke [ID¹¹⁰](#), A. Betti [ID^{75a,75b}](#), A.J. Bevan [ID⁹⁴](#), M. Bhamjee [ID^{33c}](#), S. Bhatta [ID¹⁴⁵](#), D.S. Bhattacharya [ID¹⁶⁶](#), P. Bhattachari [ID²⁶](#), V.S. Bhopatkar [ID¹²¹](#), R. Bi^{29,al}, R.M. Bianchi [ID¹²⁹](#), O. Biebel [ID¹⁰⁹](#), R. Bielski [ID¹²³](#), M. Biglietti [ID^{77a}](#), T.R.V. Billoud [ID¹³²](#), M. Bindi [ID⁵⁵](#), A. Bingul [ID^{21b}](#), C. Bini [ID^{75a,75b}](#), A. Biondini [ID⁹²](#), C.J. Birch-sykes [ID¹⁰¹](#), G.A. Bird [ID^{20,134}](#), M. Birman [ID¹⁶⁹](#), M. Biros [ID¹³³](#), T. Bisanz [ID³⁶](#), E. Bisceglie [ID^{43b,43a}](#), D. Biswas [ID¹⁷⁰](#), A. Bitadze [ID¹⁰¹](#), K. Bjørke [ID¹²⁵](#), I. Bloch [ID⁴⁸](#), C. Blocker [ID²⁶](#), A. Blue [ID⁵⁹](#), U. Blumenschein [ID⁹⁴](#), J. Blumenthal [ID¹⁰⁰](#), G.J. Bobbink [ID¹¹⁴](#), V.S. Bobrovnikov [ID³⁷](#), M. Boehler [ID⁵⁴](#), D. Bogavac [ID³⁶](#), A.G. Bogdanchikov [ID³⁷](#), C. Bohm [ID^{47a}](#), V. Boisvert [ID⁹⁵](#), P. Bokan [ID⁴⁸](#), T. Bold [ID^{85a}](#), M. Bomben [ID⁵](#), M. Bona [ID⁹⁴](#), M. Boonekamp [ID¹³⁵](#), C.D. Booth [ID⁹⁵](#), A.G. Borbely [ID⁵⁹](#), H.M. Borecka-Bielska [ID¹⁰⁸](#), L.S. Borgna [ID⁹⁶](#), G. Borissov [ID⁹¹](#), D. Bortoletto [ID¹²⁶](#), D. Boscherini [ID^{23b}](#), M. Bosman [ID¹³](#), J.D. Bossio Sola [ID³⁶](#), K. Bouaouda [ID^{35a}](#), N. Bouchhar [ID¹⁶³](#), J. Boudreau [ID¹²⁹](#), E.V. Bouhova-Thacker [ID⁹¹](#), D. Boumediene [ID⁴⁰](#), R. Bouquet [ID⁵](#), A. Boveia [ID¹¹⁹](#), J. Boyd [ID³⁶](#), D. Boye [ID²⁹](#), I.R. Boyko [ID³⁸](#), J. Bracinik [ID²⁰](#), N. Brahimi [ID^{62d}](#), G. Brandt [ID¹⁷¹](#), O. Brandt [ID³²](#), F. Braren [ID⁴⁸](#), B. Brau [ID¹⁰³](#), J.E. Brau [ID¹²³](#), K. Brendlinger [ID⁴⁸](#), R. Brener [ID¹⁶⁹](#), L. Brenner [ID¹¹⁴](#), R. Brenner [ID¹⁶¹](#), S. Bressler [ID¹⁶⁹](#), D. Britton [ID⁵⁹](#), D. Britzger [ID¹¹⁰](#), I. Brock [ID²⁴](#), G. Brooijmans [ID⁴¹](#), W.K. Brooks [ID^{137f}](#), E. Brost [ID²⁹](#), L.M. Brown [ID¹⁶⁵](#), T.L. Bruckler [ID¹²⁶](#), P.A. Bruckman de Renstrom [ID⁸⁶](#), B. Briuers [ID⁴⁸](#), D. Bruncko [ID^{28b,*}](#), A. Bruni [ID^{23b}](#), G. Bruni [ID^{23b}](#), M. Bruschi [ID^{23b}](#), N. Bruscino [ID^{75a,75b}](#), T. Buanes [ID¹⁶](#), Q. Buat [ID¹³⁸](#), A.G. Buckley [ID⁵⁹](#), I.A. Budagov [ID^{38,*}](#), M.K. Bugge [ID¹²⁵](#), O. Bulekov [ID³⁷](#), B.A. Bullard [ID¹⁴³](#), S. Burdin [ID⁹²](#), C.D. Burgard [ID⁴⁹](#), A.M. Burger [ID⁴⁰](#), B. Burghgrave [ID⁸](#), J.T.P. Burr [ID³²](#), C.D. Burton [ID¹¹](#), J.C. Burzynski [ID¹⁴²](#), E.L. Busch [ID⁴¹](#), V. Büscher [ID¹⁰⁰](#), P.J. Bussey [ID⁵⁹](#), J.M. Butler [ID²⁵](#), C.M. Buttar [ID⁵⁹](#), J.M. Butterworth [ID⁹⁶](#), W. Buttinger [ID¹³⁴](#), C.J. Buxo Vazquez¹⁰⁷, A.R. Buzykaev [ID³⁷](#), G. Cabras [ID^{23b}](#), S. Cabrera Urbán [ID¹⁶³](#), D. Caforio [ID⁵⁸](#), H. Cai [ID¹²⁹](#), Y. Cai [ID^{14a,14d}](#), V.M.M. Cairo [ID³⁶](#), O. Cakir [ID^{3a}](#), N. Calace [ID³⁶](#), P. Calafiura [ID^{17a}](#), G. Calderini [ID¹²⁷](#), P. Calfayan [ID⁶⁸](#), G. Callea [ID⁵⁹](#), L.P. Caloba^{82b}, D. Calvet [ID⁴⁰](#), S. Calvet [ID⁴⁰](#), T.P. Calvet [ID¹⁰²](#), M. Calvetti [ID^{74a,74b}](#), R. Camacho Toro [ID¹²⁷](#), S. Camarda [ID³⁶](#), D. Camarero Munoz [ID²⁶](#), P. Camarri [ID^{76a,76b}](#), M.T. Camerlingo [ID^{72a,72b}](#), D. Cameron [ID¹²⁵](#), C. Camincher [ID¹⁶⁵](#), M. Campanelli [ID⁹⁶](#), A. Camplani [ID⁴²](#), V. Canale [ID^{72a,72b}](#), A. Canesse [ID¹⁰⁴](#), M. Cano Bret [ID⁸⁰](#), J. Cantero [ID¹⁶³](#), Y. Cao [ID¹⁶²](#), F. Capocasa [ID²⁶](#), M. Capua [ID^{43b,43a}](#), A. Carbone [ID^{71a,71b}](#), R. Cardarelli [ID^{76a}](#), J.C.J. Cardenas [ID⁸](#), F. Cardillo [ID¹⁶³](#), T. Carli [ID³⁶](#), G. Carlino [ID^{72a}](#), J.I. Carlotto [ID¹³](#), B.T. Carlson [ID^{129,t}](#), E.M. Carlson [ID^{165,156a}](#), L. Carminati [ID^{71a,71b}](#), M. Carnesale [ID^{75a,75b}](#), S. Caron [ID¹¹³](#), E. Carquin [ID^{137f}](#), S. Carrá [ID^{71a,71b}](#), G. Carratta [ID^{23b,23a}](#), F. Carrio Argos [ID^{33g}](#), J.W.S. Carter [ID¹⁵⁵](#), T.M. Carter [ID⁵²](#), M.P. Casado [ID^{13,j}](#), A.F. Casha¹⁵⁵, M. Caspar [ID⁴⁸](#), E.G. Castiglia [ID¹⁷²](#), F.L. Castillo [ID^{63a}](#), L. Castillo Garcia [ID¹³](#), V. Castillo Gimenez [ID¹⁶³](#), N.F. Castro [ID^{130a,130e}](#), A. Catinaccio [ID³⁶](#), J.R. Catmore [ID¹²⁵](#), V. Cavaliere [ID²⁹](#), N. Cavalli [ID^{23b,23a}](#), V. Cavasinni [ID^{74a,74b}](#), E. Celebi [ID^{21a}](#), F. Celli [ID¹²⁶](#), M.S. Centonze [ID^{70a,70b}](#), K. Cerny [ID¹²²](#), A.S. Cerqueira [ID^{82a}](#), A. Cerri [ID¹⁴⁶](#), L. Cerrito [ID^{76a,76b}](#), F. Cerutti [ID^{17a}](#), A. Cervelli [ID^{23b}](#), G. Cesarini [ID⁵³](#), S.A. Cetin [ID^{21d}](#), Z. Chadi [ID^{35a}](#), D. Chakraborty [ID¹¹⁵](#), M. Chala [ID^{130f}](#), J. Chan [ID¹⁷⁰](#), W.Y. Chan [ID¹⁵³](#), J.D. Chapman [ID³²](#), B. Chargeishvili [ID^{149b}](#), D.G. Charlton [ID²⁰](#), T.P. Charman [ID⁹⁴](#), M. Chatterjee [ID¹⁹](#), S. Chekanov [ID⁶](#), S.V. Chekulaev [ID^{156a}](#), G.A. Chelkov [ID^{38,a}](#), A. Chen [ID¹⁰⁶](#), B. Chen [ID¹⁵¹](#), B. Chen [ID¹⁶⁵](#), H. Chen [ID^{14c}](#), H. Chen [ID²⁹](#), J. Chen [ID^{62c}](#), J. Chen [ID¹⁴²](#), S. Chen [ID¹⁵³](#), S.J. Chen [ID^{14c}](#), X. Chen [ID^{62c}](#), X. Chen [ID^{14b,ah}](#), Y. Chen [ID^{62a}](#), C.L. Cheng [ID¹⁷⁰](#), H.C. Cheng [ID^{64a}](#), S. Cheong [ID¹⁴³](#), A. Cheplakov [ID³⁸](#), E. Cheremushkina [ID⁴⁸](#), E. Cherepanova [ID¹¹⁴](#), R. Cherkaoui El Moursli [ID^{35e}](#), E. Cheu [ID⁷](#), K. Cheung [ID⁶⁵](#), L. Chevalier [ID¹³⁵](#), V. Chiarella [ID⁵³](#), G. Chiarelli [ID^{74a}](#), N. Chiedde [ID¹⁰²](#), G. Chiodini [ID^{70a}](#), A.S. Chisholm [ID²⁰](#), A. Chitan [ID^{27b}](#), M. Chitishvili [ID¹⁶³](#), M.V. Chizhov [ID³⁸](#), K. Choi [ID¹¹](#), A.R. Chomont [ID^{75a,75b}](#), Y. Chou [ID¹⁰³](#), E.Y.S. Chow [ID¹¹⁴](#), T. Chowdhury [ID^{33g}](#), L.D. Christopher [ID^{33g}](#), K.L. Chu^{64a}, M.C. Chu [ID^{64a}](#), X. Chu [ID^{14a,14d}](#), J. Chudoba [ID¹³¹](#), J.J. Chwastowski [ID⁸⁶](#), D. Cieri [ID¹¹⁰](#),

K.M. Ciesla **ID**^{85a}, V. Cindro **ID**⁹³, A. Ciocio **ID**^{17a}, F. Cirootto **ID**^{72a,72b}, Z.H. Citron **ID**^{169,m},
 M. Citterio **ID**^{71a}, D.A. Ciubotaru **ID**^{27b}, B.M. Ciungu **ID**¹⁵⁵, A. Clark **ID**⁵⁶, P.J. Clark **ID**⁵²,
 J.M. Clavijo Columbie **ID**⁴⁸, S.E. Clawson **ID**¹⁰¹, C. Clement **ID**^{47a,47b}, J. Clercx **ID**⁴⁸, L. Clissa **ID**^{23b,23a},
 Y. Coadou **ID**¹⁰², M. Cobal **ID**^{69a,69c}, A. Coccaro **ID**^{57b}, R.F. Coelho Barrue **ID**^{130a},
 R. Coelho Lopes De Sa **ID**¹⁰³, S. Coelli **ID**^{71a}, H. Cohen **ID**¹⁵¹, A.E.C. Coimbra **ID**^{71a,71b}, B. Cole **ID**⁴¹,
 J. Collot **ID**⁶⁰, P. Conde Muiño **ID**^{130a,130g}, M.P. Connell **ID**^{33c}, S.H. Connell **ID**^{33c}, I.A. Connelly **ID**⁵⁹,
 E.I. Conroy **ID**¹²⁶, F. Conventi **ID**^{72a,aj}, H.G. Cooke **ID**²⁰, A.M. Cooper-Sarkar **ID**¹²⁶, F. Cormier **ID**¹⁶⁴,
 L.D. Corpe **ID**³⁶, M. Corradi **ID**^{75a,75b}, F. Corriveau **ID**^{104,z}, A. Cortes-Gonzalez **ID**¹⁸, M.J. Costa **ID**¹⁶³,
 F. Costanza **ID**⁴, D. Costanzo **ID**¹³⁹, B.M. Cote **ID**¹¹⁹, G. Cowan **ID**⁹⁵, J.W. Cowley **ID**³², K. Cranmer **ID**¹¹⁷,
 S. Crépé-Renaudin **ID**⁶⁰, F. Crescioli **ID**¹²⁷, M. Cristinziani **ID**¹⁴¹, M. Cristoforetti **ID**^{78a,78b,d}, V. Croft **ID**¹¹⁴,
 G. Crosetti **ID**^{43b,43a}, A. Cueto **ID**³⁶, T. Cuhadar Donszelmann **ID**¹⁶⁰, H. Cui **ID**^{14a,14d}, Z. Cui **ID**⁷,
 W.R. Cunningham **ID**⁵⁹, F. Curcio **ID**^{43b,43a}, P. Czodrowski **ID**³⁶, M.M. Czurylo **ID**^{63b},
 M.J. Da Cunha Sargedas De Sousa **ID**^{62a}, J.V. Da Fonseca Pinto **ID**^{82b}, C. Da Via **ID**¹⁰¹, W. Dabrowski **ID**^{85a},
 T. Dado **ID**⁴⁹, S. Dahbi **ID**^{33g}, T. Dai **ID**¹⁰⁶, C. Dallapiccola **ID**¹⁰³, M. Dam **ID**⁴², G. D'amen **ID**²⁹,
 V. D'Amico **ID**¹⁰⁹, J. Damp **ID**¹⁰⁰, J.R. Dandoy **ID**¹²⁸, M.F. Daneri **ID**³⁰, M. Danninger **ID**¹⁴², V. Dao **ID**³⁶,
 G. Darbo **ID**^{57b}, S. Darmora **ID**⁶, S.J. Das **ID**^{29,al}, S. D'Auria **ID**^{71a,71b}, C. David **ID**^{156b}, T. Davidek **ID**¹³³,
 B. Davis-Purcell **ID**³⁴, I. Dawson **ID**⁹⁴, K. De **ID**⁸, R. De Asmundis **ID**^{72a}, N. De Biase **ID**⁴⁸,
 S. De Castro **ID**^{23b,23a}, N. De Groot **ID**¹¹³, P. de Jong **ID**¹¹⁴, H. De la Torre **ID**¹⁰⁷, A. De Maria **ID**^{14c},
 A. De Salvo **ID**^{75a}, U. De Sanctis **ID**^{76a,76b}, A. De Santo **ID**¹⁴⁶, J.B. De Vivie De Regie **ID**⁶⁰, D.V. Dedovich ³⁸,
 J. Degens **ID**¹¹⁴, A.M. Deiana **ID**⁴⁴, F. Del Corso **ID**^{23b,23a}, J. Del Peso **ID**⁹⁹, F. Del Rio **ID**^{63a}, F. Deliot **ID**¹³⁵,
 C.M. Delitzsch **ID**⁴⁹, M. Della Pietra **ID**^{72a,72b}, D. Della Volpe **ID**⁵⁶, A. Dell'Acqua **ID**³⁶,
 L. Dell'Asta **ID**^{71a,71b}, M. Delmastro **ID**⁴, P.A. Delsart **ID**⁶⁰, S. Demers **ID**¹⁷², M. Demichev **ID**³⁸,
 S.P. Denisov **ID**³⁷, L. D'Eramo **ID**¹¹⁵, D. Derendarz **ID**⁸⁶, F. Derue **ID**¹²⁷, P. Dervan **ID**⁹², K. Desch **ID**²⁴,
 K. Dette **ID**¹⁵⁵, C. Deutsch **ID**²⁴, F.A. Di Bello **ID**^{57b,57a}, A. Di Ciaccio **ID**^{76a,76b}, L. Di Ciaccio **ID**⁴,
 A. Di Domenico **ID**^{75a,75b}, C. Di Donato **ID**^{72a,72b}, A. Di Girolamo **ID**³⁶, G. Di Gregorio **ID**⁵,
 A. Di Luca **ID**^{78a,78b}, B. Di Micco **ID**^{77a,77b}, R. Di Nardo **ID**^{77a,77b}, C. Diaconu **ID**¹⁰², F.A. Dias **ID**¹¹⁴,
 T. Dias Do Vale **ID**¹⁴², M.A. Diaz **ID**^{137a,137b}, F.G. Diaz Capriles **ID**²⁴, M. Didenko **ID**¹⁶³, E.B. Diehl **ID**¹⁰⁶,
 L. Diehl **ID**⁵⁴, S. Díez Cornell **ID**⁴⁸, C. Diez Pardos **ID**¹⁴¹, C. Dimitriadi **ID**^{24,161}, A. Dimitrieva **ID**^{17a},
 J. Dingfelder **ID**²⁴, I-M. Dinu **ID**^{27b}, S.J. Dittmeier **ID**^{63b}, F. Dittus **ID**³⁶, F. Djama **ID**¹⁰², T. Djobava **ID**^{149b},
 J.I. Djupsland **ID**¹⁶, C. Doglioni **ID**^{101,98}, J. Dolejsi **ID**¹³³, Z. Dolezal **ID**¹³³, M. Donadelli **ID**^{82c},
 B. Dong **ID**¹⁰⁷, J. Domini **ID**⁴⁰, A. D'Onofrio **ID**^{77a,77b}, M. D'Onofrio **ID**⁹², J. Dopke **ID**¹³⁴, A. Doria **ID**^{72a},
 M.T. Dova **ID**⁹⁰, A.T. Doyle **ID**⁵⁹, M.A. Draguet **ID**¹²⁶, E. Drechsler **ID**¹⁴², E. Dreyer **ID**¹⁶⁹,
 I. Drivas-koulouris **ID**¹⁰, A.S. Drobac **ID**¹⁵⁸, M. Drozdova **ID**⁵⁶, D. Du **ID**^{62a}, T.A. du Pree **ID**¹¹⁴,
 F. Dubinin **ID**³⁷, M. Dubovsky **ID**^{28a}, E. Duchovni **ID**¹⁶⁹, G. Duckeck **ID**¹⁰⁹, O.A. Ducu **ID**^{27b}, D. Duda **ID**¹¹⁰,
 A. Dudarev **ID**³⁶, E.R. Duden **ID**²⁶, M. D'uffizi **ID**¹⁰¹, L. Duflot **ID**⁶⁶, M. Dührssen **ID**³⁶, C. Dülsen **ID**¹⁷¹,
 A.E. Dumitriu **ID**^{27b}, M. Dunford **ID**^{63a}, S. Dungs **ID**⁴⁹, K. Dunne **ID**^{47a,47b}, A. Duperrin **ID**¹⁰²,
 H. Duran Yildiz **ID**^{3a}, M. Düren **ID**⁵⁸, A. Durglishvili **ID**^{149b}, B.L. Dwyer **ID**¹¹⁵, G.I. Dyckes **ID**^{17a},
 M. Dyndal **ID**^{85a}, S. Dysch **ID**¹⁰¹, B.S. Dziedzic **ID**⁸⁶, Z.O. Earnshaw **ID**¹⁴⁶, B. Eckerova **ID**^{28a},
 S. Eggebrecht **ID**⁵⁵, M.G. Eggleston ⁵¹, E. Egidio Purcino De Souza **ID**¹²⁷, L.F. Ehrke **ID**⁵⁶, G. Eigen **ID**¹⁶,
 K. Einsweiler **ID**^{17a}, T. Ekelof **ID**¹⁶¹, P.A. Ekman **ID**⁹⁸, Y. El Ghazali **ID**^{35b}, H. El Jarrari **ID**^{35e,148},
 A. El Moussaoui **ID**^{35a}, V. Ellajosyula **ID**¹⁶¹, M. Ellert **ID**¹⁶¹, F. Ellinghaus **ID**¹⁷¹, A.A. Elliot **ID**⁹⁴,
 N. Ellis **ID**³⁶, J. Elmsheuser **ID**²⁹, M. Elsing **ID**³⁶, D. Emeliyanov **ID**¹³⁴, Y. Enari **ID**¹⁵³, I. Ene **ID**^{17a},
 S. Epari **ID**¹³, J. Erdmann **ID**⁴⁹, P.A. Erland **ID**⁸⁶, M. Errenst **ID**¹⁷¹, M. Escalier **ID**⁶⁶, C. Escobar **ID**¹⁶³,
 E. Etzion **ID**¹⁵¹, G. Evans **ID**^{130a}, H. Evans **ID**⁶⁸, M.O. Evans **ID**¹⁴⁶, A. Ezhilov **ID**³⁷, S. Ezzarqtouni **ID**^{35a},
 F. Fabbri **ID**⁵⁹, L. Fabbri **ID**^{23b,23a}, G. Facini **ID**⁹⁶, V. Fadeyev **ID**¹³⁶, R.M. Fakhrutdinov **ID**³⁷,
 S. Falciano **ID**^{75a}, L.F. Falda Ulhoa Coelho **ID**³⁶, P.J. Falke **ID**²⁴, S. Falke **ID**³⁶, J. Faltova **ID**¹³³, Y. Fan **ID**^{14a},
 Y. Fang **ID**^{14a,14d}, M. Fanti **ID**^{71a,71b}, M. Faraj **ID**^{69a,69b}, Z. Farazpay ⁹⁷, A. Farbin **ID**⁸, A. Farilla **ID**^{77a},

T. Farooque [ID¹⁰⁷](#), S.M. Farrington [ID⁵²](#), F. Fassi [ID^{35e}](#), D. Fassouliotis [ID⁹](#), M. Faucci Giannelli [ID^{76a,76b}](#), W.J. Fawcett [ID³²](#), L. Fayard [ID⁶⁶](#), P. Federic [ID¹³³](#), P. Federicova [ID¹³¹](#), O.L. Fedin [ID^{37,a}](#), G. Fedotov [ID³⁷](#), M. Feickert [ID¹⁷⁰](#), L. Feligioni [ID¹⁰²](#), A. Fell [ID¹³⁹](#), D.E. Fellers [ID¹²³](#), C. Feng [ID^{62b}](#), M. Feng [ID^{14b}](#), Z. Feng [ID¹¹⁴](#), M.J. Fenton [ID¹⁶⁰](#), A.B. Fenyuk [ID³⁷](#), L. Ferencz [ID⁴⁸](#), R.A.M. Ferguson [ID⁹¹](#), S.I. Fernandez Luengo [ID^{137f}](#), J. Ferrando [ID⁴⁸](#), A. Ferrari [ID¹⁶¹](#), P. Ferrari [ID^{114,113}](#), R. Ferrari [ID^{73a}](#), D. Ferrere [ID⁵⁶](#), C. Ferretti [ID¹⁰⁶](#), F. Fiedler [ID¹⁰⁰](#), A. Filipčič [ID⁹³](#), E.K. Filmer [ID¹](#), F. Filthaut [ID¹¹³](#), M.C.N. Fiolhais [ID^{130a,130c,c}](#), L. Fiorini [ID¹⁶³](#), F. Fischer [ID¹⁴¹](#), W.C. Fisher [ID¹⁰⁷](#), T. Fitschen [ID¹⁰¹](#), I. Fleck [ID¹⁴¹](#), P. Fleischmann [ID¹⁰⁶](#), T. Flick [ID¹⁷¹](#), L. Flores [ID¹²⁸](#), M. Flores [ID^{33d,af}](#), L.R. Flores Castillo [ID^{64a}](#), F.M. Follega [ID^{78a,78b}](#), N. Fomin [ID¹⁶](#), J.H. Foo [ID¹⁵⁵](#), B.C. Forland [ID⁶⁸](#), A. Formica [ID¹³⁵](#), A.C. Forti [ID¹⁰¹](#), E. Fortin [ID¹⁰²](#), A.W. Fortman [ID⁶¹](#), M.G. Foti [ID^{17a}](#), L. Fountas [ID^{9,k}](#), D. Fournier [ID⁶⁶](#), H. Fox [ID⁹¹](#), P. Francavilla [ID^{74a,74b}](#), S. Francescato [ID⁶¹](#), S. Franchellucci [ID⁵⁶](#), M. Franchini [ID^{23b,23a}](#), S. Franchino [ID^{63a}](#), D. Francis [ID³⁶](#), L. Franco [ID¹¹³](#), L. Franconi [ID¹⁹](#), M. Franklin [ID⁶¹](#), G. Frattari [ID²⁶](#), A.C. Freegard [ID⁹⁴](#), W.S. Freund [ID^{82b}](#), Y.Y. Frid [ID¹⁵¹](#), N. Fritzsch [ID⁵⁰](#), A. Froch [ID⁵⁴](#), D. Froidevaux [ID³⁶](#), J.A. Frost [ID¹²⁶](#), Y. Fu [ID^{62a}](#), M. Fujimoto [ID¹¹⁸](#), E. Fullana Torregrosa [ID^{163,*}](#), J. Fuster [ID¹⁶³](#), A. Gabrielli [ID^{23b,23a}](#), A. Gabrielli [ID¹⁵⁵](#), P. Gadow [ID⁴⁸](#), G. Gagliardi [ID^{57b,57a}](#), L.G. Gagnon [ID^{17a}](#), G.E. Gallardo [ID¹²⁶](#), E.J. Gallas [ID¹²⁶](#), B.J. Gallop [ID¹³⁴](#), R. Gamboa Goni [ID⁹⁴](#), K.K. Gan [ID¹¹⁹](#), S. Ganguly [ID¹⁵³](#), J. Gao [ID^{62a}](#), Y. Gao [ID⁵²](#), F.M. Garay Walls [ID^{137a,137b}](#), B. Garcia [ID^{29,al}](#), C. García [ID¹⁶³](#), J.E. García Navarro [ID¹⁶³](#), M. Garcia-Sciveres [ID^{17a}](#), R.W. Gardner [ID³⁹](#), D. Garg [ID⁸⁰](#), R.B. Garg [ID^{143,q}](#), C.A. Garner [ID¹⁵⁵](#), S.J. Gasiorowski [ID¹³⁸](#), P. Gaspar [ID^{82b}](#), G. Gaudio [ID^{73a}](#), V. Gautam [ID¹³](#), P. Gauzzi [ID^{75a,75b}](#), I.L. Gavrilenko [ID³⁷](#), A. Gavrilyuk [ID³⁷](#), C. Gay [ID¹⁶⁴](#), G. Gaycken [ID⁴⁸](#), E.N. Gazis [ID¹⁰](#), A.A. Geanta [ID^{27b,27e}](#), C.M. Gee [ID¹³⁶](#), C. Gemme [ID^{57b}](#), M.H. Genest [ID⁶⁰](#), S. Gentile [ID^{75a,75b}](#), S. George [ID⁹⁵](#), W.F. George [ID²⁰](#), T. Geralis [ID⁴⁶](#), L.O. Gerlach [ID⁵⁵](#), P. Gessinger-Befurt [ID³⁶](#), M.E. Geyik [ID¹⁷¹](#), M. Ghneimat [ID¹⁴¹](#), K. Ghorbanian [ID⁹⁴](#), A. Ghosal [ID¹⁴¹](#), A. Ghosh [ID¹⁶⁰](#), A. Ghosh [ID⁷](#), B. Giacobbe [ID^{23b}](#), S. Giagu [ID^{75a,75b}](#), P. Giannetti [ID^{74a}](#), A. Giannini [ID^{62a}](#), S.M. Gibson [ID⁹⁵](#), M. Gignac [ID¹³⁶](#), D.T. Gil [ID^{85b}](#), A.K. Gilbert [ID^{85a}](#), B.J. Gilbert [ID⁴¹](#), D. Gillberg [ID³⁴](#), G. Gilles [ID¹¹⁴](#), N.E.K. Gillwald [ID⁴⁸](#), L. Ginabat [ID¹²⁷](#), D.M. Gingrich [ID^{2,ai}](#), M.P. Giordani [ID^{69a,69c}](#), P.F. Giraud [ID¹³⁵](#), G. Giugliarelli [ID^{69a,69c}](#), D. Giugni [ID^{71a}](#), F. Giuli [ID³⁶](#), I. Gkalias [ID^{9,k}](#), L.K. Gladilin [ID³⁷](#), C. Glasman [ID⁹⁹](#), G.R. Gledhill [ID¹²³](#), M. Glisic [ID¹²³](#), I. Gnesi [ID^{43b,g}](#), Y. Go [ID^{29,al}](#), M. Goblirsch-Kolb [ID²⁶](#), B. Gocke [ID⁴⁹](#), D. Godin [ID¹⁰⁸](#), B. Gokturk [ID^{21a}](#), S. Goldfarb [ID¹⁰⁵](#), T. Golling [ID⁵⁶](#), M.G.D. Gololo [ID^{33g}](#), D. Golubkov [ID³⁷](#), J.P. Gombas [ID¹⁰⁷](#), A. Gomes [ID^{130a,130b}](#), G. Gomes Da Silva [ID¹⁴¹](#), A.J. Gomez Delegido [ID¹⁶³](#), R. Gonçalo [ID^{130a,130c}](#), G. Gonella [ID¹²³](#), L. Gonella [ID²⁰](#), A. Gongadze [ID³⁸](#), F. Gonnella [ID²⁰](#), J.L. Gonski [ID⁴¹](#), R.Y. González Andana [ID⁵²](#), S. González de la Hoz [ID¹⁶³](#), S. Gonzalez Fernandez [ID¹³](#), R. Gonzalez Lopez [ID⁹²](#), C. Gonzalez Renteria [ID^{17a}](#), R. Gonzalez Suarez [ID¹⁶¹](#), S. Gonzalez-Sevilla [ID⁵⁶](#), G.R. Gonzalvo Rodriguez [ID¹⁶³](#), L. Goossens [ID³⁶](#), P.A. Gorbounov [ID³⁷](#), B. Gorini [ID³⁶](#), E. Gorini [ID^{70a,70b}](#), A. Gorišek [ID⁹³](#), A.T. Goshaw [ID⁵¹](#), M.I. Gostkin [ID³⁸](#), S. Goswami [ID¹²¹](#), C.A. Gottardo [ID³⁶](#), M. Gouighri [ID^{35b}](#), V. Goumarre [ID⁴⁸](#), A.G. Goussiou [ID¹³⁸](#), N. Govender [ID^{33c}](#), I. Grabowska-Bold [ID^{85a}](#), K. Graham [ID³⁴](#), E. Gramstad [ID¹²⁵](#), S. Grancagnolo [ID¹⁸](#), M. Grandi [ID¹⁴⁶](#), V. Gratchev [ID^{37,*}](#), P.M. Gravila [ID^{27f}](#), F.G. Gravili [ID^{70a,70b}](#), H.M. Gray [ID^{17a}](#), M. Greco [ID^{70a,70b}](#), C. Grefe [ID²⁴](#), I.M. Gregor [ID⁴⁸](#), P. Grenier [ID¹⁴³](#), C. Grieco [ID¹³](#), A.A. Grillo [ID¹³⁶](#), K. Grimm [ID^{31,n}](#), S. Grinstein [ID^{13,v}](#), J.-F. Grivaz [ID⁶⁶](#), E. Gross [ID¹⁶⁹](#), J. Grosse-Knetter [ID⁵⁵](#), C. Grud [ID¹⁰⁶](#), J.C. Grundy [ID¹²⁶](#), L. Guan [ID¹⁰⁶](#), W. Guan [ID¹⁷⁰](#), C. Gubbels [ID¹⁶⁴](#), J.G.R. Guerrero Rojas [ID¹⁶³](#), G. Guerrieri [ID^{69a,69b}](#), F. Guescini [ID¹¹⁰](#), R. Gugel [ID¹⁰⁰](#), J.A.M. Guhit [ID¹⁰⁶](#), A. Guida [ID⁴⁸](#), T. Guillemin [ID⁴](#), E. Guilloton [ID^{167,134}](#), S. Guindon [ID³⁶](#), F. Guo [ID^{14a,14d}](#), J. Guo [ID^{62c}](#), L. Guo [ID⁶⁶](#), Y. Guo [ID¹⁰⁶](#), R. Gupta [ID⁴⁸](#), S. Gurbuz [ID²⁴](#), S.S. Gurdasani [ID⁵⁴](#), G. Gustavino [ID³⁶](#), M. Guth [ID⁵⁶](#), P. Gutierrez [ID¹²⁰](#), L.F. Gutierrez Zagazeta [ID¹²⁸](#), C. Gutschow [ID⁹⁶](#), C. Gwenlan [ID¹²⁶](#), C.B. Gwilliam [ID⁹²](#), E.S. Haaland [ID¹²⁵](#), A. Haas [ID¹¹⁷](#), M. Habedank [ID⁴⁸](#), C. Haber [ID^{17a}](#), H.K. Hadavand [ID⁸](#), A. Hadef [ID¹⁰⁰](#), S. Hadzic [ID¹¹⁰](#), E.H. Haines [ID⁹⁶](#), M. Haleem [ID¹⁶⁶](#), J. Haley [ID¹²¹](#), J.J. Hall [ID¹³⁹](#), G.D. Hallewell [ID¹⁰²](#), L. Halser [ID¹⁹](#), K. Hamano [ID¹⁶⁵](#), H. Hamdaoui [ID^{35e}](#),

M. Hamer [ID²⁴](#), G.N. Hamity [ID⁵²](#), J. Han [ID^{62b}](#), K. Han [ID^{62a}](#), L. Han [ID^{14c}](#), S. Han [ID^{17a}](#), Y.F. Han [ID¹⁵⁵](#), K. Hanagaki [ID⁸³](#), M. Hance [ID¹³⁶](#), D.A. Hangal [ID^{41,ae}](#), H. Hanif [ID¹⁴²](#), M.D. Hank [ID¹²⁸](#), R. Hankache [ID¹⁰¹](#), J.B. Hansen [ID⁴²](#), J.D. Hansen [ID⁴²](#), P.H. Hansen [ID⁴²](#), K. Hara [ID¹⁵⁷](#), D. Harada [ID⁵⁶](#), T. Harenberg [ID¹⁷¹](#), S. Harkusha [ID³⁷](#), Y.T. Harris [ID¹²⁶](#), N.M. Harrison [ID¹¹⁹](#), P.F. Harrison [ID¹⁶⁷](#), N.M. Hartman [ID¹⁴³](#), N.M. Hartmann [ID¹⁰⁹](#), Y. Hasegawa [ID¹⁴⁰](#), A. Hasib [ID⁵²](#), S. Haug [ID¹⁹](#), R. Hauser [ID¹⁰⁷](#), M. Havranek [ID¹³²](#), C.M. Hawkes [ID²⁰](#), R.J. Hawkings [ID³⁶](#), S. Hayashida [ID¹¹¹](#), D. Hayden [ID¹⁰⁷](#), C. Hayes [ID¹⁰⁶](#), R.L. Hayes [ID¹¹⁴](#), C.P. Hays [ID¹²⁶](#), J.M. Hays [ID⁹⁴](#), H.S. Hayward [ID⁹²](#), F. He [ID^{62a}](#), Y. He [ID¹⁵⁴](#), Y. He [ID¹²⁷](#), N.B. Heatley [ID⁹⁴](#), V. Hedberg [ID⁹⁸](#), A.L. Heggelund [ID¹²⁵](#), N.D. Hehir [ID⁹⁴](#), C. Heidegger [ID⁵⁴](#), K.K. Heidegger [ID⁵⁴](#), W.D. Heidorn [ID⁸¹](#), J. Heilman [ID³⁴](#), S. Heim [ID⁴⁸](#), T. Heim [ID^{17a}](#), J.G. Heinlein [ID¹²⁸](#), J.J. Heinrich [ID¹²³](#), L. Heinrich [ID^{110,ag}](#), J. Hejbal [ID¹³¹](#), L. Helary [ID⁴⁸](#), A. Held [ID¹⁷⁰](#), S. Hellesund [ID¹²⁵](#), C.M. Helling [ID¹⁶⁴](#), S. Hellman [ID^{47a,47b}](#), C. Helsens [ID³⁶](#), R.C.W. Henderson⁹¹, L. Henkelmann [ID³²](#), A.M. Henriques Correia³⁶, H. Herde [ID⁹⁸](#), Y. Hernández Jiménez [ID¹⁴⁵](#), L.M. Herrmann [ID²⁴](#), T. Herrmann [ID⁵⁰](#), G. Herten [ID⁵⁴](#), R. Hertenberger [ID¹⁰⁹](#), L. Hervas [ID³⁶](#), N.P. Hessey [ID^{156a}](#), H. Hibi [ID⁸⁴](#), S.J. Hillier [ID²⁰](#), F. Hinterkeuser [ID²⁴](#), M. Hirose [ID¹²⁴](#), S. Hirose [ID¹⁵⁷](#), D. Hirschbuehl [ID¹⁷¹](#), T.G. Hitchings [ID¹⁰¹](#), B. Hiti [ID⁹³](#), J. Hobbs [ID¹⁴⁵](#), R. Hobincu [ID^{27e}](#), N. Hod [ID¹⁶⁹](#), M.C. Hodgkinson [ID¹³⁹](#), B.H. Hodkinson [ID³²](#), A. Hoecker [ID³⁶](#), J. Hofer [ID⁴⁸](#), T. Holm [ID²⁴](#), M. Holzbock [ID¹¹⁰](#), L.B.A.H. Hommels [ID³²](#), B.P. Honan [ID¹⁰¹](#), J. Hong [ID^{62c}](#), T.M. Hong [ID¹²⁹](#), J.C. Honig [ID⁵⁴](#), B.H. Hooberman [ID¹⁶²](#), W.H. Hopkins [ID⁶](#), Y. Horii [ID¹¹¹](#), S. Hou [ID¹⁴⁸](#), A.S. Howard [ID⁹³](#), J. Howarth [ID⁵⁹](#), J. Hoya [ID⁶](#), M. Hrabovsky [ID¹²²](#), A. Hrynevich [ID⁴⁸](#), T. Hrynev'ova [ID⁴](#), P.J. Hsu [ID⁶⁵](#), S.-C. Hsu [ID¹³⁸](#), Q. Hu [ID⁴¹](#), Y.F. Hu [ID^{14a,14d,ak}](#), D.P. Huang [ID⁹⁶](#), S. Huang [ID^{64b}](#), X. Huang [ID^{14c}](#), Y. Huang [ID^{62a}](#), Y. Huang [ID^{14a}](#), Z. Huang [ID¹⁰¹](#), Z. Hubacek [ID¹³²](#), M. Huebner [ID²⁴](#), F. Huegging [ID²⁴](#), T.B. Huffman [ID¹²⁶](#), M. Huhtinen [ID³⁶](#), S.K. Huiberts [ID¹⁶](#), R. Hulskens [ID¹⁰⁴](#), N. Huseynov [ID^{12,a}](#), J. Huston [ID¹⁰⁷](#), J. Huth [ID⁶¹](#), R. Hyneman [ID¹⁴³](#), G. Iacobucci [ID⁵⁶](#), G. Iakovidis [ID²⁹](#), I. Ibragimov [ID¹⁴¹](#), L. Iconomidou-Fayard [ID⁶⁶](#), P. Iengo [ID^{72a,72b}](#), R. Iguchi [ID¹⁵³](#), T. Iizawa [ID⁵⁶](#), Y. Ikegami [ID⁸³](#), A. Ilg [ID¹⁹](#), N. Ilic [ID¹⁵⁵](#), H. Imam [ID^{35a}](#), T. Ingebretsen Carlson [ID^{47a,47b}](#), G. Introzzi [ID^{73a,73b}](#), M. Iodice [ID^{77a}](#), V. Ippolito [ID^{75a,75b}](#), M. Ishino [ID¹⁵³](#), W. Islam [ID¹⁷⁰](#), C. Issever [ID^{18,48}](#), S. Istin [ID^{21a,an}](#), H. Ito [ID¹⁶⁸](#), J.M. Iturbe Ponce [ID^{64a}](#), R. Iuppa [ID^{78a,78b}](#), A. Ivina [ID¹⁶⁹](#), J.M. Izen [ID⁴⁵](#), V. Izzo [ID^{72a}](#), P. Jacka [ID^{131,132}](#), P. Jackson [ID¹](#), R.M. Jacobs [ID⁴⁸](#), B.P. Jaeger [ID¹⁴²](#), C.S. Jagfeld [ID¹⁰⁹](#), P. Jain [ID⁵⁴](#), G. Jäkel [ID¹⁷¹](#), K. Jakobs [ID⁵⁴](#), T. Jakoubek [ID¹⁶⁹](#), J. Jamieson [ID⁵⁹](#), K.W. Janas [ID^{85a}](#), A.E. Jaspan [ID⁹²](#), M. Javurkova [ID¹⁰³](#), F. Jeanneau [ID¹³⁵](#), L. Jeanty [ID¹²³](#), J. Jejelava [ID^{149a,ac}](#), P. Jenni [ID^{54,h}](#), C.E. Jessiman [ID³⁴](#), S. Jézéquel [ID⁴](#), C. Jia^{62b}, J. Jia [ID¹⁴⁵](#), X. Jia [ID⁶¹](#), X. Jia [ID^{14a,14d}](#), Z. Jia [ID^{14c}](#), Y. Jiang^{62a}, S. Jiggins [ID⁴⁸](#), J. Jimenez Pena [ID¹¹⁰](#), S. Jin [ID^{14c}](#), A. Jinaru [ID^{27b}](#), O. Jinnouchi [ID¹⁵⁴](#), P. Johansson [ID¹³⁹](#), K.A. Johns [ID⁷](#), J.W. Johnson [ID¹³⁶](#), D.M. Jones [ID³²](#), E. Jones [ID¹⁶⁷](#), P. Jones [ID³²](#), R.W.L. Jones [ID⁹¹](#), T.J. Jones [ID⁹²](#), R. Joshi [ID¹¹⁹](#), J. Jovicevic [ID¹⁵](#), X. Ju [ID^{17a}](#), J.J. Junggeburth [ID³⁶](#), T. Junkermann [ID^{63a}](#), A. Juste Rozas [ID^{13,v}](#), S. Kabana [ID^{137e}](#), A. Kaczmarska [ID⁸⁶](#), M. Kado [ID¹¹⁰](#), H. Kagan [ID¹¹⁹](#), M. Kagan [ID¹⁴³](#), A. Kahn⁴¹, A. Kahn [ID¹²⁸](#), C. Kahra [ID¹⁰⁰](#), T. Kaji [ID¹⁶⁸](#), E. Kajomovitz [ID¹⁵⁰](#), N. Kakati [ID¹⁶⁹](#), C.W. Kalderon [ID²⁹](#), A. Kamenshchikov [ID¹⁵⁵](#), S. Kanayama [ID¹⁵⁴](#), N.J. Kang [ID¹³⁶](#), D. Kar [ID^{33g}](#), K. Karava [ID¹²⁶](#), M.J. Kareem [ID^{156b}](#), E. Karentzos [ID⁵⁴](#), I. Karkanias [ID^{152,f}](#), S.N. Karpov [ID³⁸](#), Z.M. Karpova [ID³⁸](#), V. Kartvelishvili [ID⁹¹](#), A.N. Karyukhin [ID³⁷](#), E. Kasimi [ID^{152,f}](#), J. Katzy [ID⁴⁸](#), S. Kaur [ID³⁴](#), K. Kawade [ID¹⁴⁰](#), T. Kawamoto [ID¹³⁵](#), G. Kawamura⁵⁵, E.F. Kay [ID¹⁶⁵](#), F.I. Kaya [ID¹⁵⁸](#), S. Kazakos [ID¹³](#), V.F. Kazanin [ID³⁷](#), Y. Ke [ID¹⁴⁵](#), J.M. Keaveney [ID^{33a}](#), R. Keeler [ID¹⁶⁵](#), G.V. Kehris [ID⁶¹](#), J.S. Keller [ID³⁴](#), A.S. Kelly⁹⁶, D. Kelsey [ID¹⁴⁶](#), J.J. Kempster [ID¹⁴⁶](#), K.E. Kennedy [ID⁴¹](#), P.D. Kennedy [ID¹⁰⁰](#), O. Kepka [ID¹³¹](#), B.P. Kerridge [ID¹⁶⁷](#), S. Kersten [ID¹⁷¹](#), B.P. Kerševan [ID⁹³](#), S. Keshri [ID⁶⁶](#), L. Keszeghova [ID^{28a}](#), S. Ketabchi Haghight [ID¹⁵⁵](#), M. Khandoga [ID¹²⁷](#), A. Khanov [ID¹²¹](#), A.G. Kharlamov [ID³⁷](#), T. Kharlamova [ID³⁷](#), E.E. Khoda [ID¹³⁸](#), T.J. Khoo [ID¹⁸](#), G. Khoriauli [ID¹⁶⁶](#), J. Khubua [ID^{149b}](#), Y.A.R. Khwaira [ID⁶⁶](#), M. Kiehn [ID³⁶](#), A. Kilgallon [ID¹²³](#), D.W. Kim [ID^{47a,47b}](#), E. Kim [ID¹⁵⁴](#), Y.K. Kim [ID³⁹](#), N. Kimura [ID⁹⁶](#), A. Kirchhoff [ID⁵⁵](#), C. Kirfel [ID²⁴](#), J. Kirk [ID¹³⁴](#),

A.E. Kiryunin [ID¹¹⁰](#), T. Kishimoto [ID¹⁵³](#), D.P. Kisliuk¹⁵⁵, C. Kitsaki [ID¹⁰](#), O. Kivernyk [ID²⁴](#),
 M. Klassen [ID^{63a}](#), C. Klein [ID³⁴](#), L. Klein [ID¹⁶⁶](#), M.H. Klein [ID¹⁰⁶](#), M. Klein [ID⁹²](#), S.B. Klein [ID⁵⁶](#),
 U. Klein [ID⁹²](#), P. Klimek [ID³⁶](#), A. Klimentov [ID²⁹](#), F. Klimpel [ID¹¹⁰](#), T. Klioutchnikova [ID³⁶](#), P. Kluit [ID¹¹⁴](#),
 S. Kluth [ID¹¹⁰](#), E. Knerner [ID⁷⁹](#), T.M. Knight [ID¹⁵⁵](#), A. Knue [ID⁵⁴](#), R. Kobayashi [ID⁸⁷](#), M. Kocian [ID¹⁴³](#),
 P. Kodyš [ID¹³³](#), D.M. Koeck [ID¹⁴⁶](#), P.T. Koenig [ID²⁴](#), T. Koffas [ID³⁴](#), M. Kolb [ID¹³⁵](#), I. Koletsou [ID⁴](#),
 T. Komarek [ID¹²²](#), K. Köneke [ID⁵⁴](#), A.X.Y. Kong [ID¹](#), T. Kono [ID¹¹⁸](#), N. Konstantinidis [ID⁹⁶](#), B. Konya [ID⁹⁸](#),
 R. Kopeliansky [ID⁶⁸](#), S. Koperny [ID^{85a}](#), K. Korcyl [ID⁸⁶](#), K. Kordas [ID^{152,f}](#), G. Koren [ID¹⁵¹](#), A. Korn [ID⁹⁶](#),
 S. Korn [ID⁵⁵](#), I. Korolkov [ID¹³](#), N. Korotkova [ID³⁷](#), B. Kortman [ID¹¹⁴](#), O. Kortner [ID¹¹⁰](#), S. Kortner [ID¹¹⁰](#),
 W.H. Kostecka [ID¹¹⁵](#), V.V. Kostyukhin [ID¹⁴¹](#), A. Kotsokechagia [ID¹³⁵](#), A. Kotwal [ID⁵¹](#), A. Koulouris [ID³⁶](#),
 A. Kourkoumeli-Charalampidi [ID^{73a,73b}](#), C. Kourkoumelis [ID⁹](#), E. Kourlitis [ID⁶](#), O. Kovanda [ID¹⁴⁶](#),
 R. Kowalewski [ID¹⁶⁵](#), W. Kozanecki [ID¹³⁵](#), A.S. Kozhin [ID³⁷](#), V.A. Kramarenko [ID³⁷](#), G. Kramberger [ID⁹³](#),
 P. Kramer [ID¹⁰⁰](#), M.W. Krasny [ID¹²⁷](#), A. Krasznahorkay [ID³⁶](#), J.A. Kremer [ID¹⁰⁰](#), T. Kresse [ID⁵⁰](#),
 J. Kretzschmar [ID⁹²](#), K. Kreul [ID¹⁸](#), P. Krieger [ID¹⁵⁵](#), S. Krishnamurthy [ID¹⁰³](#), M. Krivos [ID¹³³](#),
 K. Krizka [ID²⁰](#), K. Kroeninger [ID⁴⁹](#), H. Kroha [ID¹¹⁰](#), J. Kroll [ID¹³¹](#), J. Kroll [ID¹²⁸](#), K.S. Krowpman [ID¹⁰⁷](#),
 U. Kruchonak [ID³⁸](#), H. Krüger [ID²⁴](#), N. Krumnack⁸¹, M.C. Kruse [ID⁵¹](#), J.A. Krzysiak [ID⁸⁶](#),
 O. Kuchinskaia [ID³⁷](#), S. Kuday [ID^{3a}](#), S. Kuehn [ID³⁶](#), R. Kuesters [ID⁵⁴](#), T. Kuhl [ID⁴⁸](#), V. Kukhtin [ID³⁸](#),
 Y. Kulchitsky [ID^{37,a}](#), S. Kuleshov [ID^{137d,137b}](#), M. Kumar [ID^{33g}](#), N. Kumari [ID¹⁰²](#), A. Kupco [ID¹³¹](#), T. Kupfer⁴⁹,
 A. Kupich [ID³⁷](#), O. Kuprash [ID⁵⁴](#), H. Kurashige [ID⁸⁴](#), L.L. Kurchaninov [ID^{156a}](#), Y.A. Kurochkin [ID³⁷](#),
 A. Kurova [ID³⁷](#), M. Kuze [ID¹⁵⁴](#), A.K. Kvam [ID¹⁰³](#), J. Kvita [ID¹²²](#), T. Kwan [ID¹⁰⁴](#), N.G. Kyriacou [ID¹⁰⁶](#),
 L.A.O. Laatu [ID¹⁰²](#), C. Lacasta [ID¹⁶³](#), F. Lacava [ID^{75a,75b}](#), H. Lacker [ID¹⁸](#), D. Lacour [ID¹²⁷](#), N.N. Lad [ID⁹⁶](#),
 E. Ladygin [ID³⁸](#), B. Laforge [ID¹²⁷](#), T. Lagouri [ID^{137e}](#), S. Lai [ID⁵⁵](#), I.K. Lakomiec [ID^{85a}](#), N. Lalloue [ID⁶⁰](#),
 J.E. Lambert [ID¹²⁰](#), S. Lammers [ID⁶⁸](#), W. Lampl [ID⁷](#), C. Lampoudis [ID^{152,f}](#), A.N. Lancaster [ID¹¹⁵](#),
 E. Lançon [ID²⁹](#), U. Landgraf [ID⁵⁴](#), M.P.J. Landon [ID⁹⁴](#), V.S. Lang [ID⁵⁴](#), R.J. Langenberg [ID¹⁰³](#),
 A.J. Lankford [ID¹⁶⁰](#), F. Lanni [ID³⁶](#), K. Lantzsch [ID²⁴](#), A. Lanza [ID^{73a}](#), A. Lapertosa [ID^{57b,57a}](#),
 J.F. Laporte [ID¹³⁵](#), T. Lari [ID^{71a}](#), F. Lasagni Manghi [ID^{23b}](#), M. Lassnig [ID³⁶](#), V. Latonova [ID¹³¹](#),
 A. Laudrain [ID¹⁰⁰](#), A. Laurier [ID¹⁵⁰](#), S.D. Lawlor [ID⁹⁵](#), Z. Lawrence [ID¹⁰¹](#), M. Lazzaroni [ID^{71a,71b}](#), B. Le¹⁰¹,
 E.M. Le Boulicaut [ID⁵¹](#), B. Leban [ID⁹³](#), A. Lebedev [ID⁸¹](#), M. LeBlanc [ID³⁶](#), F. Ledroit-Guillon [ID⁶⁰](#),
 A.C.A. Lee [ID⁹⁶](#), G.R. Lee [ID¹⁶](#), S.C. Lee [ID¹⁴⁸](#), S. Lee [ID^{47a,47b}](#), T.F. Lee [ID⁹²](#), L.L. Leeuw [ID^{33c}](#),
 H.P. Lefebvre [ID⁹⁵](#), M. Lefebvre [ID¹⁶⁵](#), C. Leggett [ID^{17a}](#), K. Lehmann [ID¹⁴²](#), G. Lehmann Miotto [ID³⁶](#),
 M. Leigh [ID⁵⁶](#), W.A. Leight [ID¹⁰³](#), A. Leisos [ID^{152,u}](#), M.A.L. Leite [ID^{82c}](#), C.E. Leitgeb [ID⁴⁸](#), R. Leitner [ID¹³³](#),
 K.J.C. Leney [ID⁴⁴](#), T. Lenz [ID²⁴](#), S. Leone [ID^{74a}](#), C. Leonidopoulos [ID⁵²](#), A. Leopold [ID¹⁴⁴](#), C. Leroy [ID¹⁰⁸](#),
 R. Les [ID¹⁰⁷](#), C.G. Lester [ID³²](#), M. Levchenko [ID³⁷](#), J. Levêque [ID⁴](#), D. Levin [ID¹⁰⁶](#), L.J. Levinson [ID¹⁶⁹](#),
 M.P. Lewicki [ID⁸⁶](#), D.J. Lewis [ID⁴](#), A. Li [ID⁵](#), B. Li [ID^{62b}](#), C. Li^{62a}, C-Q. Li [ID^{62c}](#), H. Li [ID^{62a}](#), H. Li [ID^{62b}](#),
 H. Li [ID^{14c}](#), H. Li [ID^{62b}](#), J. Li [ID^{62c}](#), K. Li [ID¹³⁸](#), L. Li [ID^{62c}](#), M. Li [ID^{14a,14d}](#), Q.Y. Li [ID^{62a}](#), S. Li [ID^{14a,14d}](#),
 S. Li [ID^{62d,62c,e}](#), T. Li [ID^{62b}](#), X. Li [ID¹⁰⁴](#), Z. Li [ID^{62b}](#), Z. Li [ID¹²⁶](#), Z. Li [ID¹⁰⁴](#), Z. Li [ID⁹²](#), Z. Li [ID^{14a,14d}](#),
 Z. Liang [ID^{14a}](#), M. Liberatore [ID⁴⁸](#), B. Liberti [ID^{76a}](#), K. Lie [ID^{64c}](#), J. Lieber Marin [ID^{82b}](#), H. Lien [ID⁶⁸](#),
 K. Lin [ID¹⁰⁷](#), R.A. Linck [ID⁶⁸](#), R.E. Lindley [ID⁷](#), J.H. Lindon [ID²](#), A. Linss [ID⁴⁸](#), E. Lipeles [ID¹²⁸](#),
 A. Lipniacka [ID¹⁶](#), A. Lister [ID¹⁶⁴](#), J.D. Little [ID⁴](#), B. Liu [ID^{14a}](#), B.X. Liu [ID¹⁴²](#), D. Liu [ID^{62d,62c}](#),
 J.B. Liu [ID^{62a}](#), J.K.K. Liu [ID³²](#), K. Liu [ID^{62d,62c}](#), M. Liu [ID^{62a}](#), M.Y. Liu [ID^{62a}](#), P. Liu [ID^{14a}](#),
 Q. Liu [ID^{62d,138,62c}](#), X. Liu [ID^{62a}](#), Y. Liu [ID^{14c,14d}](#), Y.L. Liu [ID¹⁰⁶](#), Y.W. Liu [ID^{62a}](#), J. Llorente Merino [ID¹⁴²](#),
 S.L. Lloyd [ID⁹⁴](#), E.M. Lobodzinska [ID⁴⁸](#), P. Loch [ID⁷](#), S. Loffredo [ID^{76a,76b}](#), T. Lohse [ID¹⁸](#),
 K. Lohwasser [ID¹³⁹](#), E. Loiacono [ID⁴⁸](#), M. Lokajicek [ID^{131,*}](#), J.D. Long [ID¹⁶²](#), I. Longarini [ID¹⁶⁰](#),
 L. Longo [ID^{70a,70b}](#), R. Longo [ID¹⁶²](#), I. Lopez Paz [ID⁶⁷](#), A. Lopez Solis [ID⁴⁸](#), J. Lorenz [ID¹⁰⁹](#),
 N. Lorenzo Martinez [ID⁴](#), A.M. Lory [ID¹⁰⁹](#), X. Lou [ID^{47a,47b}](#), X. Lou [ID^{14a,14d}](#), A. Lounis [ID⁶⁶](#), J. Love [ID⁶](#),
 P.A. Love [ID⁹¹](#), G. Lu [ID^{14a,14d}](#), M. Lu [ID⁸⁰](#), S. Lu [ID¹²⁸](#), Y.J. Lu [ID⁶⁵](#), H.J. Lubatti [ID¹³⁸](#), C. Luci [ID^{75a,75b}](#),
 F.L. Lucio Alves [ID^{14c}](#), A. Lucotte [ID⁶⁰](#), F. Luehring [ID⁶⁸](#), I. Luise [ID¹⁴⁵](#), O. Lukianchuk [ID⁶⁶](#),
 O. Lundberg [ID¹⁴⁴](#), B. Lund-Jensen [ID¹⁴⁴](#), N.A. Luongo [ID¹²³](#), M.S. Lutz [ID¹⁵¹](#), D. Lynn [ID²⁹](#), H. Lyons⁹²,

R. Lysak [ID¹³¹](#), E. Lytken [ID⁹⁸](#), V. Lyubushkin [ID³⁸](#), T. Lyubushkina [ID³⁸](#), M.M. Lyukova [ID¹⁴⁵](#), H. Ma [ID²⁹](#), L.L. Ma [ID^{62b}](#), Y. Ma [ID⁹⁶](#), D.M. Mac Donell [ID¹⁶⁵](#), G. Maccarrone [ID⁵³](#), J.C. MacDonald [ID¹³⁹](#), R. Madar [ID⁴⁰](#), W.F. Mader [ID⁵⁰](#), J. Maeda [ID⁸⁴](#), T. Maeno [ID²⁹](#), M. Maerker [ID⁵⁰](#), H. Maguire [ID¹³⁹](#), A. Maio [ID^{130a,130b,130d}](#), K. Maj [ID^{85a}](#), O. Majersky [ID⁴⁸](#), S. Majewski [ID¹²³](#), N. Makovec [ID⁶⁶](#), V. Maksimovic [ID¹⁵](#), B. Malaescu [ID¹²⁷](#), Pa. Malecki [ID⁸⁶](#), V.P. Maleev [ID³⁷](#), F. Malek [ID⁶⁰](#), D. Malito [ID^{43b,43a}](#), U. Mallik [ID⁸⁰](#), C. Malone [ID³²](#), S. Maltezos¹⁰, S. Malyukov³⁸, J. Mamuzic [ID¹³](#), G. Mancini [ID⁵³](#), G. Manco [ID^{73a,73b}](#), J.P. Mandalia [ID⁹⁴](#), I. Mandić [ID⁹³](#), L. Manhaes de Andrade Filho [ID^{82a}](#), I.M. Maniatis [ID¹⁶⁹](#), J. Manjarres Ramos [ID^{102,ad}](#), D.C. Mankad [ID¹⁶⁹](#), A. Mann [ID¹⁰⁹](#), B. Mansoulie [ID¹³⁵](#), S. Manzoni [ID³⁶](#), A. Marantis [ID^{152,u}](#), G. Marchiori [ID⁵](#), M. Marcisovsky [ID¹³¹](#), C. Marcon [ID^{71a,71b}](#), M. Marinescu [ID²⁰](#), M. Marjanovic [ID¹²⁰](#), E.J. Marshall [ID⁹¹](#), Z. Marshall [ID^{17a}](#), S. Marti-Garcia [ID¹⁶³](#), T.A. Martin [ID¹⁶⁷](#), V.J. Martin [ID⁵²](#), B. Martin dit Latour [ID¹⁶](#), L. Martinelli [ID^{75a,75b}](#), M. Martinez [ID^{13,v}](#), P. Martinez Agullo [ID¹⁶³](#), V.I. Martinez Outschoorn [ID¹⁰³](#), P. Martinez Suarez [ID¹³](#), S. Martin-Haugh [ID¹³⁴](#), V.S. Martoiu [ID^{27b}](#), A.C. Martyniuk [ID⁹⁶](#), A. Marzin [ID³⁶](#), S.R. Maschek [ID¹¹⁰](#), D. Mascione [ID^{78a,78b}](#), L. Masetti [ID¹⁰⁰](#), T. Mashimo [ID¹⁵³](#), J. Masik [ID¹⁰¹](#), A.L. Maslennikov [ID³⁷](#), L. Massa [ID^{23b}](#), P. Massarotti [ID^{72a,72b}](#), P. Mastrandrea [ID^{74a,74b}](#), A. Mastroberardino [ID^{43b,43a}](#), T. Masubuchi [ID¹⁵³](#), T. Mathisen [ID¹⁶¹](#), N. Matsuzawa¹⁵³, J. Maurer [ID^{27b}](#), B. Maček [ID⁹³](#), D.A. Maximov [ID³⁷](#), R. Mazini [ID¹⁴⁸](#), I. Maznas [ID^{152,f}](#), M. Mazza [ID¹⁰⁷](#), S.M. Mazza [ID¹³⁶](#), C. Mc Ginn [ID²⁹](#), J.P. Mc Gowan [ID¹⁰⁴](#), S.P. Mc Kee [ID¹⁰⁶](#), E.F. McDonald [ID¹⁰⁵](#), A.E. McDougall [ID¹¹⁴](#), J.A. Mcfayden [ID¹⁴⁶](#), G. Mchedlidze [ID^{149b}](#), R.P. Mckenzie [ID^{33g}](#), T.C. McLachlan [ID⁴⁸](#), D.J. McLaughlin [ID⁹⁶](#), K.D. McLean [ID¹⁶⁵](#), S.J. McMahon [ID¹³⁴](#), P.C. McNamara [ID¹⁰⁵](#), C.M. Mcpartland [ID⁹²](#), R.A. McPherson [ID^{165,z}](#), T. Megy [ID⁴⁰](#), S. Mehlhase [ID¹⁰⁹](#), A. Mehta [ID⁹²](#), D. Melini [ID¹⁵⁰](#), B.R. Mellado Garcia [ID^{33g}](#), A.H. Melo [ID⁵⁵](#), F. Meloni [ID⁴⁸](#), A.M. Mendes Jacques Da Costa [ID¹⁰¹](#), H.Y. Meng [ID¹⁵⁵](#), L. Meng [ID⁹¹](#), S. Menke [ID¹¹⁰](#), M. Mentink [ID³⁶](#), E. Meoni [ID^{43b,43a}](#), C. Merlassino [ID¹²⁶](#), L. Merola [ID^{72a,72b}](#), C. Meroni [ID^{71a}](#), G. Merz¹⁰⁶, O. Meshkov [ID³⁷](#), J. Metcalfe [ID⁶](#), A.S. Mete [ID⁶](#), C. Meyer [ID⁶⁸](#), J-P. Meyer [ID¹³⁵](#), R.P. Middleton [ID¹³⁴](#), L. Mijović [ID⁵²](#), G. Mikenberg [ID¹⁶⁹](#), M. Mikestikova [ID¹³¹](#), M. Mikuž [ID⁹³](#), H. Mildner [ID¹³⁹](#), A. Milic [ID³⁶](#), C.D. Milke [ID⁴⁴](#), D.W. Miller [ID³⁹](#), L.S. Miller [ID³⁴](#), A. Milov [ID¹⁶⁹](#), D.A. Milstead^{47a,47b}, T. Min^{14c}, A.A. Minaenko [ID³⁷](#), I.A. Minashvili [ID^{149b}](#), L. Mince [ID⁵⁹](#), A.I. Mincer [ID¹¹⁷](#), B. Mindur [ID^{85a}](#), M. Mineev [ID³⁸](#), Y. Mino [ID⁸⁷](#), L.M. Mir [ID¹³](#), M. Miralles Lopez [ID¹⁶³](#), M. Mironova [ID¹²⁶](#), M.C. Missio [ID¹¹³](#), T. Mitani [ID¹⁶⁸](#), A. Mitra [ID¹⁶⁷](#), V.A. Mitsou [ID¹⁶³](#), O. Miu [ID¹⁵⁵](#), P.S. Miyagawa [ID⁹⁴](#), Y. Miyazaki⁸⁹, A. Mizukami [ID⁸³](#), T. Mkrtchyan [ID^{63a}](#), M. Mlinarevic [ID⁹⁶](#), T. Mlinarevic [ID⁹⁶](#), M. Mlynariкова [ID³⁶](#), S. Mobius [ID⁵⁵](#), K. Mochizuki [ID¹⁰⁸](#), P. Moder [ID⁴⁸](#), P. Mogg [ID¹⁰⁹](#), A.F. Mohammed [ID^{14a,14d}](#), S. Mohapatra [ID⁴¹](#), G. Mokgatitswane [ID^{33g}](#), B. Mondal [ID¹⁴¹](#), S. Mondal [ID¹³²](#), K. Mönig [ID⁴⁸](#), E. Monnier [ID¹⁰²](#), L. Monsonis Romero¹⁶³, J. Montejø Berlingen [ID⁸³](#), M. Montella [ID¹¹⁹](#), F. Monticelli [ID⁹⁰](#), N. Morange [ID⁶⁶](#), A.L. Moreira De Carvalho [ID^{130a}](#), M. Moreno Llácer [ID¹⁶³](#), C. Moreno Martinez [ID⁵⁶](#), P. Morettini [ID^{57b}](#), S. Morgenstern [ID¹⁶⁷](#), M. Morii [ID⁶¹](#), M. Morinaga [ID¹⁵³](#), A.K. Morley [ID³⁶](#), F. Morodei [ID^{75a,75b}](#), L. Morvaj [ID³⁶](#), P. Moschovakos [ID³⁶](#), B. Moser [ID³⁶](#), M. Mosidze^{149b}, T. Moskalets [ID⁵⁴](#), P. Moskvitina [ID¹¹³](#), J. Moss [ID^{31,o}](#), E.J.W. Moyse [ID¹⁰³](#), O. Mtintsilana [ID^{33g}](#), S. Muanza [ID¹⁰²](#), J. Mueller [ID¹²⁹](#), D. Muenstermann [ID⁹¹](#), R. Müller [ID¹⁹](#), G.A. Mullier [ID¹⁶¹](#), J.J. Mullin¹²⁸, D.P. Mungo [ID¹⁵⁵](#), J.L. Munoz Martinez [ID¹³](#), D. Munoz Perez [ID¹⁶³](#), F.J. Munoz Sanchez [ID¹⁰¹](#), M. Murin [ID¹⁰¹](#), W.J. Murray [ID^{167,134}](#), A. Murrone [ID^{71a,71b}](#), J.M. Muse [ID¹²⁰](#), M. Muškinja [ID^{17a}](#), C. Mwewa [ID²⁹](#), A.G. Myagkov [ID^{37,a}](#), A.J. Myers [ID⁸](#), A.A. Myers¹²⁹, G. Myers [ID⁶⁸](#), M. Myska [ID¹³²](#), B.P. Nachman [ID^{17a}](#), O. Nackenhorst [ID⁴⁹](#), A. Nag [ID⁵⁰](#), K. Nagai [ID¹²⁶](#), K. Nagano [ID⁸³](#), J.L. Nagle [ID^{29,al}](#), E. Nagy [ID¹⁰²](#), A.M. Nairz [ID³⁶](#), Y. Nakahama [ID⁸³](#), K. Nakamura [ID⁸³](#), H. Nanjo [ID¹²⁴](#), R. Narayan [ID⁴⁴](#), E.A. Narayanan [ID¹¹²](#), I. Naryshkin [ID³⁷](#), M. Naseri [ID³⁴](#), C. Nass [ID²⁴](#), G. Navarro [ID^{22a}](#), J. Navarro-Gonzalez [ID¹⁶³](#), R. Nayak [ID¹⁵¹](#), A. Nayaz [ID¹⁸](#), P.Y. Nechaeva [ID³⁷](#), F. Nechansky [ID⁴⁸](#), L. Nedic [ID¹²⁶](#), T.J. Neep [ID²⁰](#), A. Negri [ID^{73a,73b}](#), M. Negrini [ID^{23b}](#), C. Nellist [ID¹¹⁴](#), C. Nelson [ID¹⁰⁴](#), K. Nelson [ID¹⁰⁶](#), S. Nemecek [ID¹³¹](#), M. Nessi [ID^{36,i}](#), M.S. Neubauer [ID¹⁶²](#), F. Neuhaus [ID¹⁰⁰](#),

J. Neundorf [ID⁴⁸](#), R. Newhouse [ID¹⁶⁴](#), P.R. Newman [ID²⁰](#), C.W. Ng [ID¹²⁹](#), Y.W.Y. Ng [ID⁴⁸](#), B. Ngair [ID^{35e}](#), H.D.N. Nguyen [ID¹⁰⁸](#), R.B. Nickerson [ID¹²⁶](#), R. Nicolaïdou [ID¹³⁵](#), J. Nielsen [ID¹³⁶](#), M. Niemeyer [ID⁵⁵](#), N. Nikiforou [ID³⁶](#), V. Nikolaenko [ID^{37,a}](#), I. Nikolic-Audit [ID¹²⁷](#), K. Nikolopoulos [ID²⁰](#), P. Nilsson [ID²⁹](#), I. Ninca [ID⁴⁸](#), H.R. Nindhito [ID⁵⁶](#), G. Ninio [ID¹⁵¹](#), A. Nisati [ID^{75a}](#), N. Nishu [ID²](#), R. Nisius [ID¹¹⁰](#), J-E. Nitschke [ID⁵⁰](#), E.K. Nkademeng [ID^{33g}](#), S.J. Noacco Rosende [ID⁹⁰](#), T. Nobe [ID¹⁵³](#), D.L. Noel [ID³²](#), Y. Noguchi [ID⁸⁷](#), T. Nommensen [ID¹⁴⁷](#), M.A. Nomura²⁹, M.B. Norfolk [ID¹³⁹](#), R.R.B. Norisam [ID⁹⁶](#), B.J. Norman [ID³⁴](#), J. Novak [ID⁹³](#), T. Novak [ID⁴⁸](#), L. Novotny [ID¹³²](#), R. Novotny [ID¹¹²](#), L. Nozka [ID¹²²](#), K. Ntekas [ID¹⁶⁰](#), N.M.J. Nunes De Moura Junior [ID^{82b}](#), E. Nurse⁹⁶, J. Ocariz [ID¹²⁷](#), A. Ochi [ID⁸⁴](#), I. Ochoa [ID^{130a}](#), S. Oerdekk [ID¹⁶¹](#), J.T. Offermann [ID³⁹](#), A. Ogrodnik [ID^{85a}](#), A. Oh [ID¹⁰¹](#), C.C. Ohm [ID¹⁴⁴](#), H. Oide [ID⁸³](#), R. Oishi [ID¹⁵³](#), M.L. Ojeda [ID⁴⁸](#), Y. Okazaki [ID⁸⁷](#), M.W. O'Keefe⁹², Y. Okumura [ID¹⁵³](#), L.F. Oleiro Seabra [ID^{130a}](#), S.A. Olivares Pino [ID^{137d}](#), D. Oliveira Damazio [ID²⁹](#), D. Oliveira Goncalves [ID^{82a}](#), J.L. Oliver [ID¹⁶⁰](#), M.J.R. Olsson [ID¹⁶⁰](#), A. Olszewski [ID⁸⁶](#), J. Olszowska [ID^{86,*}](#), Ö.O. Öncel [ID⁵⁴](#), D.C. O'Neil [ID¹⁴²](#), A.P. O'Neill [ID¹⁹](#), A. Onofre [ID^{130a,130e}](#), P.U.E. Onyisi [ID¹¹](#), M.J. Oreglia [ID³⁹](#), G.E. Orellana [ID⁹⁰](#), D. Orestano [ID^{77a,77b}](#), N. Orlando [ID¹³](#), R.S. Orr [ID¹⁵⁵](#), V. O'Shea [ID⁵⁹](#), R. Ospanov [ID^{62a}](#), G. Otero y Garzon [ID³⁰](#), H. Otono [ID⁸⁹](#), P.S. Ott [ID^{63a}](#), G.J. Ottino [ID^{17a}](#), M. Ouchrif [ID^{35d}](#), J. Ouellette [ID²⁹](#), F. Ould-Saada [ID¹²⁵](#), M. Owen [ID⁵⁹](#), R.E. Owen [ID¹³⁴](#), K.Y. Oyulmaz [ID^{21a}](#), V.E. Ozcan [ID^{21a}](#), N. Ozturk [ID⁸](#), S. Ozturk [ID^{21d}](#), H.A. Pacey [ID³²](#), K. Pachal [ID⁵¹](#), A. Pacheco Pages [ID¹³](#), C. Padilla Aranda [ID¹³](#), G. Padovano [ID^{75a,75b}](#), S. Pagan Griso [ID^{17a}](#), G. Palacino [ID⁶⁸](#), A. Palazzo [ID^{70a,70b}](#), S. Palestini [ID³⁶](#), J. Pan [ID¹⁷²](#), T. Pan [ID^{64a}](#), D.K. Panchal [ID¹¹](#), C.E. Pandini [ID¹¹⁴](#), J.G. Panduro Vazquez [ID⁹⁵](#), H. Pang [ID^{14b}](#), P. Pani [ID⁴⁸](#), G. Panizzo [ID^{69a,69c}](#), L. Paolozzi [ID⁵⁶](#), C. Papadatos [ID¹⁰⁸](#), S. Parajuli [ID⁴⁴](#), A. Paramonov [ID⁶](#), C. Paraskevopoulos [ID¹⁰](#), D. Paredes Hernandez [ID^{64b}](#), T.H. Park [ID¹⁵⁵](#), M.A. Parker [ID³²](#), F. Parodi [ID^{57b,57a}](#), E.W. Parrish [ID¹¹⁵](#), V.A. Parrish [ID⁵²](#), J.A. Parsons [ID⁴¹](#), U. Parzefall [ID⁵⁴](#), B. Pascual Dias [ID¹⁰⁸](#), L. Pascual Dominguez [ID¹⁵¹](#), F. Pasquali [ID¹¹⁴](#), E. Pasqualucci [ID^{75a}](#), S. Passaggio [ID^{57b}](#), F. Pastore [ID⁹⁵](#), P. Pasuwani [ID^{47a,47b}](#), P. Patel [ID⁸⁶](#), U.M. Patel [ID⁵¹](#), J.R. Pater [ID¹⁰¹](#), T. Pauly [ID³⁶](#), J. Pearkes [ID¹⁴³](#), M. Pedersen [ID¹²⁵](#), R. Pedro [ID^{130a}](#), S.V. Peleganchuk [ID³⁷](#), O. Penc [ID³⁶](#), E.A. Pender [ID⁵²](#), H. Peng [ID^{62a}](#), K.E. Penski [ID¹⁰⁹](#), M. Penzin [ID³⁷](#), B.S. Peralva [ID^{82d}](#), A.P. Pereira Peixoto [ID⁶⁰](#), L. Pereira Sanchez [ID^{47a,47b}](#), D.V. Perepelitsa [ID^{29,al}](#), E. Perez Codina [ID^{156a}](#), M. Perganti [ID¹⁰](#), L. Perini [ID^{71a,71b,*}](#), H. Pernegger [ID³⁶](#), S. Perrella [ID³⁶](#), A. Perrevoort [ID¹¹³](#), O. Perrin [ID⁴⁰](#), K. Peters [ID⁴⁸](#), R.F.Y. Peters [ID¹⁰¹](#), B.A. Petersen [ID³⁶](#), T.C. Petersen [ID⁴²](#), E. Petit [ID¹⁰²](#), V. Petousis [ID¹³²](#), C. Petridou [ID^{152,f}](#), A. Petrukhin [ID¹⁴¹](#), M. Pettee [ID^{17a}](#), N.E. Pettersson [ID³⁶](#), A. Petukhov [ID³⁷](#), K. Petukhova [ID¹³³](#), A. Peyaud [ID¹³⁵](#), R. Pezoa [ID^{137f}](#), L. Pezzotti [ID³⁶](#), G. Pezzullo [ID¹⁷²](#), T.M. Pham [ID¹⁷⁰](#), T. Pham [ID¹⁰⁵](#), P.W. Phillips [ID¹³⁴](#), M.W. Phipps [ID¹⁶²](#), G. Piacquadio [ID¹⁴⁵](#), E. Pianori [ID^{17a}](#), F. Piazza [ID^{71a,71b}](#), R. Piegaia [ID³⁰](#), D. Pietreanu [ID^{27b}](#), A.D. Pilkington [ID¹⁰¹](#), M. Pinamonti [ID^{69a,69c}](#), J.L. Pinfold [ID²](#), B.C. Pinheiro Pereira [ID^{130a}](#), C. Pitman Donaldson⁹⁶, D.A. Pizzi [ID³⁴](#), L. Pizzimento [ID^{76a,76b}](#), A. Pizzini [ID¹¹⁴](#), M.-A. Pleier [ID²⁹](#), V. Plesanovs⁵⁴, V. Pleskot [ID¹³³](#), E. Plotnikova³⁸, G. Poddar [ID⁴](#), R. Poettgen [ID⁹⁸](#), L. Poggioli [ID¹²⁷](#), D. Pohl [ID²⁴](#), I. Pokharel [ID⁵⁵](#), S. Polacek [ID¹³³](#), G. Polesello [ID^{73a}](#), A. Poley [ID^{142,156a}](#), R. Polifka [ID¹³²](#), A. Polini [ID^{23b}](#), C.S. Pollard [ID¹⁶⁷](#), Z.B. Pollock [ID¹¹⁹](#), V. Polychronakos [ID²⁹](#), E. Pompa Pacchi [ID^{75a,75b}](#), D. Ponomarenko [ID¹¹³](#), L. Pontecorvo [ID³⁶](#), S. Popa [ID^{27a}](#), G.A. Popeneciu [ID^{27d}](#), D.M. Portillo Quintero [ID^{156a}](#), S. Pospisil [ID¹³²](#), P. Postolache [ID^{27c}](#), K. Potamianos [ID¹²⁶](#), P.A. Potepa [ID^{85a}](#), I.N. Potrap [ID³⁸](#), C.J. Potter [ID³²](#), H. Potti [ID¹](#), T. Poulsen [ID⁴⁸](#), J. Poveda [ID¹⁶³](#), M.E. Pozo Astigarraga [ID³⁶](#), A. Prades Ibanez [ID¹⁶³](#), M.M. Prapa [ID⁴⁶](#), J. Pretel [ID⁵⁴](#), D. Price [ID¹⁰¹](#), M. Primavera [ID^{70a}](#), M.A. Principe Martin [ID⁹⁹](#), R. Privara [ID¹²²](#), M.L. Proffitt [ID¹³⁸](#), N. Proklova [ID¹²⁸](#), K. Prokofiev [ID^{64c}](#), G. Proto [ID^{76a,76b}](#), S. Protopopescu [ID²⁹](#), J. Proudfoot [ID⁶](#), M. Przybycien [ID^{85a}](#), W.W. Przygoda [ID^{85b}](#), J.E. Puddefoot [ID¹³⁹](#), D. Pudzha [ID³⁷](#), D. Pyatiizbyantseva [ID³⁷](#), J. Qian [ID¹⁰⁶](#), D. Qichen [ID¹⁰¹](#), Y. Qin [ID¹⁰¹](#), T. Qiu [ID⁹⁴](#), A. Quadt [ID⁵⁵](#), M. Queitsch-Maitland [ID¹⁰¹](#), G. Quetant [ID⁵⁶](#), G. Rabanal Bolanos [ID⁶¹](#), D. Rafanoharana [ID⁵⁴](#), F. Ragusa [ID^{71a,71b}](#), J.L. Rainbolt [ID³⁹](#), J.A. Raine [ID⁵⁶](#), S. Rajagopalan [ID²⁹](#), E. Ramakoti [ID³⁷](#), K. Ran [ID^{48,14d}](#), N.P. Rapheeha [ID^{33g}](#), V. Raskina [ID¹²⁷](#), D.F. Rassloff [ID^{63a}](#), S. Rave [ID¹⁰⁰](#),

- B. Ravina [ID⁵⁵](#), I. Ravinovich [ID¹⁶⁹](#), M. Raymond [ID³⁶](#), A.L. Read [ID¹²⁵](#), N.P. Readioff [ID¹³⁹](#), D.M. Rebuzzi [ID^{73a,73b}](#), G. Redlinger [ID²⁹](#), K. Reeves [ID⁴⁵](#), J.A. Reidelsturz [ID¹⁷¹](#), D. Reikher [ID¹⁵¹](#), A. Rej [ID¹⁴¹](#), C. Rembser [ID³⁶](#), A. Renardi [ID⁴⁸](#), M. Renda [ID^{27b}](#), M.B. Rendel [ID¹¹⁰](#), F. Renner [ID⁴⁸](#), A.G. Rennie [ID⁵⁹](#), S. Resconi [ID^{71a}](#), M. Ressegotti [ID^{57b,57a}](#), E.D. Ressegueie [ID^{17a}](#), S. Rettie [ID³⁶](#), J.G. Reyes Rivera [ID¹⁰⁷](#), B. Reynolds [ID¹¹⁹](#), E. Reynolds [ID^{17a}](#), M. Rezaei Estabragh [ID¹⁷¹](#), O.L. Rezanova [ID³⁷](#), P. Reznicek [ID¹³³](#), N. Ribaric [ID⁹¹](#), E. Ricci [ID^{78a,78b}](#), R. Richter [ID¹¹⁰](#), S. Richter [ID^{47a,47b}](#), E. Richter-Was [ID^{85b}](#), M. Ridel [ID¹²⁷](#), S. Ridouani [ID^{35d}](#), P. Rieck [ID¹¹⁷](#), P. Riedler [ID³⁶](#), M. Rijssenbeek [ID¹⁴⁵](#), A. Rimoldi [ID^{73a,73b}](#), M. Rimoldi [ID⁴⁸](#), L. Rinaldi [ID^{23b,23a}](#), T.T. Rinn [ID²⁹](#), M.P. Rinnagel [ID¹⁰⁹](#), G. Ripellino [ID¹⁶¹](#), I. Riu [ID¹³](#), P. Rivadeneira [ID⁴⁸](#), J.C. Rivera Vergara [ID¹⁶⁵](#), F. Rizatdinova [ID¹²¹](#), E. Rizvi [ID⁹⁴](#), C. Rizzi [ID⁵⁶](#), B.A. Roberts [ID¹⁶⁷](#), B.R. Roberts [ID^{17a}](#), S.H. Robertson [ID^{104,z}](#), M. Robin [ID⁴⁸](#), D. Robinson [ID³²](#), C.M. Robles Gajardo [ID^{137f}](#), M. Robles Manzano [ID¹⁰⁰](#), A. Robson [ID⁵⁹](#), A. Rocchi [ID^{76a,76b}](#), C. Roda [ID^{74a,74b}](#), S. Rodriguez Bosca [ID^{63a}](#), Y. Rodriguez Garcia [ID^{22a}](#), A. Rodriguez Rodriguez [ID⁵⁴](#), A.M. Rodríguez Vera [ID^{156b}](#), S. Roe [ID³⁶](#), J.T. Roemer [ID¹⁶⁰](#), A.R. Roepe-Gier [ID¹³⁶](#), J. Roggel [ID¹⁷¹](#), O. Røhne [ID¹²⁵](#), R.A. Rojas [ID¹⁰³](#), B. Roland [ID⁵⁴](#), C.P.A. Roland [ID⁶⁸](#), J. Roloff [ID²⁹](#), A. Romanouk [ID³⁷](#), E. Romano [ID^{73a,73b}](#), M. Romano [ID^{23b}](#), A.C. Romero Hernandez [ID¹⁶²](#), N. Rompotis [ID⁹²](#), L. Roos [ID¹²⁷](#), S. Rosati [ID^{75a}](#), B.J. Rosser [ID³⁹](#), E. Rossi [ID⁴](#), E. Rossi [ID^{72a,72b}](#), L.P. Rossi [ID^{57b}](#), L. Rossini [ID⁴⁸](#), R. Rosten [ID¹¹⁹](#), M. Rotaru [ID^{27b}](#), B. Rottler [ID⁵⁴](#), C. Rougier [ID^{102,ad}](#), D. Rousseau [ID⁶⁶](#), D. Rousso [ID³²](#), G. Rovelli [ID^{73a,73b}](#), A. Roy [ID¹⁶²](#), S. Roy-Garand [ID¹⁵⁵](#), A. Rozanov [ID¹⁰²](#), Y. Rozen [ID¹⁵⁰](#), X. Ruan [ID^{33g}](#), A. Rubio Jimenez [ID¹⁶³](#), A.J. Ruby [ID⁹²](#), V.H. Ruelas Rivera [ID¹⁸](#), T.A. Ruggeri [ID¹](#), F. Rühr [ID⁵⁴](#), A. Ruiz-Martinez [ID¹⁶³](#), A. Rummler [ID³⁶](#), Z. Rurikova [ID⁵⁴](#), N.A. Rusakovich [ID³⁸](#), H.L. Russell [ID¹⁶⁵](#), J.P. Rutherford [ID⁷](#), K. Rybacki [ID⁹¹](#), M. Rybar [ID¹³³](#), E.B. Rye [ID¹²⁵](#), A. Ryzhov [ID³⁷](#), J.A. Sabater Iglesias [ID⁵⁶](#), P. Sabatini [ID¹⁶³](#), L. Sabetta [ID^{75a,75b}](#), H.F-W. Sadrozinski [ID¹³⁶](#), F. Safai Tehrani [ID^{75a}](#), B. Safarzadeh Samani [ID¹⁴⁶](#), M. Safdarri [ID¹⁴³](#), S. Saha [ID¹⁰⁴](#), M. Sahin soy [ID¹¹⁰](#), M. Saimpert [ID¹³⁵](#), M. Saito [ID¹⁵³](#), T. Saito [ID¹⁵³](#), D. Salamani [ID³⁶](#), A. Salnikov [ID¹⁴³](#), J. Salt [ID¹⁶³](#), A. Salvador Salas [ID¹³](#), D. Salvatore [ID^{43b,43a}](#), F. Salvatore [ID¹⁴⁶](#), A. Salzburger [ID³⁶](#), D. Sammel [ID⁵⁴](#), D. Sampsonidis [ID^{152,f}](#), D. Sampsonidou [ID^{62d,62c}](#), J. Sánchez [ID¹⁶³](#), A. Sanchez Pineda [ID⁴](#), V. Sanchez Sebastian [ID¹⁶³](#), H. Sandaker [ID¹²⁵](#), C.O. Sander [ID⁴⁸](#), J.A. Sandesara [ID¹⁰³](#), M. Sandhoff [ID¹⁷¹](#), C. Sandoval [ID^{22b}](#), D.P.C. Sankey [ID¹³⁴](#), T. Sano [ID⁸⁷](#), A. Sansoni [ID⁵³](#), L. Santi [ID^{75a,75b}](#), C. Santoni [ID⁴⁰](#), H. Santos [ID^{130a,130b}](#), S.N. Santpur [ID^{17a}](#), A. Santra [ID¹⁶⁹](#), K.A. Saoucha [ID¹³⁹](#), J.G. Saraiva [ID^{130a,130d}](#), J. Sardain [ID⁷](#), O. Sasaki [ID⁸³](#), K. Sato [ID¹⁵⁷](#), C. Sauer [ID^{63b}](#), F. Sauerburger [ID⁵⁴](#), E. Sauvan [ID⁴](#), P. Savard [ID^{155,ai}](#), R. Sawada [ID¹⁵³](#), C. Sawyer [ID¹³⁴](#), L. Sawyer [ID⁹⁷](#), I. Sayago Galvan [ID¹⁶³](#), C. Sbarra [ID^{23b}](#), A. Sbrizzi [ID^{23b,23a}](#), T. Scanlon [ID⁹⁶](#), J. Schaarschmidt [ID¹³⁸](#), P. Schacht [ID¹¹⁰](#), D. Schaefer [ID³⁹](#), U. Schäfer [ID¹⁰⁰](#), A.C. Schaffer [ID^{66,44}](#), D. Schaile [ID¹⁰⁹](#), R.D. Schamberger [ID¹⁴⁵](#), E. Schanet [ID¹⁰⁹](#), C. Scharf [ID¹⁸](#), M.M. Schefer [ID¹⁹](#), V.A. Schegelsky [ID³⁷](#), D. Scheirich [ID¹³³](#), F. Schenck [ID¹⁸](#), M. Schernau [ID¹⁶⁰](#), C. Scheulen [ID⁵⁵](#), C. Schiavi [ID^{57b,57a}](#), Z.M. Schillaci [ID²⁶](#), E.J. Schioppa [ID^{70a,70b}](#), M. Schioppa [ID^{43b,43a}](#), B. Schlag [ID¹⁰⁰](#), K.E. Schleicher [ID⁵⁴](#), S. Schlenker [ID³⁶](#), J. Schmeing [ID¹⁷¹](#), M.A. Schmidt [ID¹⁷¹](#), K. Schmieden [ID¹⁰⁰](#), C. Schmitt [ID¹⁰⁰](#), S. Schmitt [ID⁴⁸](#), L. Schoeffel [ID¹³⁵](#), A. Schoening [ID^{63b}](#), P.G. Scholer [ID⁵⁴](#), E. Schopf [ID¹²⁶](#), M. Schott [ID¹⁰⁰](#), J. Schovancova [ID³⁶](#), S. Schramm [ID⁵⁶](#), F. Schroeder [ID¹⁷¹](#), H-C. Schultz-Coulon [ID^{63a}](#), M. Schumacher [ID⁵⁴](#), B.A. Schumm [ID¹³⁶](#), Ph. Schune [ID¹³⁵](#), H.R. Schwartz [ID¹³⁶](#), A. Schwartzman [ID¹⁴³](#), T.A. Schwarz [ID¹⁰⁶](#), Ph. Schwemling [ID¹³⁵](#), R. Schwienhorst [ID¹⁰⁷](#), A. Sciandra [ID¹³⁶](#), G. Sciolla [ID²⁶](#), F. Scuri [ID^{74a}](#), F. Scutti [ID¹⁰⁵](#), C.D. Sebastiani [ID⁹²](#), K. Sedlaczek [ID⁴⁹](#), P. Seema [ID¹⁸](#), S.C. Seidel [ID¹¹²](#), A. Seiden [ID¹³⁶](#), B.D. Seidlitz [ID⁴¹](#), C. Seitz [ID⁴⁸](#), J.M. Seixas [ID^{82b}](#), G. Sekhniaidze [ID^{72a}](#), S.J. Sekula [ID⁴⁴](#), L. Selem [ID⁴](#), N. Semprini-Cesari [ID^{23b,23a}](#), S. Sen [ID⁵¹](#), D. Sengupta [ID⁵⁶](#), V. Senthilkumar [ID¹⁶³](#), L. Serin [ID⁶⁶](#), L. Serkin [ID^{69a,69b}](#), M. Sessa [ID^{77a,77b}](#), H. Severini [ID¹²⁰](#), F. Sforza [ID^{57b,57a}](#), A. Sfyrla [ID⁵⁶](#), E. Shabalina [ID⁵⁵](#), R. Shaheen [ID¹⁴⁴](#), J.D. Shahinian [ID¹²⁸](#), D. Shaked Renous [ID¹⁶⁹](#), L.Y. Shan [ID^{14a}](#), M. Shapiro [ID^{17a}](#), A. Sharma [ID³⁶](#),

A.S. Sharma [ID¹⁶⁴](#), P. Sharma [ID⁸⁰](#), S. Sharma [ID⁴⁸](#), P.B. Shatalov [ID³⁷](#), K. Shaw [ID¹⁴⁶](#), S.M. Shaw [ID¹⁰¹](#), Q. Shen [ID^{62c,5}](#), P. Sherwood [ID⁹⁶](#), L. Shi [ID⁹⁶](#), C.O. Shimmin [ID¹⁷²](#), Y. Shimogama [ID¹⁶⁸](#), J.D. Shinner [ID⁹⁵](#), I.P.J. Shipsey [ID¹²⁶](#), S. Shirabe [ID⁶⁰](#), M. Shiyakova [ID^{38,x}](#), J. Shlomi [ID¹⁶⁹](#), M.J. Shochet [ID³⁹](#), J. Shojaii [ID¹⁰⁵](#), D.R. Shope [ID¹²⁵](#), S. Shrestha [ID^{119,am}](#), E.M. Shrif [ID^{33g}](#), M.J. Shroff [ID¹⁶⁵](#), P. Sicho [ID¹³¹](#), A.M. Sickles [ID¹⁶²](#), E. Sideras Haddad [ID^{33g}](#), A. Sidoti [ID^{23b}](#), F. Siegert [ID⁵⁰](#), Dj. Sijacki [ID¹⁵](#), R. Sikora [ID^{85a}](#), F. Sili [ID⁹⁰](#), J.M. Silva [ID²⁰](#), M.V. Silva Oliveira [ID³⁶](#), S.B. Silverstein [ID^{47a}](#), S. Simion [ID⁶⁶](#), R. Simoniello [ID³⁶](#), E.L. Simpson [ID⁵⁹](#), H. Simpson [ID¹⁴⁶](#), L.R. Simpson [ID¹⁰⁶](#), N.D. Simpson [ID⁹⁸](#), S. Simsek [ID^{21d}](#), S. Sindhu [ID⁵⁵](#), P. Sinervo [ID¹⁵⁵](#), S. Singh [ID¹⁴²](#), S. Singh [ID¹⁵⁵](#), S. Sinha [ID⁴⁸](#), S. Sinha [ID^{33g}](#), M. Sioli [ID^{23b,23a}](#), I. Siral [ID³⁶](#), S.Yu. Sivoklokov [ID^{37,*}](#), J. Sjölin [ID^{47a,47b}](#), A. Skaf [ID⁵⁵](#), E. Skorda [ID⁹⁸](#), P. Skubic [ID¹²⁰](#), M. Slawinska [ID⁸⁶](#), V. Smakhtin [ID¹⁶⁹](#), B.H. Smart [ID¹³⁴](#), J. Smiesko [ID³⁶](#), S.Yu. Smirnov [ID³⁷](#), Y. Smirnov [ID³⁷](#), L.N. Smirnova [ID^{37,a}](#), O. Smirnova [ID⁹⁸](#), A.C. Smith [ID⁴¹](#), E.A. Smith [ID³⁹](#), H.A. Smith [ID¹²⁶](#), J.L. Smith [ID⁹²](#), R. Smith [ID¹⁴³](#), M. Smizanska [ID⁹¹](#), K. Smolek [ID¹³²](#), A. Smykiewicz [ID⁸⁶](#), A.A. Snesarev [ID³⁷](#), H.L. Snoek [ID¹¹⁴](#), S. Snyder [ID²⁹](#), R. Sobie [ID^{165,z}](#), A. Soffer [ID¹⁵¹](#), C.A. Solans Sanchez [ID³⁶](#), E.Yu. Soldatov [ID³⁷](#), U. Soldevila [ID¹⁶³](#), A.A. Solodkov [ID³⁷](#), S. Solomon [ID⁵⁴](#), A. Soloshenko [ID³⁸](#), K. Solovieva [ID⁵⁴](#), O.V. Solovyanov [ID⁴⁰](#), V. Solovyev [ID³⁷](#), P. Sommer [ID³⁶](#), A. Sonay [ID¹³](#), W.Y. Song [ID^{156b}](#), J.M. Sonneveld [ID¹¹⁴](#), A. Sopczak [ID¹³²](#), A.L. Sopio [ID⁹⁶](#), F. Sopkova [ID^{28b}](#), V. Sothilingam [ID^{63a}](#), S. Sottocornola [ID⁶⁸](#), R. Soualah [ID^{116b}](#), Z. Soumaini [ID^{35e}](#), D. South [ID⁴⁸](#), S. Spagnolo [ID^{70a,70b}](#), M. Spalla [ID¹¹⁰](#), D. Sperlich [ID⁵⁴](#), G. Spigo [ID³⁶](#), M. Spina [ID¹⁴⁶](#), S. Spinali [ID⁹¹](#), D.P. Spiteri [ID⁵⁹](#), M. Spousta [ID¹³³](#), E.J. Staats [ID³⁴](#), A. Stabile [ID^{71a,71b}](#), R. Stamen [ID^{63a}](#), M. Stamenkovic [ID¹¹⁴](#), A. Stampeki [ID²⁰](#), M. Standke [ID²⁴](#), E. Stanecka [ID⁸⁶](#), M.V. Stange [ID⁵⁰](#), B. Stanislaus [ID^{17a}](#), M.M. Stanitzki [ID⁴⁸](#), M. Stankaityte [ID¹²⁶](#), B. Stapp [ID⁴⁸](#), E.A. Starchenko [ID³⁷](#), G.H. Stark [ID¹³⁶](#), J. Stark [ID^{102,ad}](#), D.M. Starko [ID^{156b}](#), P. Staroba [ID¹³¹](#), P. Starovoitov [ID^{63a}](#), S. Stärz [ID¹⁰⁴](#), R. Staszewski [ID⁸⁶](#), G. Stavropoulos [ID⁴⁶](#), J. Steentoft [ID¹⁶¹](#), P. Steinberg [ID²⁹](#), B. Stelzer [ID^{142,156a}](#), H.J. Stelzer [ID¹²⁹](#), O. Stelzer-Chilton [ID^{156a}](#), H. Stenzel [ID⁵⁸](#), T.J. Stevenson [ID¹⁴⁶](#), G.A. Stewart [ID³⁶](#), J.R. Stewart [ID¹²¹](#), M.C. Stockton [ID³⁶](#), G. Stoicea [ID^{27b}](#), M. Stolarski [ID^{130a}](#), S. Stonjek [ID¹¹⁰](#), A. Straessner [ID⁵⁰](#), J. Strandberg [ID¹⁴⁴](#), S. Strandberg [ID^{47a,47b}](#), M. Strauss [ID¹²⁰](#), T. Strebler [ID¹⁰²](#), P. Strizenec [ID^{28b}](#), R. Ströhmer [ID¹⁶⁶](#), D.M. Strom [ID¹²³](#), L.R. Strom [ID⁴⁸](#), R. Stroynowski [ID⁴⁴](#), A. Strubig [ID^{47a,47b}](#), S.A. Stucci [ID²⁹](#), B. Stugu [ID¹⁶](#), J. Stupak [ID¹²⁰](#), N.A. Styles [ID⁴⁸](#), D. Su [ID¹⁴³](#), S. Su [ID^{62a}](#), W. Su [ID^{62d,138,62c}](#), X. Su [ID^{62a,66}](#), K. Sugizaki [ID¹⁵³](#), V.V. Sulin [ID³⁷](#), M.J. Sullivan [ID⁹²](#), D.M.S. Sultan [ID^{78a,78b}](#), L. Sultanaliyeva [ID³⁷](#), S. Sultansoy [ID^{3b}](#), T. Sumida [ID⁸⁷](#), S. Sun [ID¹⁰⁶](#), S. Sun [ID¹⁷⁰](#), O. Sunneborn Gudnadottir [ID¹⁶¹](#), M.R. Sutton [ID¹⁴⁶](#), M. Svatos [ID¹³¹](#), M. Swiatlowski [ID^{156a}](#), T. Swirski [ID¹⁶⁶](#), I. Sykora [ID^{28a}](#), M. Sykora [ID¹³³](#), T. Sykora [ID¹³³](#), D. Ta [ID¹⁰⁰](#), K. Tackmann [ID^{48,w}](#), A. Taffard [ID¹⁶⁰](#), R. Tafirout [ID^{156a}](#), J.S. Tafoya Vargas [ID⁶⁶](#), R.H.M. Taibah [ID¹²⁷](#), R. Takashima [ID⁸⁸](#), E.P. Takeva [ID⁵²](#), Y. Takubo [ID⁸³](#), M. Talby [ID¹⁰²](#), A.A. Talyshев [ID³⁷](#), K.C. Tam [ID^{64b}](#), N.M. Tamir [ID¹⁵¹](#), A. Tanaka [ID¹⁵³](#), J. Tanaka [ID¹⁵³](#), R. Tanaka [ID⁶⁶](#), M. Tanasimi [ID^{57b,57a}](#), J. Tang [ID^{62c}](#), Z. Tao [ID¹⁶⁴](#), S. Tapia Araya [ID^{137f}](#), S. Tapprogge [ID¹⁰⁰](#), A. Tarek Abouelfadl Mohamed [ID¹⁰⁷](#), S. Tarem [ID¹⁵⁰](#), K. Tariq [ID^{62b}](#), G. Tarna [ID^{102,27b}](#), G.F. Tartarelli [ID^{71a}](#), P. Tas [ID¹³³](#), M. Tasevsky [ID¹³¹](#), E. Tassi [ID^{43b,43a}](#), A.C. Tate [ID¹⁶²](#), G. Tateno [ID¹⁵³](#), Y. Tayalati [ID^{35e,y}](#), G.N. Taylor [ID¹⁰⁵](#), W. Taylor [ID^{156b}](#), H. Teagle [ID⁹²](#), A.S. Tee [ID¹⁷⁰](#), R. Teixeira De Lima [ID¹⁴³](#), P. Teixeira-Dias [ID⁹⁵](#), J.J. Teoh [ID¹⁵⁵](#), K. Terashi [ID¹⁵³](#), J. Terron [ID⁹⁹](#), S. Terzo [ID¹³](#), M. Testa [ID⁵³](#), R.J. Teuscher [ID^{155,z}](#), A. Thaler [ID⁷⁹](#), O. Theiner [ID⁵⁶](#), N. Themistokleous [ID⁵²](#), T. Theveneaux-Pelzer [ID¹⁰²](#), O. Thielmann [ID¹⁷¹](#), D.W. Thomas [ID⁹⁵](#), J.P. Thomas [ID²⁰](#), E.A. Thompson [ID^{17a}](#), P.D. Thompson [ID²⁰](#), E. Thomson [ID¹²⁸](#), E.J. Thorpe [ID⁹⁴](#), Y. Tian [ID⁵⁵](#), V. Tikhomirov [ID^{37,a}](#), Yu.A. Tikhonov [ID³⁷](#), S. Timoshenko [ID³⁷](#), E.X.L. Ting [ID¹](#), P. Tipton [ID¹⁷²](#), S.H. Tlou [ID^{33g}](#), A. Tnourji [ID⁴⁰](#), K. Todome [ID^{23b,23a}](#), S. Todorova-Nova [ID¹³³](#), S. Todt [ID⁵⁰](#), M. Togawa [ID⁸³](#), J. Tojo [ID⁸⁹](#), S. Tokár [ID^{28a}](#), K. Tokushuku [ID⁸³](#), O. Toldaiev [ID⁶⁸](#), R. Tombs [ID³²](#), M. Tomoto [ID^{83,111}](#), L. Tompkins [ID^{143,q}](#), K.W. Topolnicki [ID^{85b}](#), P. Tornambe [ID¹⁰³](#), E. Torrence [ID¹²³](#), H. Torres [ID⁵⁰](#), E. Torró Pastor [ID¹⁶³](#), M. Toscani [ID³⁰](#), C. Tosciri [ID³⁹](#), M. Tost [ID¹¹](#), D.R. Tovey [ID¹³⁹](#), A. Traeet [ID¹⁶](#),

I.S. Trandafir [ID^{27b}](#), T. Trefzger [ID¹⁶⁶](#), A. Tricoli [ID²⁹](#), I.M. Trigger [ID^{156a}](#), S. Trincaz-Duvold [ID¹²⁷](#),
 D.A. Trischuk [ID²⁶](#), B. Trocmé [ID⁶⁰](#), C. Troncon [ID^{71a}](#), L. Truong [ID^{33c}](#), M. Trzebinski [ID⁸⁶](#), A. Trzupek [ID⁸⁶](#),
 F. Tsai [ID¹⁴⁵](#), M. Tsai [ID¹⁰⁶](#), A. Tsiamis [ID^{152,f}](#), P.V. Tsiareshka³⁷, S. Tsigaridas [ID^{156a}](#), A. Tsirigotis [ID^{152,u}](#),
 V. Tsiskaridze [ID¹⁴⁵](#), E.G. Tskhadadze [ID^{149a}](#), M. Tsopoulou [ID^{152,f}](#), Y. Tsujikawa [ID⁸⁷](#), I.I. Tsukerman [ID³⁷](#),
 V. Tsulaia [ID^{17a}](#), S. Tsuno [ID⁸³](#), O. Tsur [ID¹⁵⁰](#), D. Tsybychev [ID¹⁴⁵](#), Y. Tu [ID^{64b}](#), A. Tudorache [ID^{27b}](#),
 V. Tudorache [ID^{27b}](#), A.N. Tuna [ID³⁶](#), S. Turchikhin [ID³⁸](#), I. Turk Cakir [ID^{3a}](#), R. Turra [ID^{71a}](#),
 T. Turtuvshin [ID^{38,aa}](#), P.M. Tuts [ID⁴¹](#), S. Tzamarias [ID^{152,f}](#), P. Tzanis [ID¹⁰](#), E. Tzovara [ID¹⁰⁰](#), K. Uchida¹⁵³,
 F. Ukegawa [ID¹⁵⁷](#), P.A. Ulloa Poblete [ID^{137c}](#), E.N. Umaka [ID²⁹](#), G. Unal [ID³⁶](#), M. Unal [ID¹¹](#), A. Undrus [ID²⁹](#),
 G. Unel [ID¹⁶⁰](#), J. Urban [ID^{28b}](#), P. Urquijo [ID¹⁰⁵](#), G. Usai [ID⁸](#), R. Ushioda [ID¹⁵⁴](#), M. Usman [ID¹⁰⁸](#),
 Z. Uysal [ID^{21b}](#), L. Vacavant [ID¹⁰²](#), V. Vacek [ID¹³²](#), B. Vachon [ID¹⁰⁴](#), K.O.H. Vadla [ID¹²⁵](#), T. Vafeiadis [ID³⁶](#),
 A. Vaitkus [ID⁹⁶](#), C. Valderanis [ID¹⁰⁹](#), E. Valdes Santurio [ID^{47a,47b}](#), M. Valente [ID^{156a}](#), S. Valentinetto [ID^{23b,23a}](#),
 A. Valero [ID¹⁶³](#), A. Vallier [ID^{102,ad}](#), J.A. Valls Ferrer [ID¹⁶³](#), D.R. Van Arneman [ID¹¹⁴](#), T.R. Van Daalen [ID¹³⁸](#),
 P. Van Gemmeren [ID⁶](#), M. Van Rijnbach [ID^{125,36}](#), S. Van Stroud [ID⁹⁶](#), I. Van Vulpen [ID¹¹⁴](#),
 M. Vanadia [ID^{76a,76b}](#), W. Vandelli [ID³⁶](#), M. Vandenbroucke [ID¹³⁵](#), E.R. Vandewall [ID¹²¹](#), D. Vannicola [ID¹⁵¹](#),
 L. Vannoli [ID^{57b,57a}](#), R. Vari [ID^{75a}](#), E.W. Varnes [ID⁷](#), C. Varni [ID^{17a}](#), T. Varol [ID¹⁴⁸](#), D. Varouchas [ID⁶⁶](#),
 L. Varriale [ID¹⁶³](#), K.E. Varvell [ID¹⁴⁷](#), M.E. Vasile [ID^{27b}](#), L. Vaslin⁴⁰, G.A. Vasquez [ID¹⁶⁵](#), F. Vazeille [ID⁴⁰](#),
 T. Vazquez Schroeder [ID³⁶](#), J. Veatch [ID³¹](#), V. Vecchio [ID¹⁰¹](#), M.J. Veen [ID¹⁰³](#), I. Veliseck [ID¹²⁶](#),
 L.M. Veloce [ID¹⁵⁵](#), F. Veloso [ID^{130a,130c}](#), S. Veneziano [ID^{75a}](#), A. Ventura [ID^{70a,70b}](#), A. Verbytskyi [ID¹¹⁰](#),
 M. Verducci [ID^{74a,74b}](#), C. Vergis [ID²⁴](#), M. Verissimo De Araujo [ID^{82b}](#), W. Verkerke [ID¹¹⁴](#),
 J.C. Vermeulen [ID¹¹⁴](#), C. Vernieri [ID¹⁴³](#), P.J. Verschuuren [ID⁹⁵](#), M. Vessella [ID¹⁰³](#), M.C. Vetterli [ID^{142,ai}](#),
 A. Vgenopoulos [ID^{152,f}](#), N. Viaux Maira [ID^{137f}](#), T. Vickey [ID¹³⁹](#), O.E. Vickey Boeriu [ID¹³⁹](#),
 G.H.A. Viehhäuser [ID¹²⁶](#), L. Vigani [ID^{63b}](#), M. Villa [ID^{23b,23a}](#), M. Villaplana Perez [ID¹⁶³](#), E.M. Villhauer⁵²,
 E. Vilucchi [ID⁵³](#), M.G. Vincter [ID³⁴](#), G.S. Virdee [ID²⁰](#), A. Vishwakarma [ID⁵²](#), C. Vittori [ID³⁶](#),
 I. Vivarelli [ID¹⁴⁶](#), V. Vladimirov¹⁶⁷, E. Voevodina [ID¹¹⁰](#), F. Vogel [ID¹⁰⁹](#), P. Vokac [ID¹³²](#), J. Von Ahnen [ID⁴⁸](#),
 E. Von Toerne [ID²⁴](#), B. Vormwald [ID³⁶](#), V. Vorobel [ID¹³³](#), K. Vorobev [ID³⁷](#), M. Vos [ID¹⁶³](#), K. Voss [ID¹⁴¹](#),
 J.H. Vossebeld [ID⁹²](#), M. Vozak [ID¹¹⁴](#), L. Vozdecky [ID⁹⁴](#), N. Vranjes [ID¹⁵](#), M. Vranjes Milosavljevic [ID¹⁵](#),
 M. Vreeswijk [ID¹¹⁴](#), R. Vuillermet [ID³⁶](#), O. Vujinovic [ID¹⁰⁰](#), I. Vukotic [ID³⁹](#), S. Wada [ID¹⁵⁷](#), C. Wagner¹⁰³,
 J.M. Wagner [ID^{17a}](#), W. Wagner [ID¹⁷¹](#), S. Wahdan [ID¹⁷¹](#), H. Wahlberg [ID⁹⁰](#), R. Wakasa [ID¹⁵⁷](#),
 M. Wakida [ID¹¹¹](#), J. Walder [ID¹³⁴](#), R. Walker [ID¹⁰⁹](#), W. Walkowiak [ID¹⁴¹](#), A.M. Wang [ID⁶¹](#), A.Z. Wang [ID¹⁷⁰](#),
 C. Wang [ID¹⁰⁰](#), C. Wang [ID^{62c}](#), H. Wang [ID^{17a}](#), J. Wang [ID^{64a}](#), R.-J. Wang [ID¹⁰⁰](#), R. Wang [ID⁶¹](#), R. Wang [ID⁶](#),
 S.M. Wang [ID¹⁴⁸](#), S. Wang [ID^{62b}](#), T. Wang [ID^{62a}](#), W.T. Wang [ID⁸⁰](#), X. Wang [ID^{14c}](#), X. Wang [ID¹⁶²](#),
 X. Wang [ID^{62c}](#), Y. Wang [ID^{62d}](#), Y. Wang [ID^{14c}](#), Z. Wang [ID¹⁰⁶](#), Z. Wang [ID^{62d,51,62c}](#), Z. Wang [ID¹⁰⁶](#),
 A. Warburton [ID¹⁰⁴](#), R.J. Ward [ID²⁰](#), N. Warrack [ID⁵⁹](#), A.T. Watson [ID²⁰](#), H. Watson [ID⁵⁹](#), M.F. Watson [ID²⁰](#),
 G. Watts [ID¹³⁸](#), B.M. Waugh [ID⁹⁶](#), C. Weber [ID²⁹](#), H.A. Weber [ID¹⁸](#), M.S. Weber [ID¹⁹](#), S.M. Weber [ID^{63a}](#),
 C. Wei^{62a}, Y. Wei [ID¹²⁶](#), A.R. Weidberg [ID¹²⁶](#), E.J. Weik [ID¹¹⁷](#), J. Weingarten [ID⁴⁹](#), M. Weirich [ID¹⁰⁰](#),
 C. Weiser [ID⁵⁴](#), C.J. Wells [ID⁴⁸](#), T. Wenaus [ID²⁹](#), B. Wendland [ID⁴⁹](#), T. Wengler [ID³⁶](#), N.S. Wenke¹¹⁰,
 N. Wermes [ID²⁴](#), M. Wessels [ID^{63a}](#), K. Whalen [ID¹²³](#), A.M. Wharton [ID⁹¹](#), A.S. White [ID⁶¹](#), A. White [ID⁸](#),
 M.J. White [ID¹](#), D. Whiteson [ID¹⁶⁰](#), L. Wickremasinghe [ID¹²⁴](#), W. Wiedenmann [ID¹⁷⁰](#), C. Wiel [ID⁵⁰](#),
 M. Wielers [ID¹³⁴](#), C. Wiglesworth [ID⁴²](#), L.A.M. Wiik-Fuchs [ID⁵⁴](#), D.J. Wilburn¹²⁰, H.G. Wilkens [ID³⁶](#),
 D.M. Williams [ID⁴¹](#), H.H. Williams¹²⁸, S. Williams [ID³²](#), S. Willocq [ID¹⁰³](#), B.J. Wilson [ID¹⁰¹](#),
 P.J. Windischhofer [ID³⁹](#), F. Winklmeier [ID¹²³](#), B.T. Winter [ID⁵⁴](#), J.K. Winter [ID¹⁰¹](#), M. Wittgen¹⁴³,
 M. Wobisch [ID⁹⁷](#), R. Wölker [ID¹²⁶](#), J. Wollrath¹⁶⁰, M.W. Wolter [ID⁸⁶](#), H. Wolters [ID^{130a,130c}](#),
 V.W.S. Wong [ID¹⁶⁴](#), A.F. Wongel [ID⁴⁸](#), S.D. Worm [ID⁴⁸](#), B.K. Wosiek [ID⁸⁶](#), K.W. Woźniak [ID⁸⁶](#),
 K. Wraight [ID⁵⁹](#), J. Wu [ID^{14a,14d}](#), M. Wu [ID^{64a}](#), M. Wu [ID¹¹³](#), S.L. Wu [ID¹⁷⁰](#), X. Wu [ID⁵⁶](#), Y. Wu [ID^{62a}](#),
 Z. Wu [ID^{135,62a}](#), J. Wuertzinger [ID¹¹⁰](#), T.R. Wyatt [ID¹⁰¹](#), B.M. Wynne [ID⁵²](#), S. Xella [ID⁴²](#), L. Xia [ID^{14c}](#),
 M. Xia [ID^{14b}](#), J. Xiang [ID^{64c}](#), X. Xiao [ID¹⁰⁶](#), M. Xie [ID^{62a}](#), X. Xie [ID^{62a}](#), S. Xin [ID^{14a,14d}](#), J. Xiong [ID^{17a}](#),
 I. Xiotidis¹⁴⁶, D. Xu [ID^{14a}](#), H. Xu [ID^{62a}](#), H. Xu [ID^{62a}](#), L. Xu [ID^{62a}](#), R. Xu [ID¹²⁸](#), T. Xu [ID¹⁰⁶](#), Y. Xu [ID^{14b}](#),

Z. Xu [ID](#)^{62b}, Z. Xu [ID](#)^{14a}, B. Yabsley [ID](#)¹⁴⁷, S. Yacoob [ID](#)^{33a}, N. Yamaguchi [ID](#)⁸⁹, Y. Yamaguchi [ID](#)¹⁵⁴, H. Yamauchi [ID](#)¹⁵⁷, T. Yamazaki [ID](#)^{17a}, Y. Yamazaki [ID](#)⁸⁴, J. Yan [ID](#)^{62c}, S. Yan [ID](#)¹²⁶, Z. Yan [ID](#)²⁵, H.J. Yang [ID](#)^{62c,62d}, H.T. Yang [ID](#)^{62a}, S. Yang [ID](#)^{62a}, T. Yang [ID](#)^{64c}, X. Yang [ID](#)^{62a}, X. Yang [ID](#)^{14a}, Y. Yang [ID](#)⁴⁴, Y. Yang [ID](#)^{62a}, Z. Yang [ID](#)^{62a,106}, W-M. Yao [ID](#)^{17a}, Y.C. Yap [ID](#)⁴⁸, H. Ye [ID](#)^{14c}, H. Ye [ID](#)⁵⁵, J. Ye [ID](#)⁴⁴, S. Ye [ID](#)²⁹, X. Ye [ID](#)^{62a}, Y. Yeh [ID](#)⁹⁶, I. Yeletskikh [ID](#)³⁸, B.K. Yeo [ID](#)^{17a}, M.R. Yexley [ID](#)⁹¹, P. Yin [ID](#)⁴¹, K. Yorita [ID](#)¹⁶⁸, S. Younas [ID](#)^{27b}, C.J.S. Young [ID](#)⁵⁴, C. Young [ID](#)¹⁴³, Y. Yu [ID](#)^{62a}, M. Yuan [ID](#)¹⁰⁶, R. Yuan [ID](#)^{62b,1}, L. Yue [ID](#)⁹⁶, M. Zaazoua [ID](#)^{35e}, B. Zabinski [ID](#)⁸⁶, E. Zaid [ID](#)⁵², T. Zakareishvili [ID](#)^{149b}, N. Zakharchuk [ID](#)³⁴, S. Zambito [ID](#)⁵⁶, J.A. Zamora Saa [ID](#)^{137d,137b}, J. Zang [ID](#)¹⁵³, D. Zanzi [ID](#)⁵⁴, O. Zaplatilek [ID](#)¹³², C. Zeitnitz [ID](#)¹⁷¹, J.C. Zeng [ID](#)¹⁶², D.T. Zenger Jr [ID](#)²⁶, O. Zenin [ID](#)³⁷, T. Ženiš [ID](#)^{28a}, S. Zenz [ID](#)⁹⁴, S. Zerradi [ID](#)^{35a}, D. Zerwas [ID](#)⁶⁶, M. Zhai [ID](#)^{14a,14d}, B. Zhang [ID](#)^{14c}, D.F. Zhang [ID](#)¹³⁹, J. Zhang [ID](#)^{62b}, J. Zhang [ID](#)⁶, K. Zhang [ID](#)^{14a,14d}, L. Zhang [ID](#)^{14c}, P. Zhang [ID](#)^{14a,14d}, R. Zhang [ID](#)¹⁷⁰, S. Zhang [ID](#)¹⁰⁶, T. Zhang [ID](#)¹⁵³, X. Zhang [ID](#)^{62c}, X. Zhang [ID](#)^{62b}, Y. Zhang [ID](#)^{62c,5}, Z. Zhang [ID](#)^{17a}, Z. Zhang [ID](#)⁶⁶, H. Zhao [ID](#)¹³⁸, P. Zhao [ID](#)⁵¹, T. Zhao [ID](#)^{62b}, Y. Zhao [ID](#)¹³⁶, Z. Zhao [ID](#)^{62a}, A. Zhemchugov [ID](#)³⁸, X. Zheng [ID](#)^{62a}, Z. Zheng [ID](#)¹⁴³, D. Zhong [ID](#)¹⁶², B. Zhou ¹⁰⁶, C. Zhou [ID](#)¹⁷⁰, H. Zhou [ID](#)⁷, N. Zhou [ID](#)^{62c}, Y. Zhou ⁷, C.G. Zhu [ID](#)^{62b}, H.L. Zhu [ID](#)^{62a}, J. Zhu [ID](#)¹⁰⁶, Y. Zhu [ID](#)^{62c}, Y. Zhu [ID](#)^{62a}, X. Zhuang [ID](#)^{14a}, K. Zhukov [ID](#)³⁷, V. Zhulanov [ID](#)³⁷, N.I. Zimine [ID](#)³⁸, J. Zinsser [ID](#)^{63b}, M. Ziolkowski [ID](#)¹⁴¹, L. Živković [ID](#)¹⁵, A. Zoccoli [ID](#)^{23b,23a}, K. Zoch [ID](#)⁵⁶, T.G. Zorbas [ID](#)¹³⁹, O. Zormpa [ID](#)⁴⁶, W. Zou [ID](#)⁴¹, L. Zwalski [ID](#)³⁶.

¹Department of Physics, University of Adelaide, Adelaide; Australia.

²Department of Physics, University of Alberta, Edmonton AB; Canada.

^{3(a)}Department of Physics, Ankara University, Ankara; ^(b)Division of Physics, TOBB University of Economics and Technology, Ankara; Türkiye.

⁴LAPP, Université Savoie Mont Blanc, CNRS/IN2P3, Annecy; France.

⁵APC, Université Paris Cité, CNRS/IN2P3, Paris; France.

⁶High Energy Physics Division, Argonne National Laboratory, Argonne IL; United States of America.

⁷Department of Physics, University of Arizona, Tucson AZ; United States of America.

⁸Department of Physics, University of Texas at Arlington, Arlington TX; United States of America.

⁹Physics Department, National and Kapodistrian University of Athens, Athens; Greece.

¹⁰Physics Department, National Technical University of Athens, Zografou; Greece.

¹¹Department of Physics, University of Texas at Austin, Austin TX; United States of America.

¹²Institute of Physics, Azerbaijan Academy of Sciences, Baku; Azerbaijan.

¹³Institut de Física d'Altes Energies (IFAE), Barcelona Institute of Science and Technology, Barcelona; Spain.

^{14(a)}Institute of High Energy Physics, Chinese Academy of Sciences, Beijing; ^(b)Physics Department, Tsinghua University, Beijing; ^(c)Department of Physics, Nanjing University, Nanjing; ^(d)University of Chinese Academy of Science (UCAS), Beijing; China.

¹⁵Institute of Physics, University of Belgrade, Belgrade; Serbia.

¹⁶Department for Physics and Technology, University of Bergen, Bergen; Norway.

^{17(a)}Physics Division, Lawrence Berkeley National Laboratory, Berkeley CA; ^(b)University of California, Berkeley CA; United States of America.

¹⁸Institut für Physik, Humboldt Universität zu Berlin, Berlin; Germany.

¹⁹Albert Einstein Center for Fundamental Physics and Laboratory for High Energy Physics, University of Bern, Bern; Switzerland.

²⁰School of Physics and Astronomy, University of Birmingham, Birmingham; United Kingdom.

^{21(a)}Department of Physics, Bogazici University, Istanbul; ^(b)Department of Physics Engineering, Gaziantep University, Gaziantep; ^(c)Department of Physics, Istanbul University, Istanbul; ^(d)Istinye

University, Sariyer, Istanbul; Türkiye.

^{22(a)}Facultad de Ciencias y Centro de Investigaciones, Universidad Antonio Nariño,

Bogotá; ^(b)Departamento de Física, Universidad Nacional de Colombia, Bogotá; Colombia.

^{23(a)}Dipartimento di Fisica e Astronomia A. Righi, Università di Bologna, Bologna; ^(b)INFN Sezione di Bologna; Italy.

²⁴Physikalisches Institut, Universität Bonn, Bonn; Germany.

²⁵Department of Physics, Boston University, Boston MA; United States of America.

²⁶Department of Physics, Brandeis University, Waltham MA; United States of America.

^{27(a)}Transilvania University of Brasov, Brasov; ^(b)Horia Hulubei National Institute of Physics and Nuclear Engineering, Bucharest; ^(c)Department of Physics, Alexandru Ioan Cuza University of Iasi, Iasi; ^(d)National Institute for Research and Development of Isotopic and Molecular Technologies, Physics Department, Cluj-Napoca; ^(e)University Politehnica Bucharest, Bucharest; ^(f)West University in Timisoara, Timisoara; ^(g)Faculty of Physics, University of Bucharest, Bucharest; Romania.

^{28(a)}Faculty of Mathematics, Physics and Informatics, Comenius University, Bratislava; ^(b)Department of Subnuclear Physics, Institute of Experimental Physics of the Slovak Academy of Sciences, Kosice; Slovak Republic.

²⁹Physics Department, Brookhaven National Laboratory, Upton NY; United States of America.

³⁰Universidad de Buenos Aires, Facultad de Ciencias Exactas y Naturales, Departamento de Física, y CONICET, Instituto de Física de Buenos Aires (IFIBA), Buenos Aires; Argentina.

³¹California State University, CA; United States of America.

³²Cavendish Laboratory, University of Cambridge, Cambridge; United Kingdom.

^{33(a)}Department of Physics, University of Cape Town, Cape Town; ^(b)iThemba Labs, Western

Cape; ^(c)Department of Mechanical Engineering Science, University of Johannesburg,

Johannesburg; ^(d)National Institute of Physics, University of the Philippines Diliman (Philippines); ^(e)University of South Africa, Department of Physics, Pretoria; ^(f)University of Zululand, KwaDlangezwa; ^(g)School of Physics, University of the Witwatersrand, Johannesburg; South Africa.

³⁴Department of Physics, Carleton University, Ottawa ON; Canada.

^{35(a)}Faculté des Sciences Ain Chock, Réseau Universitaire de Physique des Hautes Energies - Université Hassan II, Casablanca; ^(b)Faculté des Sciences, Université Ibn-Tofail, Kénitra; ^(c)Faculté des Sciences Semlalia, Université Cadi Ayyad, LPHEA-Marrakech; ^(d)LPMR, Faculté des Sciences, Université Mohamed Premier, Oujda; ^(e)Faculté des sciences, Université Mohammed V, Rabat; ^(f)Institute of Applied Physics, Mohammed VI Polytechnic University, Ben Guerir; Morocco.

³⁶CERN, Geneva; Switzerland.

³⁷Affiliated with an institute covered by a cooperation agreement with CERN.

³⁸Affiliated with an international laboratory covered by a cooperation agreement with CERN.

³⁹Enrico Fermi Institute, University of Chicago, Chicago IL; United States of America.

⁴⁰LPC, Université Clermont Auvergne, CNRS/IN2P3, Clermont-Ferrand; France.

⁴¹Nevis Laboratory, Columbia University, Irvington NY; United States of America.

⁴²Niels Bohr Institute, University of Copenhagen, Copenhagen; Denmark.

^{43(a)}Dipartimento di Fisica, Università della Calabria, Rende; ^(b)INFN Gruppo Collegato di Cosenza, Laboratori Nazionali di Frascati; Italy.

⁴⁴Physics Department, Southern Methodist University, Dallas TX; United States of America.

⁴⁵Physics Department, University of Texas at Dallas, Richardson TX; United States of America.

⁴⁶National Centre for Scientific Research "Demokritos", Agia Paraskevi; Greece.

^{47(a)}Department of Physics, Stockholm University; ^(b)Oskar Klein Centre, Stockholm; Sweden.

⁴⁸Deutsches Elektronen-Synchrotron DESY, Hamburg and Zeuthen; Germany.

⁴⁹Fakultät Physik , Technische Universität Dortmund, Dortmund; Germany.

- ⁵⁰Institut für Kern- und Teilchenphysik, Technische Universität Dresden, Dresden; Germany.
- ⁵¹Department of Physics, Duke University, Durham NC; United States of America.
- ⁵²SUPA - School of Physics and Astronomy, University of Edinburgh, Edinburgh; United Kingdom.
- ⁵³INFN e Laboratori Nazionali di Frascati, Frascati; Italy.
- ⁵⁴Physikalisches Institut, Albert-Ludwigs-Universität Freiburg, Freiburg; Germany.
- ⁵⁵II. Physikalisches Institut, Georg-August-Universität Göttingen, Göttingen; Germany.
- ⁵⁶Département de Physique Nucléaire et Corpusculaire, Université de Genève, Genève; Switzerland.
- ⁵⁷^(a)Dipartimento di Fisica, Università di Genova, Genova; ^(b)INFN Sezione di Genova; Italy.
- ⁵⁸II. Physikalisches Institut, Justus-Liebig-Universität Giessen, Giessen; Germany.
- ⁵⁹SUPA - School of Physics and Astronomy, University of Glasgow, Glasgow; United Kingdom.
- ⁶⁰LPSC, Université Grenoble Alpes, CNRS/IN2P3, Grenoble INP, Grenoble; France.
- ⁶¹Laboratory for Particle Physics and Cosmology, Harvard University, Cambridge MA; United States of America.
- ⁶²^(a)Department of Modern Physics and State Key Laboratory of Particle Detection and Electronics, University of Science and Technology of China, Hefei; ^(b)Institute of Frontier and Interdisciplinary Science and Key Laboratory of Particle Physics and Particle Irradiation (MOE), Shandong University, Qingdao; ^(c)School of Physics and Astronomy, Shanghai Jiao Tong University, Key Laboratory for Particle Astrophysics and Cosmology (MOE), SKLPPC, Shanghai; ^(d)Tsung-Dao Lee Institute, Shanghai; China.
- ⁶³^(a)Kirchhoff-Institut für Physik, Ruprecht-Karls-Universität Heidelberg, Heidelberg; ^(b)Physikalisches Institut, Ruprecht-Karls-Universität Heidelberg, Heidelberg; Germany.
- ⁶⁴^(a)Department of Physics, Chinese University of Hong Kong, Shatin, N.T., Hong Kong; ^(b)Department of Physics, University of Hong Kong, Hong Kong; ^(c)Department of Physics and Institute for Advanced Study, Hong Kong University of Science and Technology, Clear Water Bay, Kowloon, Hong Kong; China.
- ⁶⁵Department of Physics, National Tsing Hua University, Hsinchu; Taiwan.
- ⁶⁶IJCLab, Université Paris-Saclay, CNRS/IN2P3, 91405, Orsay; France.
- ⁶⁷Centro Nacional de Microelectrónica (IMB-CNM-CSIC), Barcelona; Spain.
- ⁶⁸Department of Physics, Indiana University, Bloomington IN; United States of America.
- ⁶⁹^(a)INFN Gruppo Collegato di Udine, Sezione di Trieste, Udine; ^(b)ICTP, Trieste; ^(c)Dipartimento Politecnico di Ingegneria e Architettura, Università di Udine, Udine; Italy.
- ⁷⁰^(a)INFN Sezione di Lecce; ^(b)Dipartimento di Matematica e Fisica, Università del Salento, Lecce; Italy.
- ⁷¹^(a)INFN Sezione di Milano; ^(b)Dipartimento di Fisica, Università di Milano, Milano; Italy.
- ⁷²^(a)INFN Sezione di Napoli; ^(b)Dipartimento di Fisica, Università di Napoli, Napoli; Italy.
- ⁷³^(a)INFN Sezione di Pavia; ^(b)Dipartimento di Fisica, Università di Pavia, Pavia; Italy.
- ⁷⁴^(a)INFN Sezione di Pisa; ^(b)Dipartimento di Fisica E. Fermi, Università di Pisa, Pisa; Italy.
- ⁷⁵^(a)INFN Sezione di Roma; ^(b)Dipartimento di Fisica, Sapienza Università di Roma, Roma; Italy.
- ⁷⁶^(a)INFN Sezione di Roma Tor Vergata; ^(b)Dipartimento di Fisica, Università di Roma Tor Vergata, Roma; Italy.
- ⁷⁷^(a)INFN Sezione di Roma Tre; ^(b)Dipartimento di Matematica e Fisica, Università Roma Tre, Roma; Italy.
- ⁷⁸^(a)INFN-TIFPA; ^(b)Università degli Studi di Trento, Trento; Italy.
- ⁷⁹Universität Innsbruck, Department of Astro and Particle Physics, Innsbruck; Austria.
- ⁸⁰University of Iowa, Iowa City IA; United States of America.
- ⁸¹Department of Physics and Astronomy, Iowa State University, Ames IA; United States of America.
- ⁸²^(a)Departamento de Engenharia Elétrica, Universidade Federal de Juiz de Fora (UFJF), Juiz de Fora; ^(b)Universidade Federal do Rio De Janeiro COPPE/EE/IF, Rio de Janeiro; ^(c)Instituto de Física, Universidade de São Paulo, São Paulo; ^(d)Rio de Janeiro State University, Rio de Janeiro; Brazil.
- ⁸³KEK, High Energy Accelerator Research Organization, Tsukuba; Japan.

- ⁸⁴Graduate School of Science, Kobe University, Kobe; Japan.
- ^{85(a)}AGH University of Science and Technology, Faculty of Physics and Applied Computer Science, Krakow; ^(b)Marian Smoluchowski Institute of Physics, Jagiellonian University, Krakow; Poland.
- ⁸⁶Institute of Nuclear Physics Polish Academy of Sciences, Krakow; Poland.
- ⁸⁷Faculty of Science, Kyoto University, Kyoto; Japan.
- ⁸⁸Kyoto University of Education, Kyoto; Japan.
- ⁸⁹Research Center for Advanced Particle Physics and Department of Physics, Kyushu University, Fukuoka ; Japan.
- ⁹⁰Instituto de Física La Plata, Universidad Nacional de La Plata and CONICET, La Plata; Argentina.
- ⁹¹Physics Department, Lancaster University, Lancaster; United Kingdom.
- ⁹²Oliver Lodge Laboratory, University of Liverpool, Liverpool; United Kingdom.
- ⁹³Department of Experimental Particle Physics, Jožef Stefan Institute and Department of Physics, University of Ljubljana, Ljubljana; Slovenia.
- ⁹⁴School of Physics and Astronomy, Queen Mary University of London, London; United Kingdom.
- ⁹⁵Department of Physics, Royal Holloway University of London, Egham; United Kingdom.
- ⁹⁶Department of Physics and Astronomy, University College London, London; United Kingdom.
- ⁹⁷Louisiana Tech University, Ruston LA; United States of America.
- ⁹⁸Fysiska institutionen, Lunds universitet, Lund; Sweden.
- ⁹⁹Departamento de Física Teórica C-15 and CIAFF, Universidad Autónoma de Madrid, Madrid; Spain.
- ¹⁰⁰Institut für Physik, Universität Mainz, Mainz; Germany.
- ¹⁰¹School of Physics and Astronomy, University of Manchester, Manchester; United Kingdom.
- ¹⁰²CPPM, Aix-Marseille Université, CNRS/IN2P3, Marseille; France.
- ¹⁰³Department of Physics, University of Massachusetts, Amherst MA; United States of America.
- ¹⁰⁴Department of Physics, McGill University, Montreal QC; Canada.
- ¹⁰⁵School of Physics, University of Melbourne, Victoria; Australia.
- ¹⁰⁶Department of Physics, University of Michigan, Ann Arbor MI; United States of America.
- ¹⁰⁷Department of Physics and Astronomy, Michigan State University, East Lansing MI; United States of America.
- ¹⁰⁸Group of Particle Physics, University of Montreal, Montreal QC; Canada.
- ¹⁰⁹Fakultät für Physik, Ludwig-Maximilians-Universität München, München; Germany.
- ¹¹⁰Max-Planck-Institut für Physik (Werner-Heisenberg-Institut), München; Germany.
- ¹¹¹Graduate School of Science and Kobayashi-Maskawa Institute, Nagoya University, Nagoya; Japan.
- ¹¹²Department of Physics and Astronomy, University of New Mexico, Albuquerque NM; United States of America.
- ¹¹³Institute for Mathematics, Astrophysics and Particle Physics, Radboud University/Nikhef, Nijmegen; Netherlands.
- ¹¹⁴Nikhef National Institute for Subatomic Physics and University of Amsterdam, Amsterdam; Netherlands.
- ¹¹⁵Department of Physics, Northern Illinois University, DeKalb IL; United States of America.
- ^{116(a)}New York University Abu Dhabi, Abu Dhabi; ^(b)University of Sharjah, Sharjah; United Arab Emirates.
- ¹¹⁷Department of Physics, New York University, New York NY; United States of America.
- ¹¹⁸Ochanomizu University, Otsuka, Bunkyo-ku, Tokyo; Japan.
- ¹¹⁹Ohio State University, Columbus OH; United States of America.
- ¹²⁰Homer L. Dodge Department of Physics and Astronomy, University of Oklahoma, Norman OK; United States of America.
- ¹²¹Department of Physics, Oklahoma State University, Stillwater OK; United States of America.

- ¹²²Palacký University, Joint Laboratory of Optics, Olomouc; Czech Republic.
- ¹²³Institute for Fundamental Science, University of Oregon, Eugene, OR; United States of America.
- ¹²⁴Graduate School of Science, Osaka University, Osaka; Japan.
- ¹²⁵Department of Physics, University of Oslo, Oslo; Norway.
- ¹²⁶Department of Physics, Oxford University, Oxford; United Kingdom.
- ¹²⁷LPNHE, Sorbonne Université, Université Paris Cité, CNRS/IN2P3, Paris; France.
- ¹²⁸Department of Physics, University of Pennsylvania, Philadelphia PA; United States of America.
- ¹²⁹Department of Physics and Astronomy, University of Pittsburgh, Pittsburgh PA; United States of America.
- ¹³⁰(*a*) Laboratório de Instrumentação e Física Experimental de Partículas - LIP, Lisboa; (*b*) Departamento de Física, Faculdade de Ciências, Universidade de Lisboa, Lisboa; (*c*) Departamento de Física, Universidade de Coimbra, Coimbra; (*d*) Centro de Física Nuclear da Universidade de Lisboa, Lisboa; (*e*) Departamento de Física, Universidade do Minho, Braga; (*f*) Departamento de Física Teórica y del Cosmos, Universidad de Granada, Granada (Spain); (*g*) Departamento de Física, Instituto Superior Técnico, Universidade de Lisboa, Lisboa; Portugal.
- ¹³¹Institute of Physics of the Czech Academy of Sciences, Prague; Czech Republic.
- ¹³²Czech Technical University in Prague, Prague; Czech Republic.
- ¹³³Charles University, Faculty of Mathematics and Physics, Prague; Czech Republic.
- ¹³⁴Particle Physics Department, Rutherford Appleton Laboratory, Didcot; United Kingdom.
- ¹³⁵IRFU, CEA, Université Paris-Saclay, Gif-sur-Yvette; France.
- ¹³⁶Santa Cruz Institute for Particle Physics, University of California Santa Cruz, Santa Cruz CA; United States of America.
- ¹³⁷(*a*) Departamento de Física, Pontificia Universidad Católica de Chile, Santiago; (*b*) Millennium Institute for Subatomic physics at high energy frontier (SAPHIR), Santiago; (*c*) Instituto de Investigación Multidisciplinario en Ciencia y Tecnología, y Departamento de Física, Universidad de La Serena; (*d*) Universidad Andres Bello, Department of Physics, Santiago; (*e*) Instituto de Alta Investigación, Universidad de Tarapacá, Arica; (*f*) Departamento de Física, Universidad Técnica Federico Santa María, Valparaíso; Chile.
- ¹³⁸Department of Physics, University of Washington, Seattle WA; United States of America.
- ¹³⁹Department of Physics and Astronomy, University of Sheffield, Sheffield; United Kingdom.
- ¹⁴⁰Department of Physics, Shinshu University, Nagano; Japan.
- ¹⁴¹Department Physik, Universität Siegen, Siegen; Germany.
- ¹⁴²Department of Physics, Simon Fraser University, Burnaby BC; Canada.
- ¹⁴³SLAC National Accelerator Laboratory, Stanford CA; United States of America.
- ¹⁴⁴Department of Physics, Royal Institute of Technology, Stockholm; Sweden.
- ¹⁴⁵Departments of Physics and Astronomy, Stony Brook University, Stony Brook NY; United States of America.
- ¹⁴⁶Department of Physics and Astronomy, University of Sussex, Brighton; United Kingdom.
- ¹⁴⁷School of Physics, University of Sydney, Sydney; Australia.
- ¹⁴⁸Institute of Physics, Academia Sinica, Taipei; Taiwan.
- ¹⁴⁹(*a*) E. Andronikashvili Institute of Physics, Iv. Javakhishvili Tbilisi State University, Tbilisi; (*b*) High Energy Physics Institute, Tbilisi State University, Tbilisi; (*c*) University of Georgia, Tbilisi; Georgia.
- ¹⁵⁰Department of Physics, Technion, Israel Institute of Technology, Haifa; Israel.
- ¹⁵¹Raymond and Beverly Sackler School of Physics and Astronomy, Tel Aviv University, Tel Aviv; Israel.
- ¹⁵²Department of Physics, Aristotle University of Thessaloniki, Thessaloniki; Greece.
- ¹⁵³International Center for Elementary Particle Physics and Department of Physics, University of Tokyo, Tokyo; Japan.

- ¹⁵⁴Department of Physics, Tokyo Institute of Technology, Tokyo; Japan.
- ¹⁵⁵Department of Physics, University of Toronto, Toronto ON; Canada.
- ^{156(a)}TRIUMF, Vancouver BC;^(b)Department of Physics and Astronomy, York University, Toronto ON; Canada.
- ¹⁵⁷Division of Physics and Tomonaga Center for the History of the Universe, Faculty of Pure and Applied Sciences, University of Tsukuba, Tsukuba; Japan.
- ¹⁵⁸Department of Physics and Astronomy, Tufts University, Medford MA; United States of America.
- ¹⁵⁹United Arab Emirates University, Al Ain; United Arab Emirates.
- ¹⁶⁰Department of Physics and Astronomy, University of California Irvine, Irvine CA; United States of America.
- ¹⁶¹Department of Physics and Astronomy, University of Uppsala, Uppsala; Sweden.
- ¹⁶²Department of Physics, University of Illinois, Urbana IL; United States of America.
- ¹⁶³Instituto de Física Corpuscular (IFIC), Centro Mixto Universidad de Valencia - CSIC, Valencia; Spain.
- ¹⁶⁴Department of Physics, University of British Columbia, Vancouver BC; Canada.
- ¹⁶⁵Department of Physics and Astronomy, University of Victoria, Victoria BC; Canada.
- ¹⁶⁶Fakultät für Physik und Astronomie, Julius-Maximilians-Universität Würzburg, Würzburg; Germany.
- ¹⁶⁷Department of Physics, University of Warwick, Coventry; United Kingdom.
- ¹⁶⁸Waseda University, Tokyo; Japan.
- ¹⁶⁹Department of Particle Physics and Astrophysics, Weizmann Institute of Science, Rehovot; Israel.
- ¹⁷⁰Department of Physics, University of Wisconsin, Madison WI; United States of America.
- ¹⁷¹Fakultät für Mathematik und Naturwissenschaften, Fachgruppe Physik, Bergische Universität Wuppertal, Wuppertal; Germany.
- ¹⁷²Department of Physics, Yale University, New Haven CT; United States of America.
- ^a Also Affiliated with an institute covered by a cooperation agreement with CERN.
- ^b Also at An-Najah National University, Nablus; Palestine.
- ^c Also at Borough of Manhattan Community College, City University of New York, New York NY; United States of America.
- ^d Also at Bruno Kessler Foundation, Trento; Italy.
- ^e Also at Center for High Energy Physics, Peking University; China.
- ^f Also at Center for Interdisciplinary Research and Innovation (CIRI-AUTH), Thessaloniki ; Greece.
- ^g Also at Centro Studi e Ricerche Enrico Fermi; Italy.
- ^h Also at CERN, Geneva; Switzerland.
- ⁱ Also at Département de Physique Nucléaire et Corpusculaire, Université de Genève, Genève; Switzerland.
- ^j Also at Departament de Fisica de la Universitat Autònoma de Barcelona, Barcelona; Spain.
- ^k Also at Department of Financial and Management Engineering, University of the Aegean, Chios; Greece.
- ^l Also at Department of Physics and Astronomy, Michigan State University, East Lansing MI; United States of America.
- ^m Also at Department of Physics, Ben Gurion University of the Negev, Beer Sheva; Israel.
- ⁿ Also at Department of Physics, California State University, East Bay; United States of America.
- ^o Also at Department of Physics, California State University, Sacramento; United States of America.
- ^p Also at Department of Physics, King's College London, London; United Kingdom.
- ^q Also at Department of Physics, Stanford University, Stanford CA; United States of America.
- ^r Also at Department of Physics, University of Fribourg, Fribourg; Switzerland.
- ^s Also at Department of Physics, University of Thessaly; Greece.
- ^t Also at Department of Physics, Westmont College, Santa Barbara; United States of America.
- ^u Also at Hellenic Open University, Patras; Greece.
- ^v Also at Institutio Catalana de Recerca i Estudis Avancats, ICREA, Barcelona; Spain.

^w Also at Institut für Experimentalphysik, Universität Hamburg, Hamburg; Germany.

^x Also at Institute for Nuclear Research and Nuclear Energy (INRNE) of the Bulgarian Academy of Sciences, Sofia; Bulgaria.

^y Also at Institute of Applied Physics, Mohammed VI Polytechnic University, Ben Guerir; Morocco.

^z Also at Institute of Particle Physics (IPP); Canada.

^{aa} Also at Institute of Physics and Technology, Ulaanbaatar; Mongolia.

^{ab} Also at Institute of Physics, Azerbaijan Academy of Sciences, Baku; Azerbaijan.

^{ac} Also at Institute of Theoretical Physics, Ilia State University, Tbilisi; Georgia.

^{ad} Also at L2IT, Université de Toulouse, CNRS/IN2P3, UPS, Toulouse; France.

^{ae} Also at Lawrence Livermore National Laboratory, Livermore; United States of America.

^{af} Also at National Institute of Physics, University of the Philippines Diliman (Philippines); Philippines.

^{ag} Also at Technical University of Munich, Munich; Germany.

^{ah} Also at The Collaborative Innovation Center of Quantum Matter (CICQM), Beijing; China.

^{ai} Also at TRIUMF, Vancouver BC; Canada.

^{aj} Also at Università di Napoli Parthenope, Napoli; Italy.

^{ak} Also at University of Chinese Academy of Sciences (UCAS), Beijing; China.

^{al} Also at University of Colorado Boulder, Department of Physics, Colorado; United States of America.

^{am} Also at Washington College, Maryland; United States of America.

^{an} Also at Yeditepe University, Physics Department, Istanbul; Türkiye.

* Deceased